



Fakultät Wissenschaftszentrum Weihenstephan für Ernährung, Landnutzung und Umwelt

Helmholtz Zentrum München, Institut für Entwicklungsgenetik

# Direct conversion of somatic cells utilizing CRISPR/Cas9

Benedict Samuel Rauser

Vollständiger Abdruck der von der Fakultät Wissenschaftszentrum Weihenstephan für Ernährung, Landnutzung und Umwelt der Technischen Universität München zur Erlangung des akademischen Grades eines

Doktors der Naturwissenschaften

genehmigten Dissertation.

Vorsitzender: Prof. Dr. Aphrodite Kapurniotu  
Prüfer der Dissertation: 1. Prof. Dr. Wolfgang Wurst  
2. Prof. Angelika Schnieke, Ph.D.

Die Dissertation wurde am 20.06.2017 bei der Technischen Universität München eingereicht und durch die Fakultät Wissenschaftszentrum Weihenstephan für Ernährung, Landnutzung und Umwelt am 04.12.2017 angenommen.

# INDEX

1	Abstract.....	2
2	Zusammenfassung.....	3
3	Introduction .....	6
3.1	Midbrain dopaminergic neurons and cell replacement strategies.....	6
3.1.1	Midbrain dopaminergic neurons and Parkinson's disease.....	6
3.1.2	Different routes for cell replacement strategies in PD.....	7
3.1.2.1	Transcription factor combinations utilized for the direct conversion of fibroblasts to DA neurons .....	9
3.1.2.2	Roles of Ascl1, Lmx1a, Nurr1 in mdDA development and direct conversion of fibroblasts to DA neurons .....	10
3.2	The CRISPR/Cas9 system and its implications for genome editing and transcriptional regulation .....	12
3.2.1	CRISPR/Cas9 - an adaptive immune system in bacteria and archaea.....	12
3.2.2	Repurposing CRISPR/Cas9 technology for genome editing.....	14
3.2.3	Transcriptional modification by CRISPR/Cas9 .....	15
4	Aim of the thesis.....	20
5	Results.....	22
5.1	Exogenous gene expression strategies for direct conversion of MEFs to DA neurons .....	22
5.1.1	Limitations of direct reprogramming utilizing multiple viruses for gene delivery ..	22
5.1.2	Limitations of multi-cistronic constructs for direct reprogramming .....	24
5.1.3	Inefficient ribosome skipping at 2A sites results in fusion proteins .....	25
5.1.4	The reprogramming efficiency of ALN is independent of doxycycline concentrations .....	27
5.1.5	Ribosome skipping at 2A sites is not affected by expression levels .....	29
5.1.6	Successful generation of PITX3 <sup>+</sup> DA neurons by forskolin treatment .....	30
5.2	Induction of endogenous genes and direct reprogramming of astrocytes to neurons utilizing the CRISPR/Cas9 technology.....	33

5.2.1	Design of gRNAs and implementation of a screening assay to detect induction of endogenous genes .....	33
5.2.2	Screening for dCas9 fusion proteins to induce endogenous Ascl1 .....	35
5.2.2.1	The SpyTag system improves endogenous gene induction.....	35
5.2.2.2	Requirement of a new screening platform for SAM and VPR systems .....	38
5.2.2.3	Increasing the number of gRNAs has a synergistic effect on gene induction	40
5.2.2.4	SAM and VPR systems are superior to SpyTag for Ascl1 activation.....	42
5.2.2.5	Combining SAM and VPR systems has a synergistic effect on Ascl1 expression.....	44
5.2.3	Design and generation of lentiviral vectors for SAM and dCas9-VPR delivery ...	47
5.2.4	Challenges in lentiviral Cas9 packaging.....	50
5.2.5	Direct reprogramming of astrocytes to neurons utilizing SAM and VPR .....	53
6	Discussion.....	58
6.1	Limitations of exogenous gene expression for direct reprogramming .....	58
6.1.1	The requirement of co-transductions limits the reprogramming efficiency .....	58
6.1.2	The high reprogramming efficiency of Caiazzo et al., seems to be influenced by the reporter system .....	58
6.1.3	Forskolin treatment enables the generation of PITX3 <sup>+</sup> DA neurons.....	59
6.1.4	Inefficient ribosome skipping at 2A sites results in fusion proteins and cell death .....	61
6.2	Utilizing CRISPR/Cas9 technology for gene induction and direct cell conversion ..	62
6.2.1	The importance of gRNA screenings for transcriptional activation.....	62
6.2.2	Screenings of dCas9 fusion proteins for an efficient gene induction.....	63
6.2.3	Synergistic activating effect of SAM and VPR systems .....	65
6.2.4	Challenges in lentiviral delivery of dCas9 systems .....	67
6.2.5	Direct conversion of astrocytes to neurons utilizing VPR and SAM .....	68
7	Conclusion and future perspectives.....	71
8	Material and methods.....	73
8.1	Material .....	73
8.2	Methods .....	85

8.2.1	Isolation and culture of primary cells and established cell lines .....	85
8.2.1.1	Storage and culture of stable cell lines .....	85
8.2.1.2	Isolation and culture of primary fibroblasts .....	85
8.2.1.3	Isolation and culture of primary astrocytes .....	86
8.2.1.4	Coating of cover slips for cell attachment .....	86
8.2.1.5	Lipofection.....	86
8.2.2	Preparation of lentiviruses and titer determination.....	87
8.2.3	Direct reprogramming of somatic cells .....	89
8.2.3.1	Reprogramming of MEFs .....	89
8.2.3.2	Reprogramming of astrocytes .....	89
8.2.4	Immunocytochemistry and microscopy .....	90
8.2.5	Luciferase assay analysis .....	90
8.2.6	RT-qPCR .....	91
8.2.7	Western blot.....	92
8.2.8	Isolation of nucleic acids .....	93
8.2.8.1	Isolation of RNA .....	93
8.2.8.2	Purification of DNA.....	93
8.2.8.3	Agarose gel electrophoresis .....	93
8.2.9	DNA plasmid preparations .....	93
8.2.10	Cloning of new constructs .....	94
8.2.10.1	Polymerase chain reaction .....	94
8.2.10.2	Digestion of DNA fragments .....	94
8.2.10.3	Ligation of DNA fragments .....	94
8.2.10.4	Design and generation of gRNA constructs .....	94
8.2.10.5	Addition of a FlagTag to the SAM construct .....	95
8.2.10.6	Design and generation of the split-Cas system with Ef1a promoters .....	95
8.2.10.7	Design and generation of CRISPR/Cas9 constructs using the Tet-O system .....	96
8.2.11	Transformation of competent bacteria.....	97
8.2.12	Glycerol stock preparations.....	97

8.2.13 Statistical analysis.....	97
9 References.....	99
10 Appendix.....	108
10.1 Supplementary data.....	108
10.2 Abbreviations.....	111
10.3 Danksagung.....	114
10.4 Lebenslauf.....	115
10.5 Eidesstattliche Erklärung.....	117

## List of figures

Figure 1: Different routes for the conversion of fibroblasts to neurons.....	7
Figure 2: Illustration of crRNA maturation, Cas9 functionality and Cas9 protein domains..	13
Figure 3: Genome editing by means of CRISPR/Cas9 technology.....	15
Figure 4: Schematic illustration of CRISPR/Cas9 systems used for gene induction in this study.....	17
Figure 5: The need for co-transduction by multiple lentiviruses limits the reprogramming efficiency.....	23
Figure 6: Utilizing the tri-cistronic ALN vector decreases the conversion efficiency to DA neurons.....	25
Figure 7: Western blot analysis reveals inefficient ribosome skipping at 2A sequences resulting in the generation of fusion proteins.....	26
Figure 8: Reducing the doxycycline concentration does not significantly affect the reprogramming efficiency.....	28
Figure 9: Lower expression levels do not affect ribosome skipping at P2A site.....	29
Figure 10: Forskolin treatment of A+L+N transduced MEFs enables the generation of TH <sup>+</sup> /PITX3 <sup>+</sup> neurons.....	31
Figure 11: gRNA A5 successfully induces Ascl1 expression in Neuro 2a cells.....	34
Figure 12: Recruitment of multiple activators to dCas9 utilizing the SpyTag system leads to an increase in transcriptional activation.....	36
Figure 13: The SpyTag system seems to be superior to the published SunTag system for the induction of ASCL1 and NURR1.....	37
Figure 14: Using VPR and Tet-O-systems influences renilla activity rendering this system unsuitable for screening purposes.....	39

Figure 15: Multiple gRNAs synergistically increase the activation of human ASCL1 in HEK293 cells.....	40
Figure 16: Combining two gRNAs synergistically increases Ascl1 induction in murine Neuro 2a cells.....	42
Figure 17: VPR and especially SAM are superior to SpyTag for gene induction of Ascl1 in Neuro 2a cells .....	43
Figure 18: Combining SAM and VPR synergistically increases Ascl1 mRNA levels in Neuro 2a cells.....	44
Figure 19: The synergistic effect of SAM and VPR seems to be based on the gRNA sequence .....	46
Figure 20: Schematic illustrations of lentiviral vectors carrying gRNAs, dCas9 and activator components .....	48
Figure 21: The SAM split-dCas9-VPR system proves to be suitable for gene induction .....	49
Figure 22: Replacement of Ef1a by Tet-O or hUBC promoters enables lentiviral packaging of dCas9 .....	52
Figure 23: Successful conversion of astrocytes to neurons utilizing the SAM split-dCas9-VPR system delivered by lentiviruses.....	54
Figure 24: The reprogramming potential of SAM or VPR alone is comparable to the SAM split-dCas9-VPR system in lipofection experiments.....	56
Figure 25: gRNA N2 successfully induces Nurr1 in Neuro 2a cells.....	108
Figure 26: Increasing the MOI of Ascl1, Lmx1a, Nurr1 encoding lentiviruses to ten results in a decrease of TH <sup>+</sup> cells .....	108
Figure 27: Switching from N2/B27 to the medium used by Caiazzo et al., does not influence the reprogramming efficiency .....	109
Figure 28: The combination of SAM and 4x-SpyTag does not reach the levels of Ascl1 activation observed for SAM and VPR .....	109
Figure 29: VP64-dCas9-VP64 fails to induce Ascl1 expression in Neuro 2a cells when used alone with gRNAs mA1 and mA2 .....	110
Figure 30: VP64-dCas9-VP64 is not sufficient to induce direct conversion of astrocytes to neurons .....	110

## List of tables

Table 1: Published combinations of transcription factors used for direct conversion of murine and human fibroblasts to DA neurons .....	9
Table 2: Equipment .....	73
Table 3: General consumables.....	73
Table 4: Chemicals .....	74
Table 5: Cell culture media and supplements .....	75
Table 6: Composition of buffers and cell culture media .....	76
Table 7: Kits .....	78
Table 8: Enzymes .....	78
Table 9: Primary antibodies.....	79
Table 10: Secondary antibodies .....	79
Table 11: Primers for amplification and sequencing .....	80
Table 12: gRNA targeting sequences.....	81
Table 13: Taqman probes .....	82
Table 14: DNA Vectors.....	83
Table 15: Cell lines.....	84
Table 16: Bacterial strains.....	84
Table 17: Mouse strains .....	85
Table 18: Software .....	85
Table 19: Transfection of DNA plasmids using Lipofectamine 2000 .....	87
Table 20: Transfection of DNA plasmids using Lipofectamine LTX .....	87
Table 21: Transfection of DNA for lentivirus production.....	88
Table 22: Settings MicroWin32 luminometer software .....	91
Table 23: Running conditions RT-qPCR .....	92

# ABSTRACT

# 1 Abstract

Midbrain dopaminergic (DA) neurons, which are implicated in the control of voluntary movement, degenerate during Parkinson's disease. Currently, there is no cure with treatments mostly focusing on alleviation of motor symptoms. Cell replacement therapy utilizing directly reprogrammed cells is therefore regarded as a promising alternative. Somatic cells such as fibroblasts can be directly converted to DA neurons e.g. by overexpression of the transcription factors *Ascl1*, *Lmx1a* and *Nurr1* (A+L+N). However, the obtained neurons were found to be negative for the midbrain DA neuron specific marker *Pitx3* and therefore do not resemble the DA subtype lost in Parkinson's disease patients. The aim of this thesis was to test new strategies in order to improve the reprogramming efficiency *in vitro* and to identify factors enabling the generation of *Pitx3* expressing DA neurons.

PITX3<sup>+</sup> DA neurons were successfully obtained by treating A+L+N transduced fibroblasts with forskolin, an activator of cAMP signaling, suggesting the promising generation of 'true' midbrain DA neurons. In these experiments, co-transduction of a single cell by three individual lentiviruses encoding *Ascl1*, *Lmx1a* and *Nurr1* seemed to be a limiting factor. Therefore, a tri-cistronic vector carrying all three transcription factors was tested. However, a substantial proportion of *Ascl1*, *Lmx1a* and *Nurr1* was expressed as fusion proteins resulting in a significant decrease of reprogrammed cells rendering the tri-cistronic approach unsuitable for increasing the yield of TH<sup>+</sup> neurons.

In order to overcome these limitations, the potential of the CRISPR/Cas9 technology regarding the induction of endogenous genes and direct reprogramming of somatic cells was investigated. Nuclease deficient dCas9 proteins together with sequence specific gRNAs were used as shuttles to deliver transcriptional activators as fusion proteins to the promoter region of target genes thus inducing their expression. For the proof-of-principle experiments in this thesis, *Ascl1* was chosen as target gene since overexpression of this transcription factor was shown to be sufficient to directly convert astrocytes or fibroblasts into neurons. Screenings for suitable gRNA combinations and dCas9 fusion proteins were performed and a novel synergistic effect of two transcriptional activator systems – VPR and SAM – was found to strongly activate murine *Ascl1* expression. Furthermore, for the first time murine cortical astrocytes were directly converted into neurons by CRISPR/Cas9 mediated induction of *Ascl1*. These are promising findings highlighting the potential of the CRISPR/Cas9 technology for direct reprogramming and cell replacement therapies.

## 2 Zusammenfassung

Bei Morbus Parkinson degenerieren dopaminerge (DA) Neurone des Mittelhirns, die an der Steuerung bewusster Bewegungen beteiligt sind. Eine Heilung ist bislang nicht möglich und die derzeitigen Therapien konzentrieren sich auf die Behandlung motorischer Symptome. Daher gelten neue Ansätze wie Zellersatztherapien mithilfe reprogrammierter Zellen als vielversprechend. Fibroblasten können beispielsweise durch die Überexpression der Transkriptionsfaktoren *Ascl1*, *Lmx1a* und *Nurr1* (A+L+N) direkt in DA Neurone reprogrammiert werden. Allerdings handelt es sich bei diesen reprogrammierten DA Neuronen nicht um den Subtyp, der bei Morbus Parkinson Patienten betroffen ist, da das Markergen *Pitx3* nicht exprimiert wird. Ziel dieser Thesis war es, neue Methoden zur Verbesserung der *in vitro* Reprogrammierungseffizienz zu entwickeln und neue Faktoren zu identifizieren, die eine Reprogrammierung zu PITX3<sup>+</sup> DA Neuronen ermöglichen.

Eine erfolgreiche Reprogrammierung von Fibroblasten zu PITX3<sup>+</sup> DA Neuronen gelang in dieser Thesis durch die Behandlung von A+L+N transduzierten Zellen mit dem cAMP-Aktivator Forskolin. Diese vielversprechenden Daten deuten auf die Generierung „echter“ Mittelhirn-DA Neurone hin. Allerdings zeigte sich auch, dass die erforderliche Ko-Transduktion einzelner Zellen mit drei Lentiviren für die Expression von *Ascl1*, *Lmx1a* und *Nurr1* einen limitierenden Faktor darstellt. Daher wurde ein tri-cistronischer Vektor getestet, welcher es ermöglicht, *Ascl1*, *Lmx1a* und *Nurr1* mit einem einzigen Virus in Zielzellen einzubringen. Ein signifikanter Anteil der drei Transkriptionsfaktoren wurde hierbei jedoch in Form von Fusionsproteinen exprimiert, was mit einer deutlich verringerten Reprogrammierungseffizienz einherging. Der tri-cistronische Ansatz eignete sich daher nicht zur Verbesserung der Ausbeute an TH<sup>+</sup> DA Neuronen.

Als eine alternative und neue Strategie wurde das Potential des CRISPR/Cas9-Systems zur Aktivierung endogener Gene und der direkten Reprogrammierung analysiert. Hierbei wurde eine Cas9-Variante ohne Nuklease Aktivität (dCas9) verwendet, die als Fusionsprotein mit verschiedenen transkriptionellen Aktivatoren exprimiert wird. Dieser Komplex bindet mithilfe sequenzspezifischer gRNAs an Promotoren von Zielgenen und induziert so deren Expression. Für die Machbarkeitsstudien in dieser Thesis wurde *Ascl1* als Zielgen ausgewählt, da dieser Transkriptionsfaktor alleine in der Lage ist, Fibroblasten oder Astrozyten in Neurone zu reprogrammieren. In der vorliegenden Thesis wurden erfolgreich Screenings für geeignete gRNA Kombinationen und dCas9-Fusionsproteine durchgeführt. Hierbei konnte ein neuartiger synergistischer Effekt durch die Kombination zweier Systeme (SAM und VPR) zur transkriptionellen Aktivierung von murinem *Ascl1* gezeigt werden. Im Weiteren wurde die CRISPR/Cas9 Technologie erstmals zur direkten Reprogrammierung

muriner kortikaler Astrozyten in Neurone verwendet. Diese vielversprechenden Ergebnisse zeigen das Potential der CRISPR/Cas9 Technologie für die direkte Reprogrammierung und die Anwendung für Zellersatztherapien.

# INTRODUCTION

## 3 Introduction

### 3.1 Midbrain dopaminergic neurons and cell replacement strategies

#### 3.1.1 Midbrain dopaminergic neurons and Parkinson's disease

The neurotransmitter dopamine is synthesized and released by dopaminergic (DA) neurons in different parts of the mammalian brain. The rate limiting enzyme and DA neuron marker Tyrosine hydroxylase (TH) converts L-Tyrosine into L-Dihydroxyphenylalanine (L-DOPA) followed by decarboxylation to dopamine which is catalyzed by Aromatic L-amino acid decarboxylase [1]. Subsequently, dopamine is packaged into synaptic vesicles and released into the synaptic cleft upon neuronal excitation. The Dopamine transporter (DAT) enables re-import into the presynaptic neuron thus stopping dopamine signaling followed by recycling of the neurotransmitter [1].

The largest and most intensively studied group of DA neurons are the meso-diencephalic dopaminergic (mdDA) neurons involved in the control of voluntary movement, working memory and reward [2]. mdDA neurons can be divided in three clusters known as retrorubral field (A8), substantia nigra pars compacta (SNc, A9) and the ventral tegmental area (VTA, A10) [3]. mdDA neurons of the VTA and the retrorubral field are mainly implicated in cognition and reward and project to the ventral striatum and limbic structures [4]. mdDA neurons of the SNc are predominantly involved in the control of voluntary movement via their axonal projections to the dorsal striatum [4]. Parkinson's disease (PD) is characterized by the progressive degeneration and loss of mdDA neurons in the SNc [5]. This leads to a reduction of dopamine in the striatum resulting in motor symptoms including bradykinesia, rigidity and resting tremor [6-8]. However, also non-motor symptoms such as cognitive impairment and mood disorders are observed [9]. PD is a neurodegenerative disorder affecting about 1% of people at the age of 60 and increasing with age [7]. PD is regarded as a sporadic disease with unclear etiology and ageing as a major risk [10]. However, exposure to environmental toxins such as rotenone, paraquat or 1-methyl-4-phenyl-1,2,3,6-tetrahydropyridine (MPTP), has also been linked to PD and approximately 5 - 10% of PD cases have a genetic component [11-13].

The DA neuron subpopulation susceptible to neurodegenerative stress is characterized by the expression of Paired-like homeodomain transcription factor 3 (*Pitx3*) [14]. *Pitx3* is not only a marker gene for mdDA neurons but has also been shown to be critical for differentiation, long term survival and stress resistance by induction of the survival factor Brain derived neurotrophic factor (*Bdnf*) [14, 15]. Interestingly, *Pitx3* deficient *aphakia* mice show a specific loss of dopaminergic neurons in the SNc and to a much lesser extend in the VTA [14, 16], thus resembling the cell loss in PD.

To date there is no cure for PD. Treatments focus on motor symptoms by replenishing and stabilizing dopamine levels in the striatum utilizing L-DOPA or by deep brain stimulation [17]. However, the effects are often only short term effective and neuronal degradation cannot be stopped or reverted [17]. New approaches such as direct reprogramming and cell replacement therapies are therefore a promising alternative.

### 3.1.2 Different routes for cell replacement strategies in PD

PD is one of the prime candidates for direct reprogramming and cell replacement therapies due to the localized degeneration of a specific cell type [18]. Since the 1980s efforts were made to replace degenerated mdDA neurons in PD patients including allografts of human fetal ventral mesencephalon tissues [19-21]. However, severe side-effects including graft-induced dyskinesias and adaptive immune responses against allografts were observed [22, 23]. A completely new field for cell replacement strategies was born when Yamanaka and colleagues reported the reprogramming of fibroblasts into induced pluripotent stem cells (iPSC) in 2006 [24].

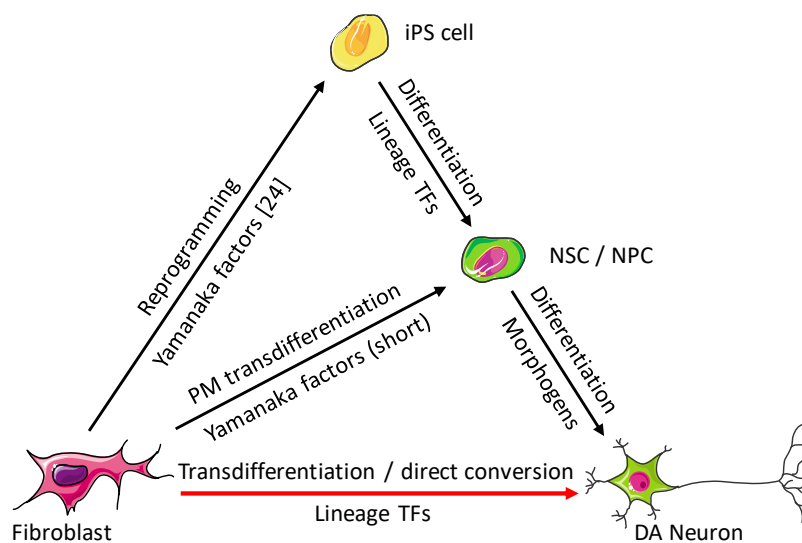


**Figure 1: Different routes for the conversion of fibroblasts to neurons**

Schematic illustration of different routes to convert one somatic cell type into another one. Reprogramming: Induced pluripotent stem cells (iPS cells) are generated by overexpression of Yamanaka factors (*Oct4*, *Sox2*, *c-Myc* and *Klf4*). Targeted differentiation by overexpression of lineage specific transcription factors (TFs) leads to the generation of neuronal stem cells (NSCs) and neuronal precursor cells (NPCs) which can be further differentiated to neuronal subtypes by addition of specific morphogens. Pluripotency mediated (PM) transdifferentiation: Overexpressing of Yamanaka factors for a limited time to generate neuronal precursor cells (NPCs) which can then be differentiated to a specific neuronal subtype by supplementing specific morphogens. Transdifferentiation or direct conversion / direct reprogramming: Overexpression of lineage specific transcription factors (TFs) is utilized to directly convert one somatic cell type into another one without passing through a pluripotent cell stage. **Abbreviations:** iPS cell: induced pluripotent stem cell, NPC: neuronal precursor cell, NSC: neuronal stem cell, PM: pluripotency mediated, TF: transcription factor.

This was achieved by overexpression of POU domain, class 5, transcription factor 1 (*Pou5f1* or *Oct4*), Sex determining region Y-box 2 (*Sox2*), Myelocytomatosis oncogene (*c-Myc*) and Kruppel-like factor 4 (*Klf4*) in mouse and human fibroblasts reprogramming them into embryonic stem cell-like cells [24, 25]. iPSCs are undifferentiated cells which undergo asymmetric cell division generating two daughter cells with different properties. While one cell stays pluripotent allowing self-renewal the second daughter cells can differentiate into all types of cells in the body [24, 25]. One of the main advantages of iPSCs compared to embryonic stem cells is that pluripotent cells can be generated from easily accessible somatic cells of the patient such as skin fibroblasts. This overcomes immunologic reactions after transplantation and does not require destruction of embryos as it is the case for the isolation of embryonic stem cells. Targeted differentiation of iPSCs to a cell type of interest such as mdDA neurons therefore has great potential for cell replacement therapies enabling personalized regenerative medicine (see Figure 1).

A commonly used model for PD are 6-hydroxy dopamine (6-OHDA) treated animals where DA neurons are selectively degenerated by the neurotoxin 6-OHDA [26]. Dopaminergic neurons derived from iPSCs have been transplanted into the striatum of 6-OHDA treated rats and were found to integrate into the host tissue leading to behavioral improvement [27]. However, teratomas which are tumors containing cell types of more than one germ layer were observed indicating the presence of undifferentiated iPSCs [27]. This tumorigenic potential which has been observed in other animal models as well is a risk of stem cell based transplantation therapies in clinical applications [28, 29].

Recently, a new approach for cell reprogramming termed transdifferentiation has emerged which can be accomplished by two ways: Via generation of expandable neuronal precursor cells [30, 31] or by direct conversion to postmitotic DA neurons [32-37] (see Figure 1). Neuronal precursor cells can be obtained by temporal expression of the Yamanaka factors described earlier [30]. These precursor cells are then differentiated into DA neurons in a second step by addition of morphogens involved in the *in vivo* development of DA neurons [30]. This method is termed pluripotency mediated (PM) transdifferentiation. While showing comparable functionality to cells derived from iPSCs and their *in vivo* counterparts, neurons derived from transdifferentiation do not have the risk of tumorigenicity as they do not pass a pluripotent state [38, 39].

Finally, by overexpression of lineage-specific transcription factors (TFs) somatic cells such as fibroblasts can be directly transdifferentiated into another somatic cell type e.g. DA neurons without passing a proliferative state [32-37]. This is also referred to as direct conversion or direct reprogramming and opens a third route for patient-specific cell replacement therapies as indicated by the red arrow in Figure 1. This route of direct reprogramming was utilized in

the underlying thesis. Transplanted DA neurons obtained by direct conversion of fibroblasts were shown to alleviate symptoms in 6-OHDA treated mice underlining the potential of direct lineage reprogramming [32].

### 3.1.2.1 Transcription factor combinations utilized for the direct conversion of fibroblasts to DA neurons

Several groups are working on the direct conversion of somatic cells into DA neurons but there is still a need to increase the reprogramming efficiency and to steer the DA neuron subtype towards mdDA neurons. Table 1 gives an overview of published combinations of transcription factors for the direct conversion of fibroblasts to DA neurons. In these cases, three to six different TFs associated with mdDA neuron development were co-expressed in fibroblasts after retro- or lentiviral gene delivery. Reprogramming efficiencies ranged from 0.05% to 18% of TH<sup>+</sup> DA neurons but a quantitative comparison is difficult due to differences in protocols, cell types used and species of origin.

**Table 1: Published combinations of transcription factors used for direct conversion of murine and human fibroblasts to DA neurons**

	<b>Caiazzo <i>et al.</i>, [37]</b>	<b>Kim <i>et al.</i>, [32]</b>	<b>Liu <i>et al.</i>, [33]</b>	<b>Pfisterer <i>et al.</i>, [34]</b>	<b>Sheng <i>et al.</i>, [36]</b>	<b>Torper <i>et al.</i>, [35]</b>
<b><i>Ascl1</i></b>	X	X	X	X	X	X
<b><i>Brn2</i></b>				X	X	X
<b><i>En1</i></b>		X				
<b><i>Foxa2</i></b>		X		X		
<b><i>Lmx1a</i></b>	X	X		X		
<b><i>Lmx1b</i></b>					X	X
<b><i>Myt1l</i></b>				X		X
<b><i>Ngn2</i></b>			X			
<b><i>Nurr1</i></b>	X	X	X		X	
<b><i>Otx2</i></b>					X	X
<b><i>Pitx3</i></b>		X	X			
<b><i>Sox2</i></b>			X			
<b>Cell type used</b>	MEFs, adult human fibroblasts	mouse tail tip fibroblasts	IMR90 human fibroblasts	human fetal lung fibroblast cell line	MEFs	human embryonic fibroblasts
<b>TH<sup>+</sup> cells/DAPI</b>	MEFs: 18% adult human fibroblasts: 3%	not determined	1 – 2% of initially plated cells	1 – 2.5%	0.05%	not determined
<b>PITX3<sup>+</sup> cells</b>	not determined	yes	not determined	not determined	yes	not determined

While TH<sup>+</sup> DA neurons are found in several areas of the mammalian brain only midbrain (TH<sup>+</sup>/PITX3<sup>+</sup>) DA neurons are degenerating in PD [6-8]. It is therefore of interest to generate 'true' mdDA (TH<sup>+</sup>/PITX3<sup>+</sup>) neurons by direct reprogramming in order to replace the DA neuron subpopulation lost during PD. Of the different transcription factor combinations shown in Table 1 however, only Kim *et al.*, and Sheng *et al.*, report the generation of TH<sup>+</sup>/PITX3<sup>+</sup> cells using five to six different transcription factors [32, 36]. This suggests that DA neurons generated by the remaining protocols may not be of midbrain identity. It is therefore of interest to both improve the reprogramming efficiency and to identify additional factors supporting the generation 'true' mdDA (PITX3<sup>+</sup>) neurons.

### 3.1.2.2 Roles of *Ascl1*, *Lmx1a*, *Nurr1* in mdDA development and direct conversion of fibroblasts to DA neurons

While the combinations of transcription factors used for direct conversion of fibroblasts to DA neurons shown in Table 1 differ considerably, one factor is always included: Achaete-scute family bHLH transcription factor 1 (*Ascl1*, also known as *Mash1*). *Ascl1* is a proneural gene of the basic helix-loop-helix family of transcription factors involved in the development of gamma-aminobutyric acid secreting neurons (GABAergic neurons) in the brain suppressing the alternative glia fate [40, 41]. *Ascl1* is also expressed in mdDA progenitor cells during embryonic development and seems to be involved in activating mdDA neuronal maturation [42, 43]. Deletion of *Ascl1* in mice leads to severe defects in neurogenesis and death at birth [44]. *Ascl1* is a central factor for neuronal reprogramming purposes as it can bind closed chromatin which makes *Ascl1* a so-called pioneer transcription factor [45]. Such a pioneer transcription factor is able to bind nucleosomal DNA by its own while regular transcription factors require cooperation with other factors [46]. This property is critical to overcome the epigenetic barriers e.g. of a fibroblast and convert it into a neuron. Exogenous *Ascl1* expression in fibroblasts [45, 47] or astrocytes [48, 49] is sufficient to directly convert these cells to neurons. Interestingly, while astrocytes are converted into inhibitory GABAergic neurons resembling the *in vivo* role of *Ascl1* [48, 49], fibroblasts become excitatory glutamatergic neurons upon overexpression of *Ascl1* [47]. These data suggest that *Ascl1* is sufficient for the induction of a neuronal fate but further factors are required to determine the neuronal subtype.

In order to generate DA neurons, up to five additional subtype specific transcription factors are commonly co-expressed [32-37]. Caiazzo *et al.*, reported a minimal set of three transcription factors comprising *Ascl1*, LIM homeobox transcription factor 1 alpha (*Lmx1a*) and Nuclear receptor subfamily 4, group A, member 2 (*Nr4a2* or *Nurr1*) [37]. Overexpression of *Ascl1*, *Lmx1a* and *Nurr1* is not sufficient to directly convert fibroblasts into PITX3<sup>+</sup> DA neurons (unpublished data, F. Meier, Helmholtz Zentrum München). This minimal

combination however, was used as a starting point for further screenings in order to improve reprogramming efficiencies and to identify new factors enabling TH<sup>+</sup>/PITX3<sup>+</sup> mdDA neuron generation with less than the published five to six different TFs.

*Lmx1a* is a member of the LIM homeodomain transcription factors and is involved in the development of mdDA neurons mainly by regulating Msh homeobox 1 (*Msx1*) [50]. *Msx1* in turn induces neurogenesis by activation of the proneural gene Neurogenin 2 and inhibition of alternative cell fates via suppression of NK6 homeobox 1 [51]. Furthermore, *Lmx1a* was found to directly induce the expression of the mdDA neuron marker *Pitx3 in vitro* [52]. *Lmx1a* is expressed from the dopaminergic progenitor cell stage (embryonic day nine (E9) in mice) onwards and stays active in mature mdDA neurons [50]. A loss of *Lmx1a* leads to a significant reduction but not complete loss of DA neurons in mouse models [53].

The orphan nuclear receptor/transcription factor *Nurr1* is expressed in postmitotic mdDA precursors of mouse embryos from E10.5 onwards but is also detected in non-dopaminergic areas such as hippocampus and cerebral cortex [54-56]. *Nurr1* is implicated in mdDA neuron specification, migration and target innervation [57]. Target genes include the survival factor *Bdnf* as well as DA neuron markers *Th*, *Dat* and the mdDA marker gene *Pitx3* [58-62]. While *Nurr1*-depleted mouse embryos develop PITX3<sup>+</sup> DA precursors, maturation of these cells is arrested and they undergo apoptosis at a neonatal stage [61]. *Nurr1*<sup>-/-</sup> mice completely lack *Th* expression and die shortly after birth [63]. This underlines *Nurr1* as an important component of post-mitotic DA neuron specification and maturation.

## 3.2 The CRISPR/Cas9 system and its implications for genome editing and transcriptional regulation

### 3.2.1 CRISPR/Cas9 - an adaptive immune system in bacteria and archaea

Clustered regularly interspaced short palindromic repeats (CRISPR) and CRISPR associated proteins (Cas) serve as adaptive immune system in approximately 40% of bacteria and 90% of archaea [64]. The CRISPR system acts via sequence specific recognition and subsequent cutting of foreign DNA by a protein-RNA complex [65]. Three types of CRISPR systems (I-III) have been described so far [64]. The type II CRISPR system is well characterized [66, 67] and was therefore used in the underlying project. Figure 2A shows the genomic organization of the type II CRISPR system comprising a Cas locus encoding the nuclease Cas9, a *CRISPR* array consisting of repeat and spacer sequences and a transactivating CRISPR RNA (*tracrRNA*) [68]. Upon infection of bacteria or archaea e.g. by bacteriophages short fragments of invader-derived DNA can be integrated as spacer sequences into the *CRISPR*-arrays of the host chromosome [65].

These new spacers subsequently serve as sequence-specific resistance to foreign DNA. Transcription of the *CRISPR* array results in a precursor transcript termed *pre-CRISPR-RNA* (*pre-crRNA*) consisting of repeats and newly integrated spacer sequences (see Figure 2A). The repeat region of *pre-crRNAs* is bound by co-expressed *tracrRNA* molecules via a 25-nucleotide sequence leading to the recruitment of RNase III and cleavage within the double-stranded repeat region (orange arrowheads in Figure 2A) [69]. Afterwards, the *crRNA* spacer is trimmed from the 5' end by a yet unknown nuclease to a length of 20 nt [68] (yellow arrowhead in Figure 2A) resulting in a mature *crRNA-tracrRNA* hybrid.

This *crRNA-tracrRNA* hybrid is bound by a Cas9 nuclease and the resulting protein-RNA complex scans invader DNA for protospacer sequences (target sequences) complementary to the 20 nucleotides of the *crRNA* as shown in Figure 2B [66, 68, 70]. Upon binding Cas9 induces a double strand break in the foreign DNA (white arrowheads in Figure 2B). It is of importance for the CRISPR immune system to discriminate between 'self' (integrated spacer sequences) and 'non-self' (foreign DNA molecules) in order to only bind and cut invading DNA molecules. In this context protospacer adjacent motifs (*PAMs*) play an important role [71]. *PAMs* consist of three nucleotides immediately downstream of the 20 nt target sequence in the foreign DNA (see Figure 2B) marking a difference to the sequence of *CRISPR* repeats in the host genome [71, 72]. Cas9 proteins from different species require distinct *PAM* sequences. The type II-A Cas9 of *Streptococcus pyogenes* used in this project detects a 5'-NGG-3' *PAM* sequence [73].

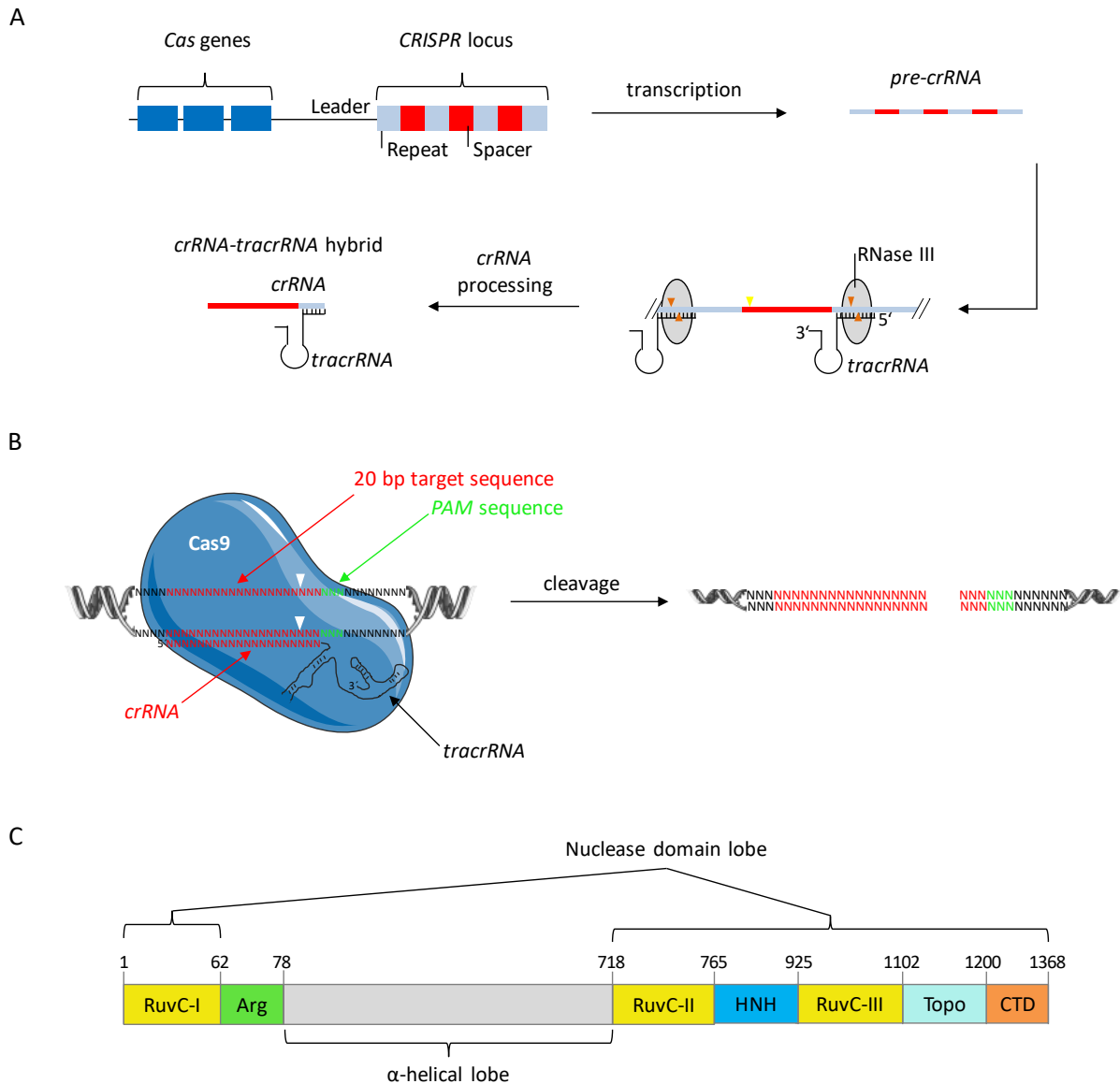


**Figure 2: Illustration of *crRNA* maturation, Cas9 functionality and Cas9 protein domains**

**(A)** Schematic illustration of *crRNA* maturation of type II CRISPR systems in bacteria and archaea serving as adaptive immune system. *Cas* genes are encoded in the *Cas* locus, the *CRISPR* locus contains repeat and spacer sequences. Short sequences of foreign DNA can be integrated as spacer sequences and serve as template for the recognition of invading DNA. A *pre-crRNA* is generated upon transcription of the *CRISPR* locus containing the newly integrated spacer sequences. *tracrRNAs* bind to repeat sequences of the *pre-crRNA* which is recognized and cleaved by RNase III (orange arrowheads). A yet unknown nuclease trims the spacer region to a length of 20 nucleotides as indicated by the yellow arrowhead. This results in a mature *crRNA-tracrRNA* hybrid. **(B)** Illustration of DNA cleavage by Cas9. *crRNA-tracrRNA* hybrids are bound by Cas9 nucleases and the protein-RNA complex recognizes and binds foreign DNA via the 20 nucleotides of the *crRNA* (red) leading to cleavage of the foreign DNA as indicated by white arrowheads. *PAM* sequences (green) are used to discriminate 'self' and 'non-self' DNA as they are only found in foreign DNA but not in the integrated spacer sequences of the *CRISPR* locus. **(C)** Illustration of *S. pyogenes* type II-A Cas9 protein domains. The nuclease activity is mediated by two domains: The discontinuous RuvC nuclease domain and the HNH nuclease domain. While the HNH nuclease domain cleaves the strand bound by the *crRNA*, RuvC cuts the non-complementary strand. The two nuclease domain lobes are separated by an  $\alpha$ -helical lobe. Further domains are Arg (arginine rich domain, involved in DNA binding), Topo (Topo homology domain) and CTD (C-terminal domain). **Abbreviations:** bp: base pairs, Cas: CRISPR associated genes, CRISPR: clustered regularly interspaced short palindromic repeats, *crRNA*: CRISPR-RNA, *PAM*: protospacer adjacent motif, *tracrRNA*: transactivating *crRNA*.

*S. pyogenes* Cas9 comprises two nuclease domains and an  $\alpha$ -helical domain illustrated in Figure 2C. The Cas9 protein is folded in a bilobed architecture with both nuclease domains in the first lobe and the  $\alpha$ -helical domain in the second lobe [67]. Loading of Cas9 by a crRNA-tracrRNA hybrid induces a structural rearrangement with a central channel that binds to target DNA mediated by the arginine rich region (Arg) [67, 74]. The HNH nuclease domain cleaves the DNA strand complementary to the crRNA sequence (target strand) and the RuvC nuclease domain cleaves the non-complementary strand [66, 67]. This generates a blunt double-strand break three nucleotides upstream of the *PAM* sequence thus destructing foreign DNA sequences [66, 75, 76].

### 3.2.2 Repurposing CRISPR/Cas9 technology for genome editing

The adaption of the CRISPR/Cas9 technology for eukaryotic genome editing has revolutionized the field of molecular biology allowing simple and quick generation of genetically modified cells and animals or genome-scale screenings [77-82]. By exchange of the 20 targeting nucleotides of the *crRNA* basically any sequence preceding a 5'-NGG-3' *PAM* can be targeted and cleaved [83, 84]. Furthermore, by using more than one gRNA multiple targets can be edited simultaneously [79, 83]. The simple and fast adaption of the CRISPR system to new target sequences is a big advantage over previously used genome editing tools such as zinc-finger nucleases and transcription activator-effector nucleases (TALENs) [85-87]. Zinc-finger nucleases and TALENs can also be modified to bind and cut specific target sequences. However, the DNA sequence specificity of these two systems is based on the protein sequence requiring individually designed proteins for each target which is cost and time intensive [88]. In contrast, targeting a new locus with the CRISPR/Cas9 system simply requires adjusting the 20 nt protospacer sequence.

For a faster and more efficient assembly of Cas9-RNA complexes so-called guide RNAs (gRNAs) were developed which are expressed as a synthetic fusion of crRNA and tracrRNA [66]. gRNAs therefore do not require the maturation process described in Figure 2A. These gRNAs are usually expressed from a RNA polymerase III promoter such as *U6* or *H1* and expression is terminated by a poly-T sequence [89-91].

The use of the CRISPR/Cas9 system for genome editing is based on the two major cell intrinsic DNA damage repair mechanisms depicted in Figure 3: Error-prone non-homologous end joining (NHEJ) and homology directed repair (HDR). Both pathways can be used to achieve distinctive goals. Re-ligation of the DNA by NHEJ leaves scars due to insertion/deletion mutations (yellow sequence in Figure 3) which can result in frame-shift mutations or premature stop-codons and is therefore often used for the generation of gene knockouts [92].

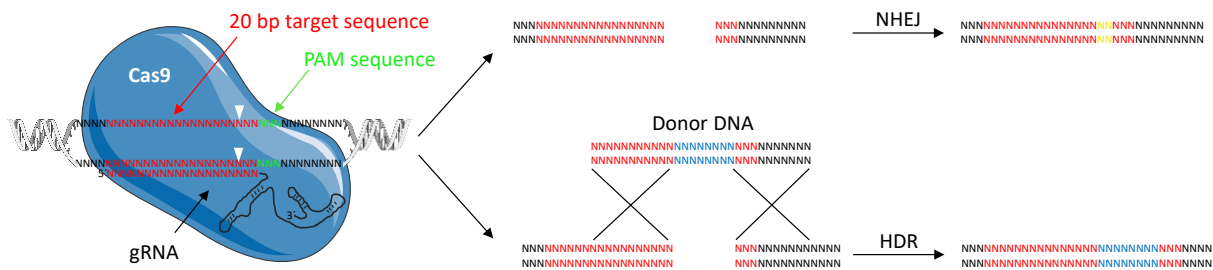


**Figure 3: Genome editing by means of CRISPR/Cas9 technology**

Illustration of genome editing utilizing the CRISPR/Cas9 system. Upon binding of the gRNA-Cas9 complex to a target sequence (red) e.g. in the eukaryotic genome Cas9 induces a double strand break three nucleotides upstream of the PAM sequence (green) as indicated by white arrowheads. The cell uses two major DNA repair mechanisms: Non-homologous end joining (NHEJ) and homology directed repair (HDR). NHEJ leads to insertion/deletion mutations (yellow) resulting in frame-shift mutations and can be used to generate gene knockouts. HDR can be used to insert a gene of interest (blue) in a scar-less fashion by offering a repair template with homology arms. Abbreviations: bp: base pairs, HDR: homology directed repair, NHEJ: non-homologous end joining, PAM: protospacer adjacent motif.

In order to insert or modify a gene of interest in a sequence specific and scar-less fashion the HDR mechanism can be utilized (blue sequence in Figure 3). For this purpose, a repair template with homology arms binding upstream and downstream of the cutting site is offered and integrated via homologous recombination [93].

### 3.2.3 Transcriptional modification by CRISPR/Cas9

The generation of a Cas9 version with depleted nuclease activity termed dead Cas9 (dCas9) opened a new field of applications for the CRISPR/Cas9 technology. For this purpose the RuvC (D10A) and HNH (H840A) nuclease domains of *S. pyogenes* Cas9 were mutated [66]. dCas9 can then be used as a shuttle to deliver epigenetic or transcriptional regulators to a sequence specific location e.g. to the promoter of a target gene without inducing a double strand break. This technology has been used to activate and suppress gene expression, to alter epigenetic marks and to change cell fate [89, 90, 94, 95]. For the induction of endogenous genes dCas9 is usually expressed as a fusion protein with different transactivation domains of transcriptional activators. Various systems have been published with varying gene induction potential depending on the transcriptional activators used. Figure 4 gives an overview on transcriptional activator systems analyzed in this thesis. The first published activation system comprises ten repeats of the transcriptional activation domain of *Herpes simplex virus* protein vmw65 (VP16) (residues 437 - 448) and is shown in Figure 4A [89]. These ten repeats of VP16 (termed VP160) are fused to the C-terminus of dCas9 and can directly interact e.g. with the General transcription factor IIB (TFIIB) [96]. TFIIB in turn binds the TATA-binding protein and is involved in the recruitment of RNA polymerase II thus contributing to the formation of the transcription initiation complex [97].

A slightly modified version termed Sso7d-dCas9-VP160 (Figure 4B) was developed at the institute by J. Truong. Here, the *S. solfataricus* DNA binding protein 7d (Sso7d) is fused to the N-terminus of dCas9 in order to putatively increase the time of dCas9 associated with the target promoter due to stronger binding and therefore potentially support transcriptional induction.

The SpyTag system shown in Figure 4C was also developed at the institute by J. Truong and allows recruitment of multiple transcriptional activators (VP160) to a single dCas9 protein. This system is based on a split version (SpyTag and SpyCatcher) of the second immunoglobulin-like collagen adhesion domain (CnaB2) of the *Streptococcus pyogenes* fibronectin-binding protein (FbaB) [98, 99]. Interaction of SpyTag and SpyCatcher leads to the formation of an isopeptide bond and thus covalent binding [98, 99]. For gene induction, multiple SpyTag repeats (four, eight or twelve) were fused to the C-terminus of the inactive nuclease (Figure 4C). These SpyTags can then be bound by SpyCatchers which in turn were fused to VP160 transcriptional activators. This allows recruitment of up to twelve copies of VP160 to a single dCas9 protein (Figure 4C). The underlying idea was that a significant increase in transcriptional activators might improve gene induction of target genes. Tanenbaum *et al.*, [100] developed a similar system termed SunTag shown in Figure 4D. Here, an array of 24 *S. cerevisiae* General control protein (GCN4) peptides termed SunTags was fused to dCas9. These tags can be targeted by single-chain variable fragment (scFv) antibodies which are in turn fused to four repeats of VP16 (VP64). This system therefore allows recruitment of up to 24 copies of VP64 to a single dCas9 molecule.

While the above-mentioned systems use varying amounts of VP16 repeats, the VPR system depicted in Figure 4E relies on a combination of three different transactivation domains [90]. Besides the commonly used VP16 repeats the VPR system also comprises transactivation domains of the P65 subunit of human NF- $\kappa$ B (residues 287 - 546). Furthermore, the transactivation domain of the Regulator of transcription activation (RTA, BRLF1: residues 416 – 605) of the *Human herpesvirus 8* is added resulting in a dCas9-VP64-P65-RTA fusion protein termed VPR system in the following. These two additional domains increase the variety of potential interaction partners which can be recruited to the dCas9 fusion protein at the promoter of a target gene. This includes e.g. the TATA-box-binding protein [101] and E1a binding protein p300 [102] by P65 or the cAMP-response-element-binding protein (CREB)-binding protein by RTA [103].

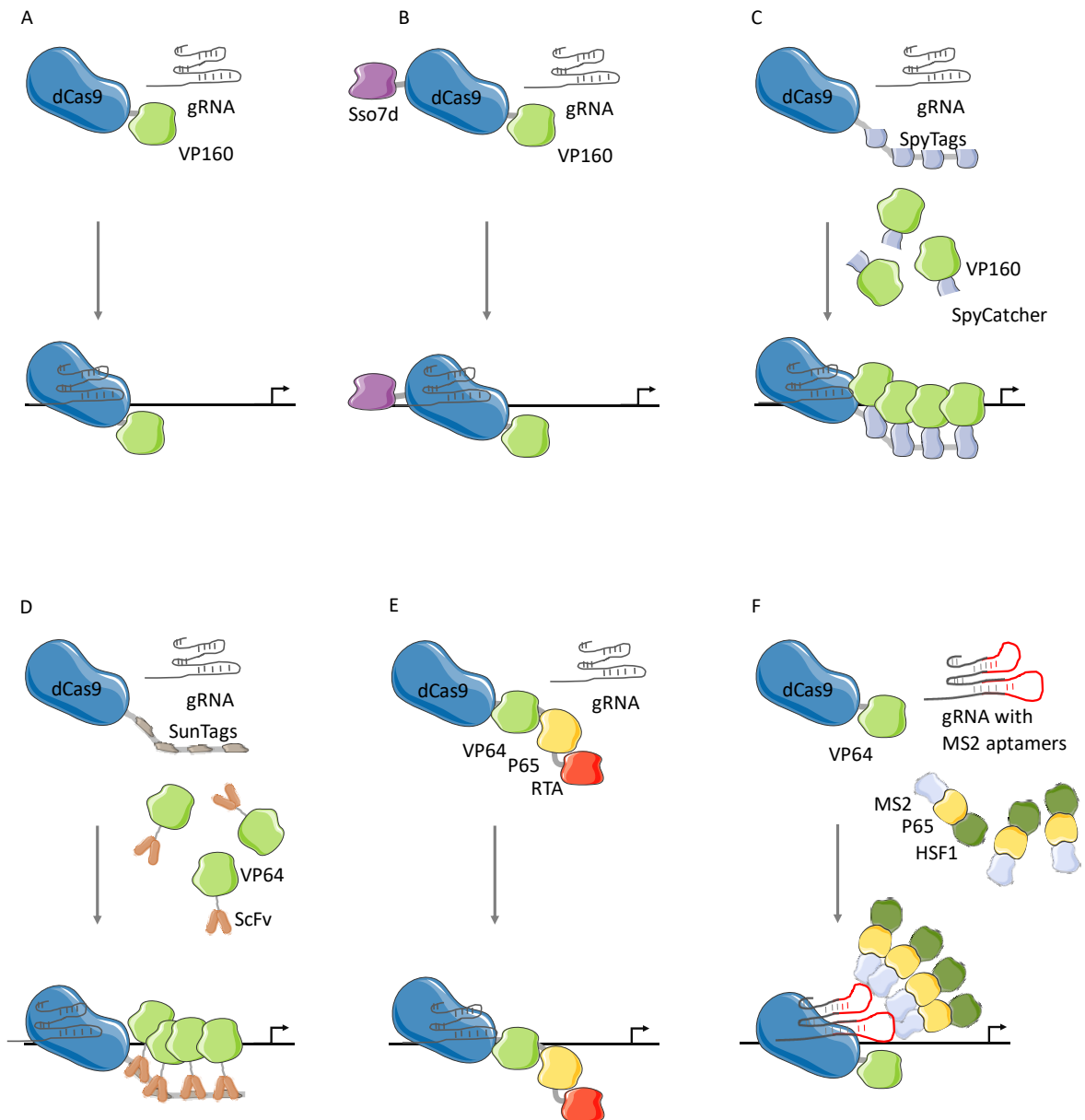


**Figure 4: Schematic illustration of CRISPR/Cas9 systems used for gene induction in this study**

Schematic illustrations of nuclease deficient *Streptococcus pyogenes* dCas9 (D10A, H840A version) fused to different transcriptional activator systems. Together with a sequence-specific gRNA dCas9 fusions are targeted to the promoter region of a gene of interest and thus induce the expression of the target gene. **(A)** dCas9-VP160 consisting of a C-terminal fusion of dCas9 with ten repeats of VP16, termed VP160. **(B)** Sso7d-dCas9-VP160 comprising dCas9 N-terminally fused to double-stranded DNA binding protein Sso7d and C-terminally to VP160. **(C)** SpyTag system consisting of dCas9 fused to multiple repeats of SpyTags (13 amino acids of the CnaB2 domain of the *Streptococcus pyogenes* fibronectin-binding protein FbaB) and SpyCatchers (complementary 116 amino acids of the CnaB2 domain). SpyCatchers are expressed as fusion proteins with VP160 thus allowing recruitment of multiple copies of VP160 to a single dCas9. **(D)** SunTag system as described by Tanenbaum *et al.*, [100]. dCas9 is fused to repeats of SunTags (GCN4 peptides) which can be bound by ScFv antibody fragments that are in turn fused to VP64 (4x repeats of VP16). **(E)** VPR system as described by Chavez *et al.*, [90] where dCas9 is fused to VP64-P65-RTA. **(F)** SAM system as described by Konermann *et al.*, [91]. A modified gRNA with two additional loops serving as MS2 aptamers is used. These aptamers are bound by MS2-P65-HSF1 fusion proteins which serve as additional transcriptional activators. This system is used in combination with a dCas9 fused to C-terminal VP64. **Abbreviations:** GCN4: general control protein 4, HSF1: heat shock transcription factor 1, MS2: bacteriophage MS2 coat protein, P65: P65 subunit of human NF- $\kappa$ B, RTA: Regulator of transcription activation, ScFv: single-chain variable fragment antibody, VP64/VP160: four/ten repeats of *Herpes simplex virus* protein VP16.

The synergistic activation mediator (SAM) system shown in Figure 4F uses an alternative strategy where transcriptional activators are recruited to hairpin aptamers added to tetraloop and stem loop 2 of the gRNA [91]. These aptamers are selectively bound by dimerized MS2 bacteriophage coat proteins indicated as MS2 in Figure 4F [104]. MS2 in turn is fused to murine P65 (residues 369 – 549) and the activation domain of the human Heat shock transcription factor 1 (HSF1) (residues 406 – 529). The HSF1 activation domain additionally allows the recruitment of e.g. chromatin remodeling complexes of the Switching defective/Sucrose non-fermenting (SWI/SNF) family [105]. The assembled complex comprising MS2-P65-HSF1 fusion proteins with a gRNA and dCas9-VP64 (Figure 4F) is termed SAM complex in the following.

In order to induce the expression of a target gene gRNAs are designed to target the promoter region of this gene. While some groups report best effects within the 250 nt upstream of the transcription start site [89, 91, 106] others have also used gRNAs binding up to 1 kb upstream of the transcription start site [90, 107]. The number of gRNAs required for a sufficient activation of the target gene seems to be gene and sequence dependent. Some reports show sufficient gene induction by a single gRNA [108, 109], whereas other reports suggest synergistic effects when a single gene is targeted by multiple gRNAs [89, 106, 110].

Early publications concentrated on improving the transcriptional levels of target genes but it soon became clear that the CRISPR/Cas9 technology could also be used to manipulate cell fates [90, 108]. The underlying idea is that targeting of the endogenous promoter rapidly remodels the epigenetic landscape and thus more closely resembles natural mechanisms which may be an advantage compared to forced overexpression of transcription factors [107]. Indeed, Black *et al.*, reported an increase in histone 3 modifications (H3K4me3 and H3K27ac) at endogenous *Ascl1* and POU domain class 3 transcription factor 2 (*Brn2*) loci induced by VP64-dCas9-VP64 three days post-transfection [107]. Tri-methylation of lysine 4 (K4me3) and acetylation of lysine 27 (K27ac) of histone 3 are both well-described markers of transcriptional activity [111, 112]. Interestingly, these modifications of endogenous promoters were not observed at this timepoint when *Ascl1* and *Brn2* were overexpressed from transfected vectors [107]. Furthermore, in contrast to neuronal transcription factors whose binding sites can be inaccessible in MEFs or astrocytes Cas9 binding was reported to be independent of the chromatin state [113]. This would give Cas9-based approaches a similar potential like pioneer factors such as *Ascl1* which was described earlier.

Mouse embryonic stem cells have been differentiated into extraembryonic lineages by dCas9-VP64 induced expression of endogenous Caudal type homeobox 2 (*Cdx2*) and GATA binding protein 6 (*Gata6*) [106]. Others however, have reported that a simple dCas9-VP64

system was not sufficient to influence cell fate [90, 108]. By using the more sophisticated VPR system and a pool of 30 gRNAs, human induced pluripotent stem cells were differentiated to neurons by inducing either Neurogenin 2 (*NGN2*) or Neurogenic differentiation 1 (*NEUROD1*) expression. Direct reprogramming of one somatic cell type to another one has only been described in two cases so far [107, 108]. Both publications used a VP64-dCas9-VP64 system where the VP16 repeats were fused to both the N- and C-terminus of dCas9. Utilizing this system MEFs were converted to skeletal myocytes (induction of Myogenic differentiation 1 (*Myod1*)) [108] and just recently MEFs were also reprogrammed to neurons [107] (induction of *Ascl1*, *Brn2* and Myelin transcription factor 1-like (*Myt1l*)). However, there is still a need to improve the CRISPR/Cas9-based direct conversion of cells, to identify new activator complexes and to apply these systems to additional cell types such as astrocytes.

## 4 Aim of the thesis

Parkinson's disease is among the prime candidates for direct reprogramming and cell replacement therapies due to the loss of a specific and spatially restricted cell type – the midbrain dopaminergic neurons. The aim of this thesis was to develop new strategies in order to improve the reprogramming efficiencies of somatic cells to dopaminergic neurons *in vitro* as this is a limiting factor of current protocols. Furthermore, new factors should be identified enabling the generation of PITX3<sup>+</sup> midbrain dopaminergic neurons. Only these PITX3<sup>+</sup> DA neurons resemble the subtype lost during Parkinson's disease which is not achieved by most of the currently published transcription factor combinations used for direct reprogramming. The CRISPR/Cas9 system is a relatively new tool to modulate gene expression and could be a promising alternative to classical reprogramming by activating the expression of endogenous genes. In this thesis, a system should be established to induce the expression of endogenous *Ascl1* utilizing transcriptional activators fused to Cas9. Furthermore, the reprogramming potential of this system should be investigated as proof-of-principle experiments to directly convert astrocytes to neurons which will then serve as a basis for cell replacement therapies.

## RESULTS

## 5 Results

Due to the specific cell loss of midbrain dopaminergic neurons Parkinson's disease is one of the prime targets for cell replacement therapy using reprogrammed cells and direct reprogramming *in vivo*. However, the reprogramming efficiency of current protocols is low and the generated DA neurons mostly do not resemble the population lost in PD as assessed by the missing expression of the mdDA marker gene *Pitx3*. It is therefore of interest to improve the reprogramming efficiency and to identify new factors enabling the generation of 'true' mdDA (PITX3<sup>+</sup>) mdDA neurons. The first part of the results concentrates on addressing these points utilizing different vector systems for the expression of exogenous transcription factors. In the second part the potential of the CRISPR/Cas9 technology regarding the induction of endogenous genes and the direct conversion of somatic cells is analyzed.

### 5.1 Exogenous gene expression strategies for direct conversion of MEFs to DA neurons

#### 5.1.1 Limitations of direct reprogramming utilizing multiple viruses for gene delivery

Caiazza *et al.*, 2011 [37], published a minimal set of transcription factors (*Ascl1*, *Lmx1a* and *Nurr1*) for the direct conversion of mouse embryonic fibroblasts (MEFs) and adult human fibroblasts to DA neurons which were delivered by individual lentiviruses. This strategy however has the disadvantage, that a single cell needs co-transduction of all three lentiviruses which may pose a limiting effect on the reprogramming efficiency. To test this hypothesis MEFs were transduced with individual lentiviruses encoding *Ascl1*, *Lmx1a* and *Nurr1* as shown in Figure 5A. Quantification of transduced cells revealed  $28.5 \pm 0.5\%$  of cells to be ASCL1<sup>+</sup> and  $19.8 \pm 0.5\%$  were NURR1<sup>+</sup> (Figure 5B). However, only  $10.1 \pm 0.9\%$  of cells expressed both genes as shown in Figure 5C. To identify successful reprogramming cells were co-stained for the DA neuron marker Tyrosine hydroxylase (TH) 14 days after transduction. When looking at these TH<sup>+</sup> cells it became clear that reprogrammed cells were always TH<sup>+</sup>/ASCL1<sup>+</sup> (Figure 5D) or TH<sup>+</sup>/NURR1<sup>+</sup> (Figure 5E). However, there was an excess of ASCL1<sup>+</sup> and NURR1<sup>+</sup> cells which did not express TH. This suggested that neither factor alone was sufficient to directly reprogram MEFs to TH<sup>+</sup> neurons thus excluding cells that were not co-transduced by at least these two lentiviruses.

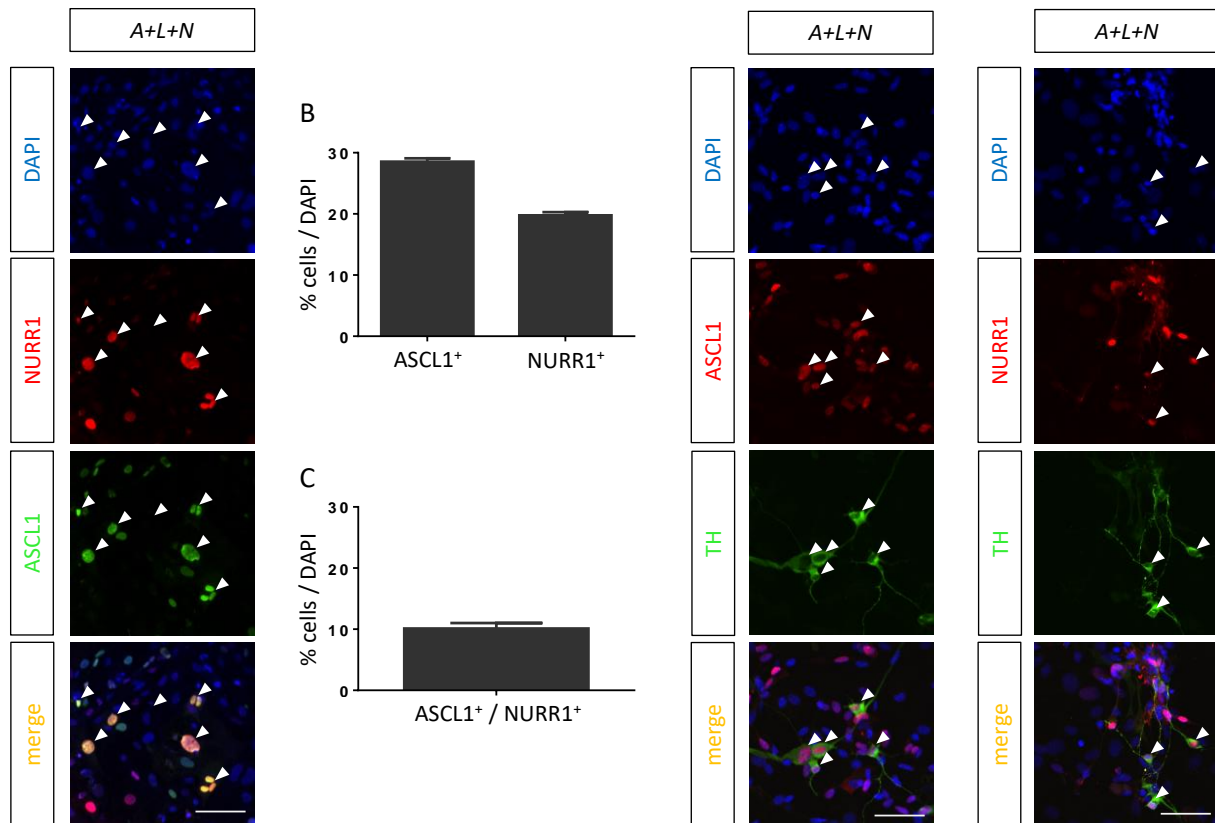


**Figure 5: The need for co-transduction by multiple lentiviruses limits the reprogramming efficiency** Immunocytochemistry at 48 h (A) or 14 days (D and E) after transduction of MEFs with *Ascl1*, *Lmx1a* and *Nurr1* encoding lentiviruses at a multiplicity of infection (MOI) of three. **(A)** Co-staining for ASCL1 and NURR1 revealed that only a fraction of cells expressed both transcription factors. **(B)** Quantification of all ASCL1<sup>+</sup> and NURR1<sup>+</sup> cells revealed a transduction efficiency of  $28.5 \pm 0.5\%$  for *Ascl1* and  $19.8 \pm 0.5\%$  for *Nurr1* encoding lentiviruses. **(C)** Quantification of double positive cells.  $10.1 \pm 0.9\%$  of cells expressed both factors. **(D)** Co-staining for ASCL1 and TH. All successfully reprogrammed TH<sup>+</sup> cells analyzed were also ASCL1<sup>+</sup> suggesting the requirement of this factor for reprogramming. Many ASCL1<sup>+</sup> cells however, were TH<sup>-</sup> indicating that *Ascl1* alone was not sufficient for the generation of dopaminergic neurons. **(E)** Co-staining for NURR1 and TH. All TH<sup>+</sup> cells observed were also NURR1<sup>+</sup> showing the importance of this factor for successful reprogramming. Similar to *Ascl1* however, *Nurr1* alone also was not sufficient for a successful conversion to TH<sup>+</sup> neurons as assessed by an excess of NURR1<sup>+</sup>/TH<sup>-</sup> cells. **Abbreviations:** A+L+N: *Ascl1*, *Lmx1a*, *Nurr1* expressed from individual lentiviruses, TH: Tyrosine hydroxylase. Scale bars: 50  $\mu\text{m}$ . Data was derived from one experiment. Error bars represent mean  $\pm$  SEM.

Caiazzo *et al.*, have shown that efficient reprogramming requires co-expression of a third factor - *Lmx1a* [37]. Due to strong and unspecific background signal of the  $\alpha$ -LMX1A antibody an immunocytochemical analysis for LMX1A<sup>+</sup> cells could not be performed. Nevertheless, the proportion of cells co-transduced by all three lentiviruses would be expected to be even lower than what was found for NURR1 and ASCL1 in Figure 5A. Furthermore, since *Tet-O* constructs were used, a fourth virus carrying the activator rTTA2 was required to co-transduce cells in order to allow expression of the three factors from *Tet-O* promoters [114]. The idea therefore was to use a tri-cistronic vector encoding all three factors.

### 5.1.2 Limitations of multi-cistronic constructs for direct reprogramming

In order to omit the limitations of single viruses described above a tri-cistronic vector was generated at the institute by F. Meier carrying *Ascl1*, *Lmx1a* and *Nurr1* termed *ALN* where individual transcription factors were separated by 2A peptides (see Figure 6A). 2A peptides consist of 18 – 22 amino acids and are cleaved at the c-terminal glycyl-prolyl peptide bond by ribosome skipping during protein synthesis [115, 116]. This leads to separation of the 2A peptide and the immediate downstream peptide which can be utilized for the expression of several genes from a single expression cassette. In comparison to internal ribosomal entry sites (IRES), 2A sequences have two advantages: 2A peptides are short (18 – 22 amino acids vs  $\geq 500$  nucleotides for IRES) and multiple proteins are produced at stoichiometric ratios [117]. In order to avoid repeated sequences which can be problematic for lentiviral packaging 2A sequences from *Porcine teschovirus-1* (P2A) and *Thoseaasigna virus* (T2A) were chosen. Using lentiviruses carrying the newly generated *Ascl1-T2A-Lmx1a-P2A-Nurr1* (*ALN*) construct depicted in Figure 6A MEFs were successfully reprogrammed to DA neurons at the institute (dissertation F. Meier).

However, reprogramming efficiencies did not reach the numbers originally published for *Ascl1*, *Lmx1a* and *Nurr1* ( $< 1\%$  TH<sup>+</sup> cells in our hands vs approximately 18% TH<sup>+</sup> by Caiazzo et al., [37]). Therefore, reprogramming efficiencies of single viruses (*A+L+N*) and the tri-cistronic (*ALN*) construct (see Figure 6A) were compared 14 days after transduction of MEFs (Figure 6B). In order to identify newly generated DA neurons cells were stained for the expression of the mature neuronal marker Microtubule-associated protein 2 (MAP2) and the DA neuron marker TH. Surprisingly, the percentages of MAP2 positive neurons (Figure 6C, *A+L+N*:  $4.1 \pm 0.8\%$ , *ALN*:  $1.0 \pm 0.3\%$  MAP2<sup>+</sup> cells / DAPI) and TH positive DA neurons (Figure 6D, *A+L+N*:  $2.2 \pm 0.6\%$ , *ALN*:  $0.3 \pm 0.1\%$  TH<sup>+</sup> cells / DAPI) were significantly decreased when using the *ALN* vector compared to single viruses.

In order to investigate a possible loss of cells after *ALN* transduction the number of cells per mm<sup>2</sup> was determined using Stereo Investigator software (MBF Bioscience) that randomly selected fields of 200 x 200  $\mu\text{m}$  for counting. Indeed, wells transduced by the tri-cistronic *ALN* construct seemed to contain a slightly decreased number of DAPI<sup>+</sup> cells per mm<sup>2</sup> when compared to the control or wells transduced with single viruses (Figure 6E, *A+L+N*:  $932 \pm 86$  vs *ALN*:  $709 \pm 54$  cells per mm<sup>2</sup>). Taken together, these results suggested possible adverse effects of the tri-cistronic *ALN* construct.

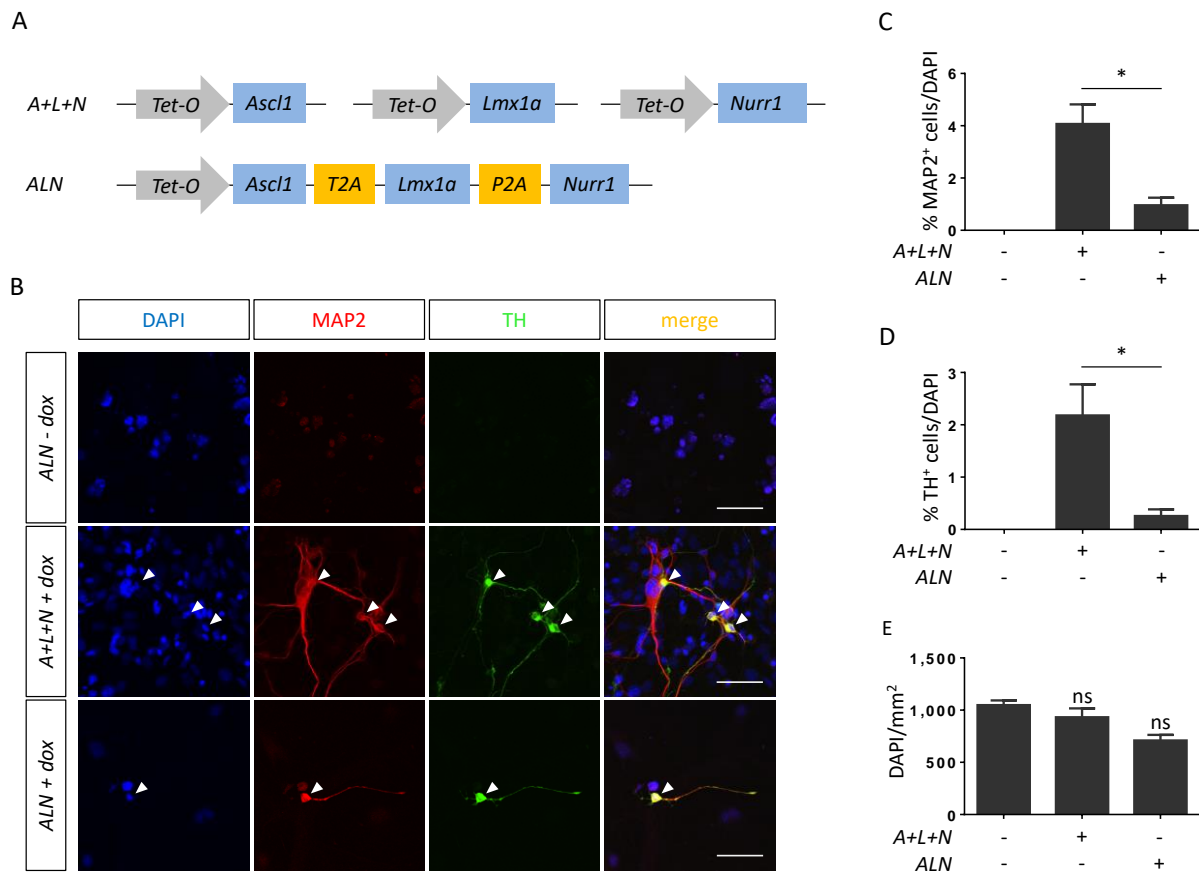


**Figure 6: Utilizing the tri-cistronic ALN vector decreases the conversion efficiency to DA neurons**

**(A)** Schematic illustration of lentiviral vectors used for reprogramming. **(B)** Cells stained for neuronal marker MAP2 and dopaminergic marker TH 14 days after transduction. Both MAP2<sup>+</sup> and TH<sup>+</sup> cells were decreased when using the tri-cistronic vector. White arrowheads indicate MAP2<sup>+</sup>/TH<sup>+</sup> cells. **(C)** Quantification of MAP2<sup>+</sup> cells/DAPI. Using the ALN virus resulted in a significant decrease in MAP2<sup>+</sup> cells when compared to the single vectors. **(D)** Quantification of TH<sup>+</sup> cells/DAPI: The amount of TH<sup>+</sup> cells was significantly lower for ALN transduced wells when compared to single viruses. **(E)** Quantification of DAPI<sup>+</sup> cells per mm<sup>2</sup> did not reveal a significant effect but hinted at lower cell numbers when using the tri-cistronic ALN construct. **Abbreviations:** ALN: *Ascl1*, *Lmx1a*, *Nurr1* expressed from a single lentiviral vector, A+L+N: *Ascl1*, *Lmx1a*, *Nurr1* expressed from individual lentiviral vectors, dox: doxycycline used for induction of *Tet-O* promoters. TH: Tyrosine hydroxylase, MAP2: Microtubule-associated protein 2. Scale bars: 50  $\mu$ m. Data was derived from three independent experiments. Error bars represent mean  $\pm$  SEM, Mann Whitney test, ns: not significant, \* $P < 0.05$ . This data was published by Theodorou and Rauser *et al.*, 2015 [118].

### 5.1.3 Inefficient ribosome skipping at 2A sites results in fusion proteins

The reason for a reduced reprogramming efficiency of the tri-cistronic ALN construct could be the generation of fusion proteins due to inefficient ribosome skipping at 2A sites [119]. To investigate this, western blots were performed using the ALN construct from the above-mentioned reprogramming experiments (*Ascl1-T2A-Lmx1a-P2A-Nurr1*) and additionally a construct where *P2A* was replaced by *IRES* (*Ascl1-T2A-Lmx1a-IRES-Nurr1*) as well as a construct with additional *eGFP* (*Ascl1-T2A-Lmx1a-P2A-Nurr1-IRES-eGFP*) and the single *Ascl1* and *Nurr1* expressing viruses (see schematic illustrations in Figure 7A).

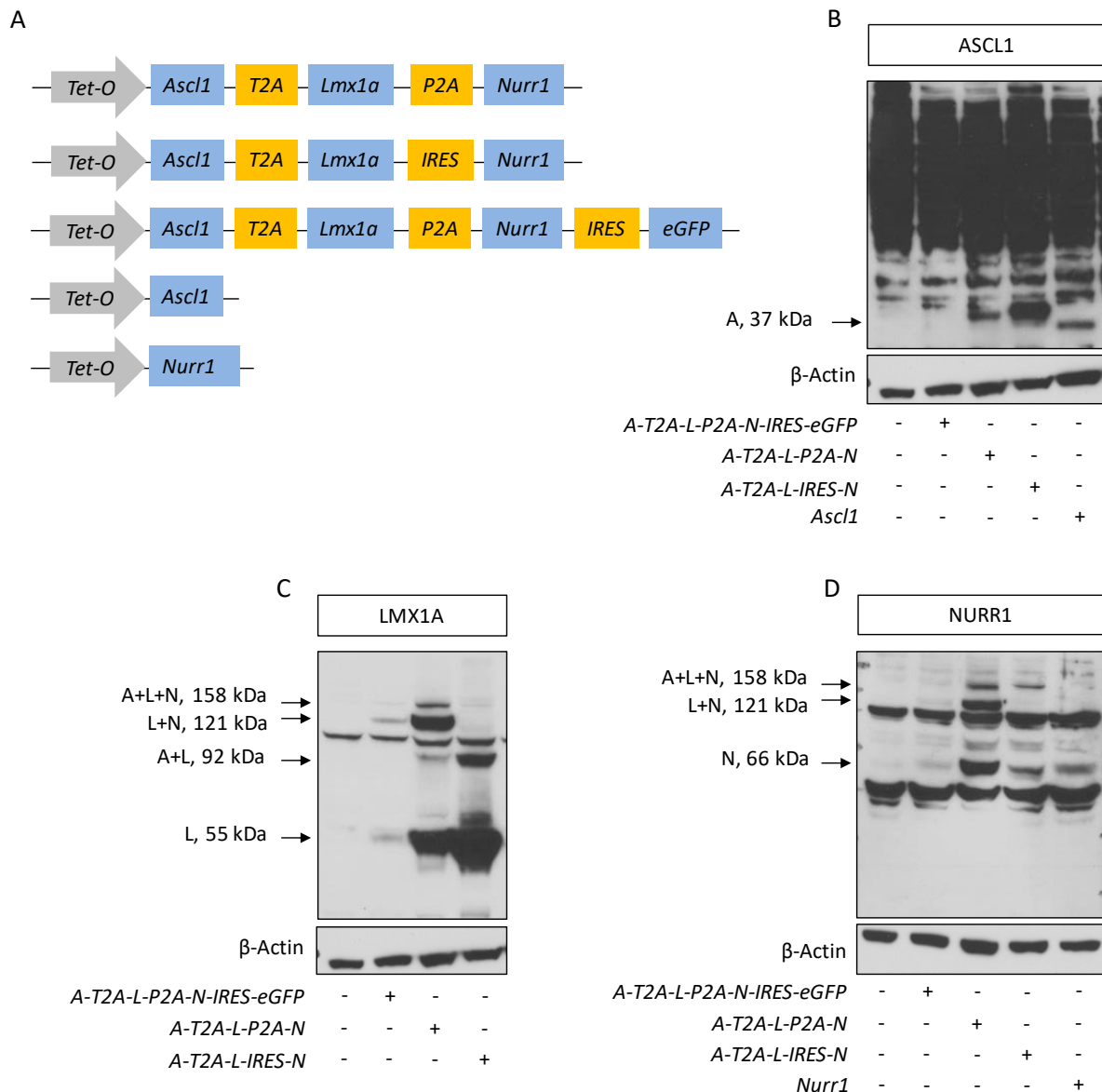


### Figure 7: Western blot analysis reveals inefficient ribosome skipping at 2A sequences resulting in the generation of fusion proteins

HEK293 cells were transduced with individual viruses and western blot analysis was performed after 48 h. **(A)** Schematic illustration of vectors used. **(B)** Western blot detecting ASCL1. The expected ASCL1 band at 37 kDa was clearly detected in the positive control. The slight shift towards a higher mass for ASCL1 from *A-T2A-L-P2A-N* and *A-T2A-L-IRES-N* vectors was due to the additional residues from the T2A element. Possible fusions with LMX1A or LMX1A and NURR1 could not be detected due to strong unspecific binding of the ASCL1 antibody. **(C)** Western blot detecting LMX1A. Besides the WT LMX1A at 55 kDa, additional fusion proteins of LMX1A with ASCL1, NURR1 or with both proteins were observed as indicated by arrows. **(D)** Western blot detecting NURR1. WT NURR1 was expected at 66 kDa. Additional fusion proteins with LMX1A or LMX1A and ASCL1 were observed as indicated by arrows. **Abbreviations:** A: ASCL1, L: LMX1A, N: NURR1, P2A: 2A sequence from *Porcine teschovirus-1*, T2A: 2A sequence from *Thosea asigna* virus, IRES: internal ribosomal entry site. This data was published by Theodorou and Rauser *et al.*, 2015 [118].

All ASCL1 western blots performed showed strong unspecific antibody binding (Figure 7 B). Therefore, only the correctly cleaved form of ASCL1 at 37 kDa could be detected (Figure 7B). For LMX1A (Figure 7C) and NURR1 (Figure 7D) however, a ladder of different fusion proteins was observed from the constructs *Ascl1-T2A-Lmx1a-P2A-Nurr1* and *Ascl1-T2A-Lmx1a-IRES-Nurr1*. LMX1A (correct size 55 kDa) was partially fused to the N-terminal

ASCL1 (92 kDa), the C-terminal NURR1 (121 kDa) or both proteins (158 kDa). NURR1 was detected at 66 kDa (correctly cleaved form), at 121 kDa (fusion with LMX1A) and at 158 kDa (ASCL1-LMX1A-NURR1 fusion). The replacement of P2A by IRES to separate LMX1A and NURR1 prevented the generation of LMX1A-NURR1 fusion proteins as expected. However, the use of *IRES* resulted in a reduced expression level of NURR1 when comparing the 66 kDa NURR1 band of *Ascl1-T2A-Lmx1a-P2A-Nurr1* and *Ascl1-T2A-Lmx1a-IRES-Nurr1* in Figure 7D. Taken together, these results confirmed incomplete ribosome skipping at 2A sites resulting in the generation of fusion proteins which are responsible for the low reprogramming efficiency.

The *Tet-O* promoter used in the *ALN* construct is known to induce gene expression at high levels [120]. In further experiments, it was therefore determined whether cleavage at 2A sites and reprogramming efficiency could be improved at lower expression levels by reducing the doxycycline concentration.

#### **5.1.4 The reprogramming efficiency of *ALN* is independent of doxycycline concentrations**

The *Tet-O-promoter* used in the previously described experiments is based on a *Tet-ON* system comprising *tet* operators upstream of a minimal promoter [114]. For the induction of the promoter a reverse Tet repressor (rTetR) fused to the transactivating domain (TA) of *Herpes simplex virus* protein vmw65 (VP16) is required [114]. This fusion protein termed rTTA only binds and induces the *tet* operator upon interacting with doxycycline [114]. This allows timing and fine tuning of the expression level by adjusting doxycycline concentrations.

In order to test whether ribosome skipping can be improved at lower expression levels, reprogramming experiments were repeated with reduced doxycycline concentrations shown in Figure 8A. Quantifications of reprogrammed cells did not reveal statistically significant differences in the percentage of MAP2<sup>+</sup> cells (Figure 8B) or TH<sup>+</sup> cells (Figure 8C) upon reducing doxycycline concentrations. However, results for the single viruses indicated a concentration dependent effect of doxycycline on the reprogramming efficiency favoring higher levels of gene expression (1.1 ± 0.3% TH<sup>+</sup> cells at 0.1 µg/ml dox vs 2.2 ± 0.6% TH<sup>+</sup> cells at 2.0 µg/ml dox). For *ALN* it seemed a concentration of 1.0 µg/ml doxycycline may be the most suitable (Figure 9C). At all conditions analyzed however, using *ALN* again seemed less suitable for direct reprogramming of MEFs to DA neurons than utilizing the single viruses. Next, it was analyzed on the protein level whether the decrease in doxycycline influences ribosome skipping at 2A sites.

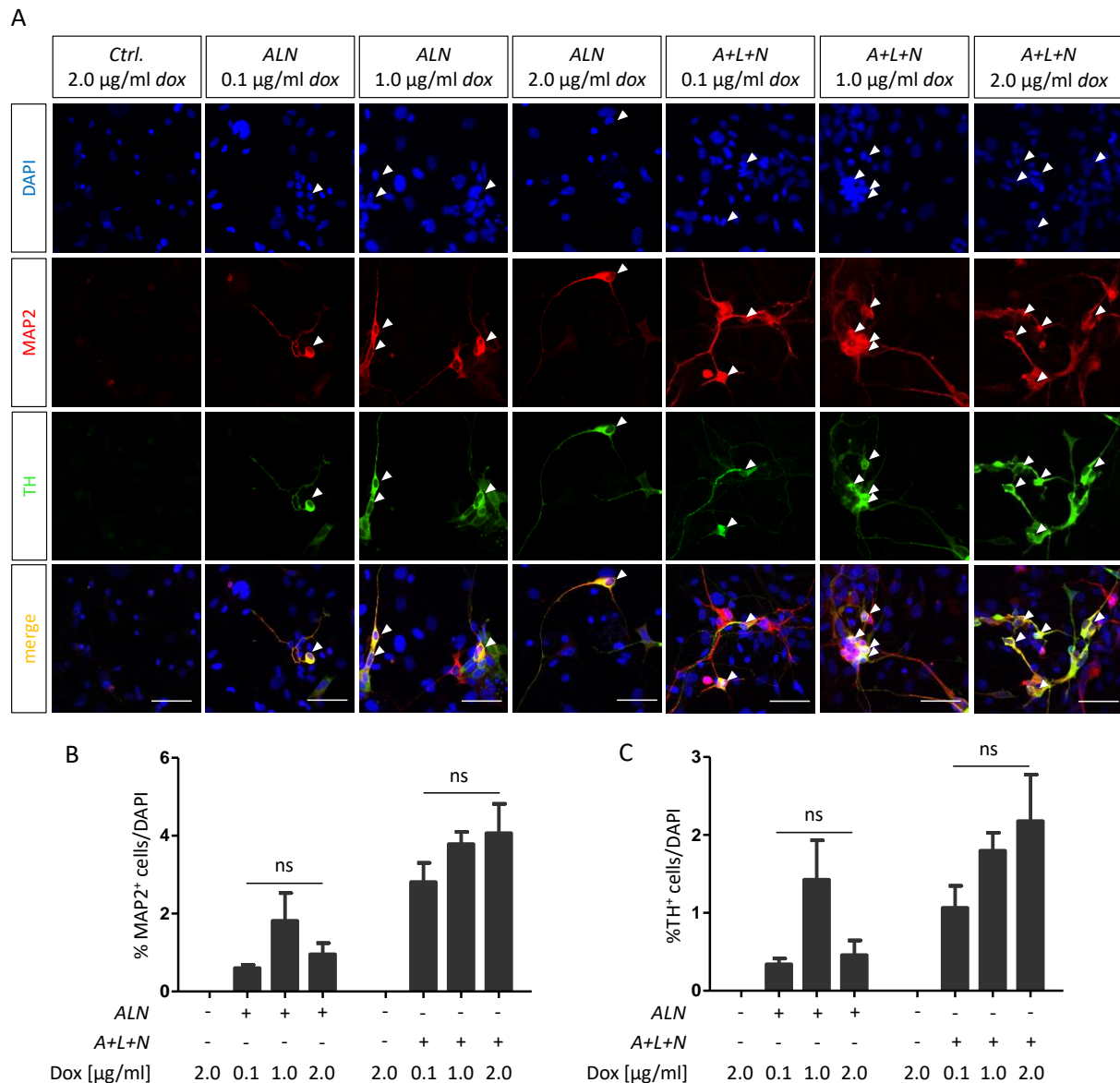


**Figure 8: Reducing the doxycycline concentration does not significantly affect the reprogramming efficiency**

MEFs were transduced either with tri-cistronic *ALN* or single viruses encoding *Ascl1*, *Lmx1a* and *Nurr1* and were cultured at different doxycycline concentrations for 14 days. **(A)** Co-staining for MAP2 and TH. Arrow heads indicate MAP2<sup>+</sup>/TH<sup>+</sup> cells. **(B)** Quantification of MAP2<sup>+</sup> cells showed no statistically significant effect on MAP2<sup>+</sup> cells upon reducing doxycycline concentration within either *ALN* or *A+L+N* transduced cells. However, a trend was observed favoring a concentration of 1 µg/ml doxycycline for *ALN* and higher levels for *A+L+N*. **(C)** Quantification of TH<sup>+</sup> cells. Reducing doxycycline concentration did not statistically significant affect the percentage of TH<sup>+</sup> cells within the *ALN* or *A+L+N* transduced cells. Similar to the results for MAP2, again best results were obtained at 1 µg/ml doxycycline for *ALN* and higher levels for *A+L+N*. **Abbreviations:** *ALN*: *Ascl1*, *Lmx1a*, *Nurr1* expressed from a tri-cistronic lentiviral vector, *A+L+N*: *Ascl1*, *Lmx1a*, *Nurr1* expressed from individual lentiviral vectors, dox: doxycycline used for induction of *Te-O* promoters. Scale bars: 50 µm. Data was derived from three independent experiments. Error bars represent mean ± SEM, Kruskal-Wallis test, Dunn's multiple comparison test. This data was published by Theodorou and Rauser *et al.*, 2015 [118].

### 5.1.5 Ribosome skipping at 2A sites is not affected by expression levels

In order to test whether ribosome skipping at 2A sites may be impaired due to the high level of protein biosynthesis, western blot analysis for NURR1 was repeated at different doxycycline levels (Figure 9A). There seemed to be a concentration dependent effect of doxycycline on the overall amount of NURR1 expressed from the *ALN* construct (see Figure 9A and B,  $23.4 \pm 9.7\%$  NURR1 protein at 0.1  $\mu\text{g/ml}$  dox vs  $45.2 \pm 26.8\%$  NURR1 protein at 2.0  $\mu\text{g/ml}$  dox normalized to *Tet-O-Nurr1*).

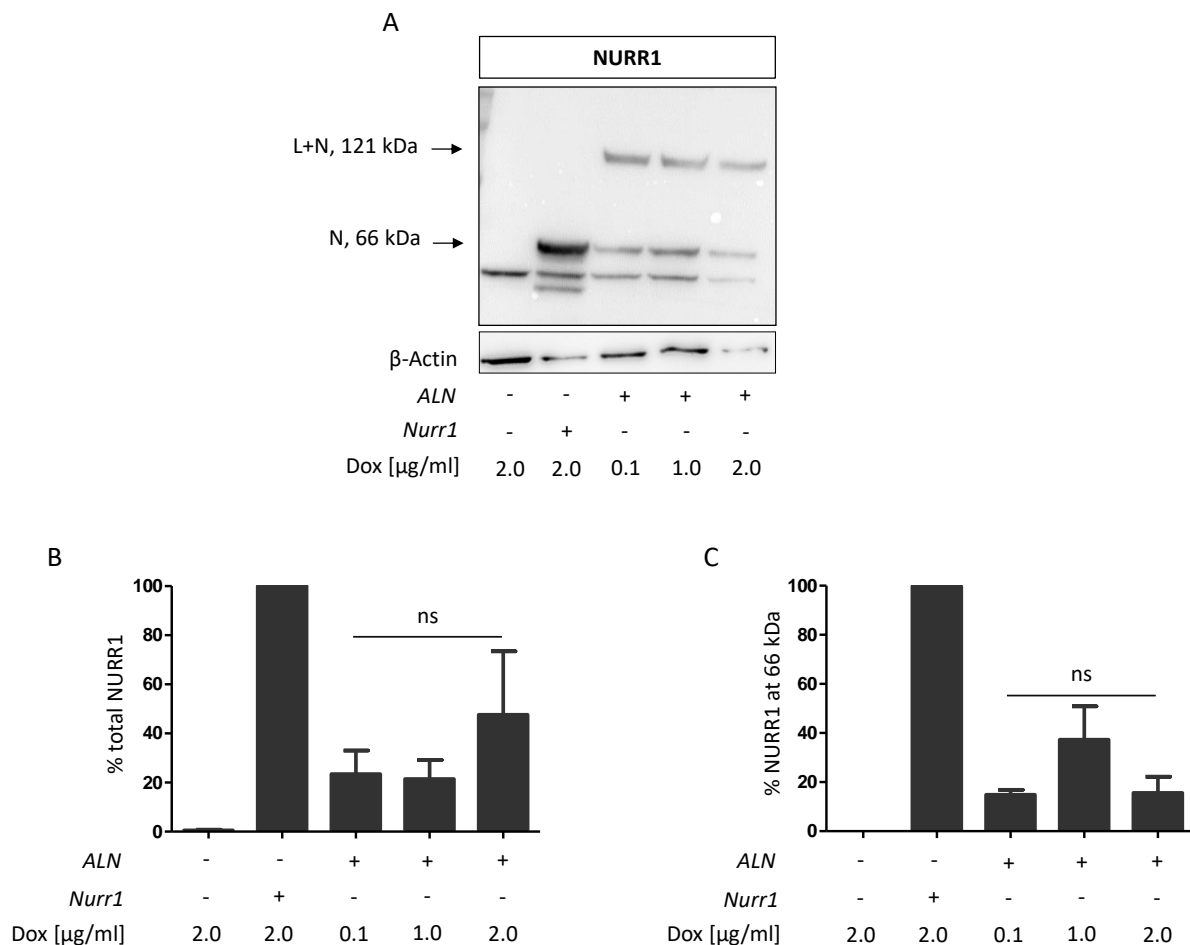


#### Figure 9: Lower expression levels do not affect ribosome skipping at P2A site

HEK293 cells were transduced with *Tet-O-Nurr1* encoding lentiviruses at different doxycycline concentrations. Western blot analysis was performed after 48 h. **(A)** Western blot detecting NURR1 shows WT NURR1 at 66 kDa and LMX1A-NURR1 fusion proteins at 121 kDa. **(B)** Quantification of total NURR1 protein. Changing the doxycycline concentration did not significantly affect the total amount of NURR1 but hinted at reduced levels upon decreasing the doxycycline concentration. **(C)** Quantification of unfused NURR1 at 66 kDa. Reducing doxycycline concentration did not significantly increase the amount of unfused NURR1 protein. Values were normalized to NURR1 overexpression from a single *Nurr1* lentivirus. **Abbreviations:** *ALN*: *Ascl1*, *Lmx1a*, *Nurr1* expressed from a single lentiviral vector, *L*: *Lmx1a*, *N*: *Nurr1* expressed from individual lentiviral vectors, dox: doxycycline used for induction of *Tet-O* promoters. Data was derived from three independent experiments. Error bars represent mean  $\pm$  SEM, Kruskal-Wallis test, Dunn's multiple comparison test, ns: not significant. This data was published by Theodorou and Rauser *et al.*, 2015 [118].

When analyzing the percentage of correctly cleaved NURR1 protein at 66 kDa it became clear that just  $15.9 \pm 6.3\%$  of total NURR1 produced from the *ALN* construct was correctly cleaved at 2.0  $\mu\text{g/ml}$  doxycycline (Figure 9C). Furthermore, the total amount of NURR1 produced by the *ALN* construct only reached about 50% of the level expressed by the single *Nurr1* encoding lentivirus (Figure 9B). This could be an explanation for the low reprogramming efficiency of the tri-cistronic *ALN* construct. Reducing the doxycycline concentration from 2.0  $\mu\text{g/ml}$  to 0.1  $\mu\text{g/ml}$  did not significantly affect the proportion of correctly cleaved NURR1. However, at 1.0  $\mu\text{g/ml}$  doxycycline the percentage of correctly cleaved NURR1 seemed to be slightly increased although not statistically significant. This corresponds to the slightly improved reprogramming efficiency of *ALN* observed at 1.0  $\mu\text{g/ml}$  doxycycline in Figure 8. These results suggest that ribosome skipping at 2A sequences was independent of the expression level and could therefore not be rescued by choosing lower levels of expression. Taken together, the use of a tri-cistronic lentiviral vector did not help to overcome the limitations of multiple single viruses described earlier and was therefore not pursued any further.

#### 5.1.6 Successful generation of PITX3<sup>+</sup> DA neurons by forskolin treatment

Single viruses encoding *A+L+N* were found to be better suited for the direct conversion of MEFs to DA neurons than the tri-cistronic *ALN* construct. However, there was still a need to improve reprogramming efficiencies. Besides overexpression of transcription factors the addition of small molecules or morphogens during reprogramming experiments can also be beneficial [30, 121]. One promising factor is forskolin, a labdane diterpenoid isolated from the roots of *Coleus Forskohlii*. Forskolin directly activates adenylate cyclase which catalyzes the conversion of adenosine triphosphate (ATP) to cyclic adenosine monophosphate (cAMP) [122-124]. cAMP signaling is involved in a wide range of cellular processes including proliferation, differentiation and chromatin condensation [125]. Interestingly, forskolin was also found to induce anti-apoptotic responses, to improve neuronal regeneration and to increase the translation of *TH* mRNA [126-130].

It was therefore tested whether forskolin treatment of *A+L+N* transduced MEFs influences the direct reprogramming efficiency. Indeed, Figure 10A+B shows a trend toward higher reprogramming efficiency upon addition of forskolin to the cells (increase from  $0.5 \pm 0.2\%$  to  $0.8 \pm 0.2\%$  TH<sup>+</sup> cells). In order to detect possible anti-apoptotic effects of forskolin, the number of DAPI<sup>+</sup> cells per mm<sup>2</sup> was determined in Figure 10C. However, forskolin treatment did not increase the overall cell survival indicating that the trend in TH<sup>+</sup> cells was not based on a generally higher survival of the cells.

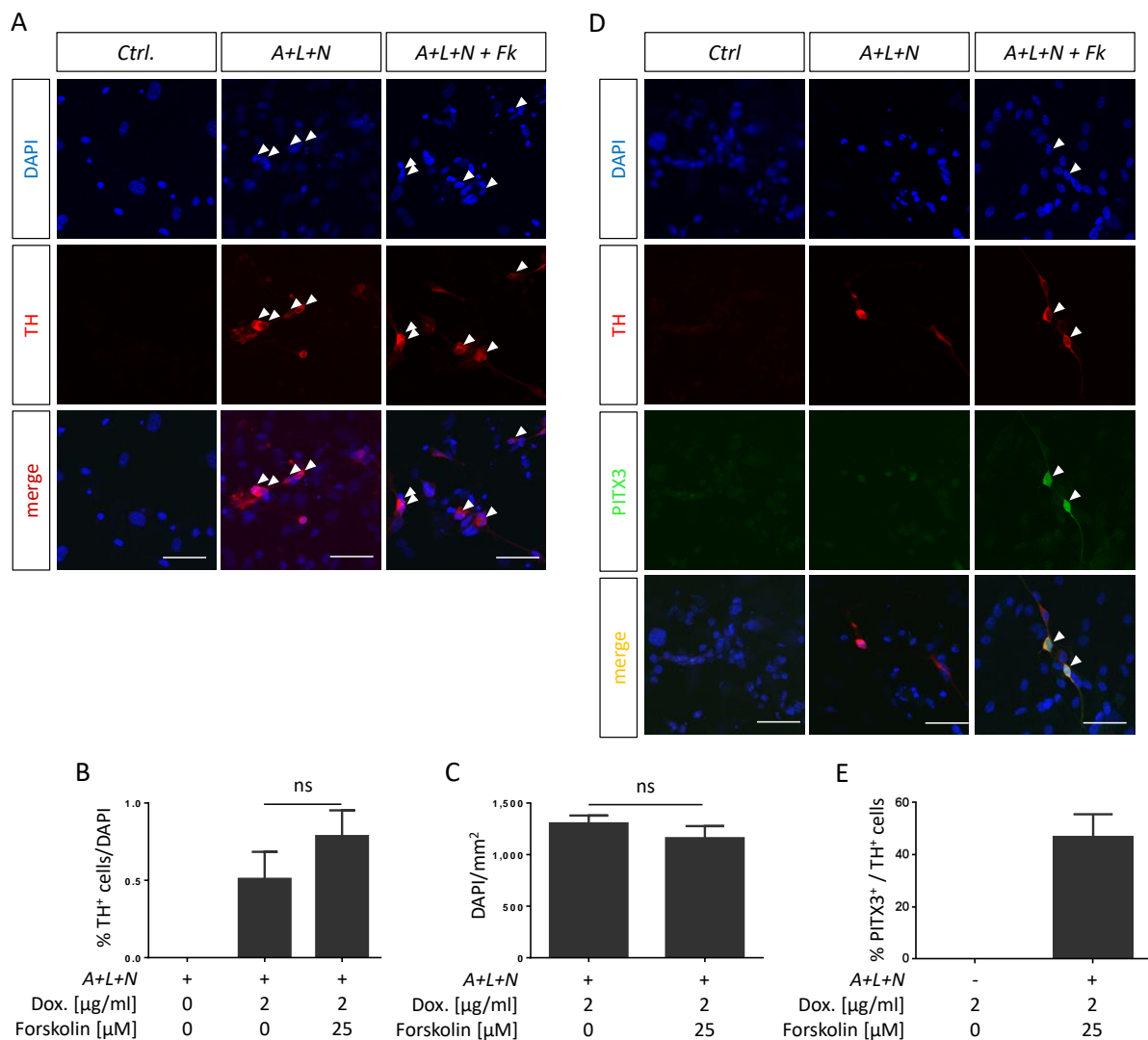


**Figure 10: Forskolin treatment of A+L+N transduced MEFs enables the generation of TH<sup>+</sup>/PITX3<sup>+</sup> neurons**

Analysis of reprogrammed MEFs 14 days after lentiviral transduction. 25 μM forskolin was added together with reprogramming medium three days after transduction. **(A)** Immunocytochemistry analysis of TH<sup>+</sup> cells showed successful generation of TH<sup>+</sup> cells for A+L+N with or without forskolin (Fk) treatment. **(B)** Quantification of TH<sup>+</sup> cells per DAPI revealed a positive trend upon addition of forskolin. **(C)** Quantification of DAPI<sup>+</sup> cells per mm<sup>2</sup> that the slight increase in TH<sup>+</sup> cells in (B) was not due to an overall increase of cells. **(D)** Immunocytochemistry analysis of reprogrammed cells from *Pitx3*<sup>GFP/+</sup> mice. GFP<sup>+</sup> cells indicate the generation of ‘true’ TH<sup>+</sup>/PITX3<sup>+</sup> mdDA neurons after addition of 25 μM forskolin to A+L+N transduced cells. **(E)** Quantification of PITX3<sup>+</sup> cells per TH. While A+L+N transduced cells were never found to express GFP (PITX3), 46.7 ± 8.8% of all TH<sup>+</sup> cells were PITX3<sup>+</sup> upon addition of forskolin. **Abbreviations:** Dox: Doxycycline, Fk: forskolin, A+L+N: *Ascl1*, *Lmx1a*, *Nurr1* expressed from individual lentiviral vectors, PITX3: Paired-like homeodomain transcription factor 3. Scale bars: 50 μm. Data was derived from three independent experiments. Error bars represent mean ± SEM, Mann-Whitney test, ns: not significant.

The subtype of the reprogrammed DA neurons obtained by A+L+N based reprogramming was still an open question. While several types of DA neurons are found in the mammalian brain only midbrain dopaminergic neurons are affected in Parkinson’s disease [6-8]. This subpopulation is characterized by the expression of *Pitx3* [14]. Various protocols and transcription factor combinations have been described for the direct conversion of fibroblasts to dopaminergic neurons [32-37]. However, the generation of TH<sup>+</sup>/PITX3<sup>+</sup> neurons was only

reported for two protocols using five or six different transcription factors respectively (*Brn2*, *Lmx1b*, *Ascl1*, *Nurr1*, *Otx2* [36] and *En1*, *Foxa2*, *Lmx1a*, *Ascl1*, *Nurr1*, *Pitx3* [32]). Overexpression of *Ascl1*, *Lmx1a* and *Nurr1* is not sufficient for the generation of TH<sup>+</sup>/PITX3<sup>+</sup> cells (unpublished data F. Meier, Helmholtz Zentrum München). It is therefore of interest to identify factors enabling the generation of 'true' midbrain dopaminergic neurons (TH<sup>+</sup>/PITX3<sup>+</sup>) requiring less than five to six individual viruses.

It was thus tested whether forskolin treatment could influence the identity of the reprogrammed cells allowing the generation of TH<sup>+</sup>/PITX3<sup>+</sup> mdDA neurons. For reprogramming experiments MEFs of *Pitx3*<sup>GFP/+</sup> mice were used which allows visualization of PITX3<sup>+</sup> cells due to GFP expression. Figure 10D shows successful generation of TH<sup>+</sup>/PITX3<sup>+</sup> cells upon addition of forskolin to A+L+N transduced MEFs. 46.7 ± 8.8% of all TH<sup>+</sup> cells were PITX3 positive (Figure 10E) which is a very promising finding for the generation of 'true' mdDA neurons.

However, the above described limitations of co-infection by multiple viruses and the inefficient ribosome skipping at 2A sequences called for a new reprogramming strategy. One promising new technology is the CRISPR/Cas9 system which can be used to induce endogenous gene expression. Due to epigenetic remodeling of targeted loci and the expression from endogenous promoters this technology more closely resembles physiological mechanisms of gene expression than forced overexpression of exogenous factors [107]. The potential of CRISPR/Cas9 for direct conversion of somatic cells is described in the following part.

## 5.2 Induction of endogenous genes and direct reprogramming of astrocytes to neurons utilizing the CRISPR/Cas9 technology

The CRISPR/Cas9 system allows targeting of virtually any locus in the genome by a protein-RNA complex consisting of a Cas9 nuclease and a specifically designed gRNA which binds complementary DNA sequences [83, 84]. Dead Cas9 (dCas9) variants which lack the DNA cutting properties are utilized as shuttles to transfer fused transcriptional regulators to a promoter of interest and modulate gene expression [89, 94, 95]. At the beginning of this project direct reprogramming of somatic cells to neurons using the CRISPR/Cas9 technology had not been described. Therefore, the aim was to set up a system which allows maximum induction of endogenous genes and to test the reprogramming properties as proof-of-principle experiments. The CRISPR/Cas9 technology enables the simultaneous induction of several genes by expressing an array of suitable gRNAs thus circumventing limitations in packaging capacity, co-transduction efficiency and fusion proteins.

For the proof-of-principle experiments of this thesis *Ascl1* was chosen as target gene since ectopic expression of this transcription factor is sufficient to successfully reprogram MEFs or astrocytes to neurons [131, 132]. Some experiments also included *Nurr1* as a second target gene since the long-term goal of this project was to directly reprogram somatic cells to DA neurons by induction of *Ascl1*, *Lmx1a*, and *Nurr1*. The following chapters describe screening experiments for suitable gRNAs, followed by screenings in which different dCas9-fusion proteins were analyzed regarding their gene induction properties.

### 5.2.1 Design of gRNAs and implementation of a screening assay to detect induction of endogenous genes

As a first step gRNAs targeting murine *Ascl1* and *Nurr1* promoters were designed to test the CRISPR/Cas9 technology for gene activation. The promoter region between -250 to -1 nucleotides (nt) upstream of the transcription start site (TSS) has been successfully targeted for gene induction using CRISPR/Cas9 by other groups [89, 91]. Therefore, eight gRNAs were designed covering these 250 nucleotides of the *Ascl1* (ENSMUST00000020243.9) and *Nurr1* (ENSMUST00000028166) promoters using an online tool at <http://crispr.mit.edu/> [133]. For each gene, four gRNAs targeting the sense strand and four gRNAs targeting the antisense strand were chosen (gRNAs *A1* – *A8* for *Ascl1*, *N1* – *N8* for *Nurr1*, see Figure 11A and B) to check for possible orientation effects. In order to detect successful induction of endogenous genes, dual luciferase assays were performed 48 h after lipofection. This allowed a quantification of the activity of the induced target protein and not just an analysis of gene induction via mRNA levels.

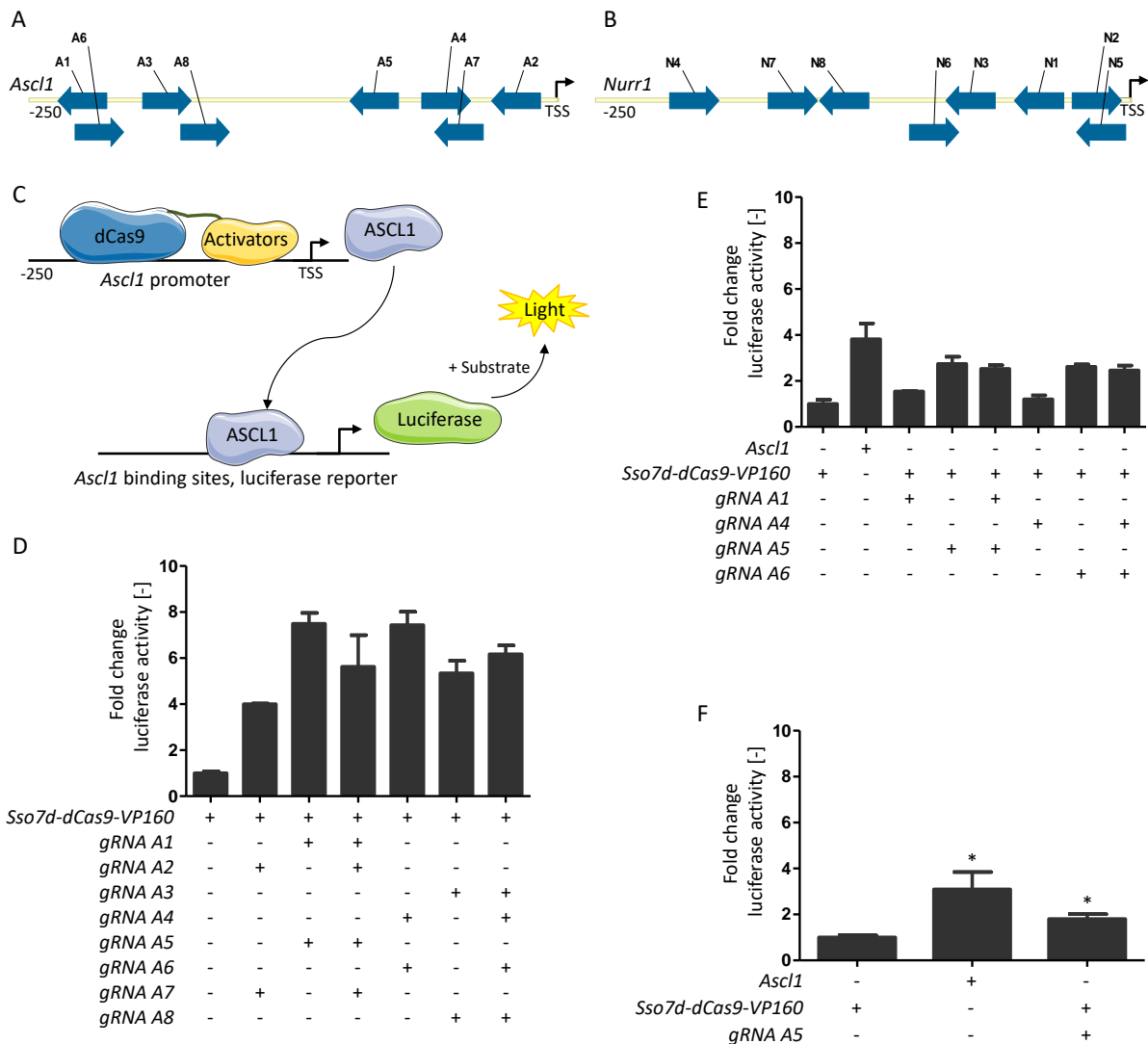


### Figure 11: gRNA A5 successfully induces *Ascl1* expression in Neuro 2a cells

Position and orientation of gRNAs targeting the 250 nucleotides upstream of the transcription start sites (TSS) of murine (A) *Ascl1* and (B) *Nurr1*. (C) Schematic illustration of the reporter system used for luciferase assays. Upon binding of dCas9 fused to transcriptional activators, the target gene i.e. *Ascl1* was expressed and bound to specific *Ascl1* binding sites on a *luciferase* reporter construct. Binding of ASCL1 then induced *firefly luciferase* expression and luciferase activity was determined by adding a suitable substrate and measurement of the generated luminescence in a luciferase assay. For normalization purposes *renilla luciferase* driven by a constitutively active promoter was co-transfected. (D) Luciferase assay screen for suitable gRNAs 48 h after transfection of Neuro 2a cells. The combination of gRNAs A1/A5 and A4/A6 showed the strongest luciferase activity. Data was derived from one experiment. (E) Luciferase assay screen for suitable gRNAs. gRNAs A5 and A6 reached similar levels of activation when tested alone or in combination with gRNAs A1 or A4, respectively. Data was derived from one experiment. (F) Luciferase assay comparing gRNA A5 and *Ascl1* overexpression. gRNA A5 induced about 60% of luciferase activity (*Ascl1* induction) when compared to *Ascl1* overexpression. Data was derived from three independent experiments. **Abbreviations:** gRNAs A1-8: gRNAs targeting the murine *Ascl1* promoter, gRNAs N1-N8: gRNAs targeting the murine *Nurr1* promoter, *Sso7d*: *S. solfataricus* DNA binding protein 7d, TSS: transcription start site, *VP160*: ten repeats of the *Herpes simplex virus* protein vmw65 (VP16) transactivation domain. Error bars represent mean  $\pm$  SEM, Kruskal-Wallis test, Dunn's multiple comparison test, \* $P < 0.05$ .

Figure 11C depicts an illustration of the established luciferase assay system in which the induced proteins ASCL1 or NURR1 bound to specific binding sites on reporter constructs inducing firefly luciferase expression [134]. The activity of the firefly luciferase could then be determined in a luciferase assay after addition of a substrate and subsequent luminescence measurement. The *firefly* luciferase activity was normalized to the activity of a co-transfected constitutively expressed *renilla* luciferase. Figure 11D-F shows an exemplary screen for suitable *Ascl1* gRNAs which was also performed for *Nurr1* (appendix, Figure 25). For these initial experiments a dCas9 version termed *Sso7d-dCas9-VP160* was used which was developed by J. Truong at the institute. *Sso7d-dCas9-VP160* consists of dCas9 C-terminally fused to ten *VP16* repeats (*VP160*) serving as transcriptional activators and N-terminally fused to the DNA binding protein *Sso7d* putatively improving DNA binding properties (see illustration in Figure 4B). In a first screen gRNA combinations with two gRNAs (*A1/A5* or *A4/A6*) targeting the *Ascl1* promoter showed the strongest activation (Figure 11D).

In a second screen gRNAs *A5* and *A6* were found to be responsible for the detected activating effect showing a comparable level of luciferase activity when used alone or in combination with gRNAs *A1* or *A4*, respectively (Figure 11E). A general influence of the gRNA orientation was not detected. gRNA *A5* was chosen for further experiments and reached about 60% of the luciferase activity (Figure 11F) when compared to direct *Ascl1* overexpression as positive control ( $1.8 \pm 0.2$  vs  $3.1 \pm 0.8$ -fold gene induction).

## 5.2.2 Screening for dCas9 fusion proteins to induce endogenous *Ascl1*

The screenings for suitable gRNAs described in the above experiments were performed using *Sso7d-dCas9-VP160*. To identify a system with potentially even stronger gene induction properties, different dCas9 versions were tested in the following chapters where dCas9 was fused to diverse combinations of transcriptional inducers including the SpyTag and SunTag systems, SAM and VPR strategies.

### 5.2.2.1 The SpyTag system improves endogenous gene induction

First, it was determined whether the fusion of the additional DNA binding domain *Sso7d* to dCas9 variants benefits the gene induction potential. For these tests, HEK293 cells were used to also apply the system to human cells. A change in gRNAs was not required since both gRNAs (*A5* for *ASCL1* and *N2* for *NURR1*) matched sequences in the corresponding human and murine promoter regions. Initial screens for *ASCL1* (Figure 12A) and *NURR1* (Figure 12B) induction suggested a positive effect of *Sso7d* on gene induction when compared to dCas9-VP160 (increased activity from  $4.0 \pm 0.5$  to  $6.4 \pm 1.2$ -fold for *ASCL1*, and  $0.9 \pm 1.2$  to  $2.1 \pm 1.6$ -fold for *NURR1*).

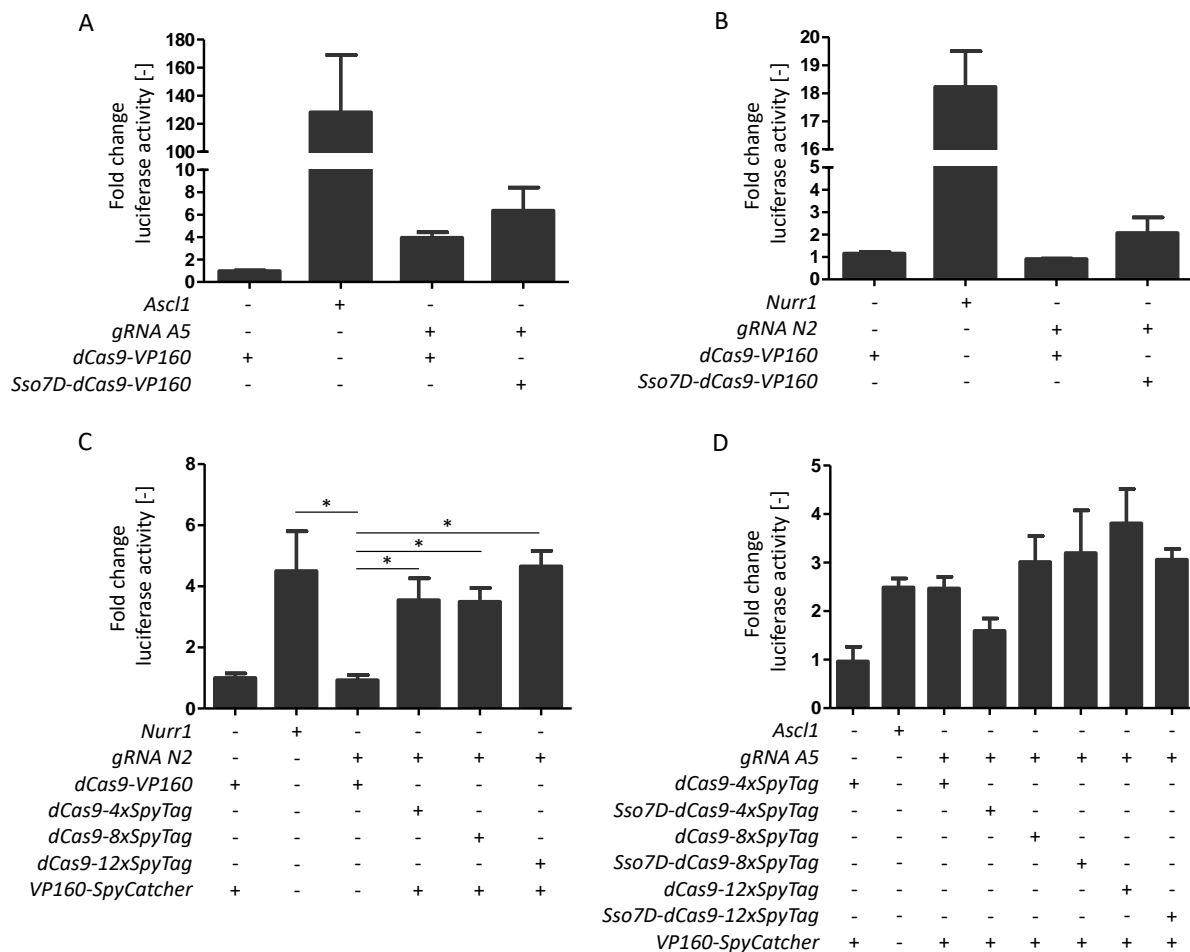


**Figure 12: Recruitment of multiple activators to dCas9 utilizing the SpyTag system leads to an increase in transcriptional activation**

Luciferase assay analysis with *ASCL1* or *NURR1* reporter constructs in HEK293 cells 48 h after lipofection. The fusion of the Sso7d DNA binding domain to dCas9-VP160 seemed to increase the activation of (A) *ASCL1* or (B) *NURR1* in a first screen (data was derived from one experiment). (C) Fusion of dCas9 to SpyTag repeats allowed recruitment of multiple VP160-SpyCatcher fusions to a single dCas9 protein. SpyTag arrays consisting of four, eight or twelve SpyTags led to a significant increase in *NURR1* transcription when compared to simple dCas9-VP160 (Data was derived from three independent experiments). (D) The addition of Sso7d to the different SpyTag arrays however did not further increase transcriptional activation (data was derived from one experiment). **Abbreviations:** gRNA A5: gRNA targeting murine and human *Ascl1*, gRNA N2: gRNA targeting murine and human *Nurr1* promoters, Sso7d: *S. solfataricus* DNA binding protein 7d, VP160: ten repeats of *Herpes simplex virus* protein VP16. Error bars represent mean  $\pm$  SEM, Kruskal-Wallis test, Dunn's multiple comparison test, \* $P < 0.05$ .

Further, it was tested whether increasing the number of transcriptional activators fused to dCas9 would influence gene expression. The SpyTag system (see Figure 4C) developed at the institute by J. Truong offered the possibility to recruit multiple copies of VP160 activators to tandem repeats of SpyTags fused to dCas9. This system is based on a split protein system consisting of SpyTags and SpyCatchers. While arrays of SpyTags are fused to dCas9, SpyCatchers are fused to VP160 transcriptional activators. Binding of SpyCatcher-VP160 to SpyTags results in the generation of an isopeptide bond and thus covalent binding of multiple VP160 copies to dCas9. Figure 12C shows that using the SpyTag system significantly increased *NURR1* expression when compared to simple dCas9-VP160

( $0.9 \pm 0.2$  vs  $3.6 \pm 0.7$ -fold activation). By rising the number of SpyTag repeats fused to dCas9 to twelve the activation level of *NURR1* was further increased to  $4.7 \pm 0.5$ -fold activation (Figure 12C). Next, it was tested whether adding the DNA binding protein Sso7d to the SpyTag system would again benefit gene induction. However, in this case no additional effect was detected suggesting that the putatively stronger binding of the dCas9 system due to the Sso7d domain only supported gene induction when the overall level of induction is moderate (Figure 12D). Therefore, the dCas9-12x-SpyTag system was chosen for further comparative studies.

In the course of these studies Tanenbaum *et. al.*, published a system similar to the SpyTag technology termed SunTag [100]. The SunTag system is based on scFV antibodies fused to four repeats of VP16 (VP64) that can bind an array of 24 SunTags fused to dCas9 (see illustration in Figure 4D). The SunTag system therefore allows recruitment of up to 24 copies of VP64 which may lead to an even higher gene induction than the 12x-SpyTag system described above.

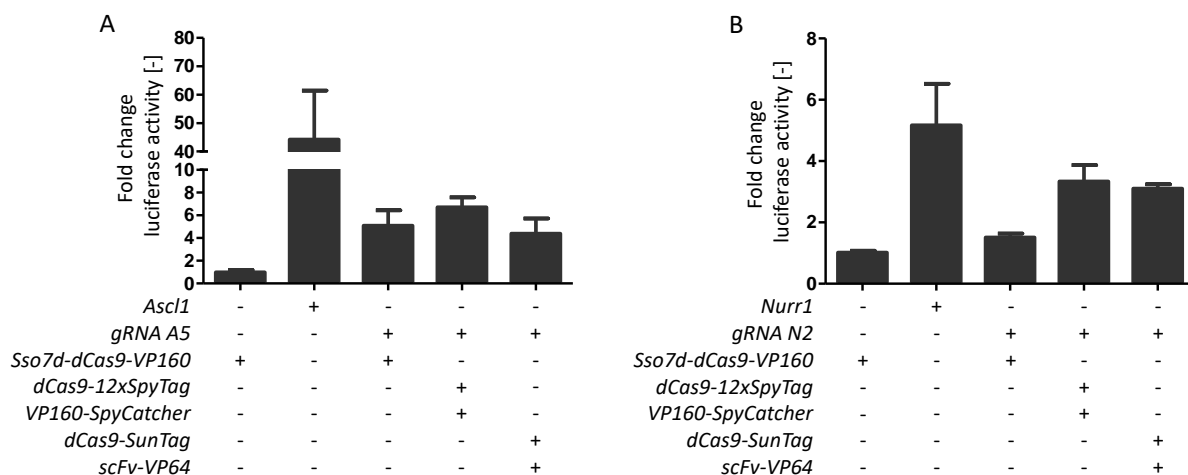


**Figure 13: The SpyTag system seems to be superior to the published SunTag system for the induction of *ASCL1* and *NURR1***

Luciferase assays comparing SpyTag and SunTag systems in HEK293 cells 48 h after transfection. Preliminary screening data suggested the SpyTag system to be better suited for gene induction of **(A)** *ASCL1* and **(B)** *NURR1* than the published SunTag system. **Abbreviations:** gRNA A5: gRNA targeting murine and human *Ascl1* promoters, gRNA N2: gRNA targeting murine and human *Nurr1* promoters, scFv: single chain variable fragment antibody, Sso7d: *S. solfataricus* DNA binding protein 7d, VP64: four repeats of *Herpes simplex virus* protein VP16, VP160: ten repeats of *Herpes simplex virus* protein VP16. Data was derived from one experiment. Error bars represent mean  $\pm$  SEM.

The activating effect of SpyTag vs SunTag system was therefore compared in a luciferase assay screen depicted in Figure 13. However, the SunTag system could not improve *ASCL1* or *NURR1* induction when compared to SpyTag and was therefore not used in further experiments (*ASCL1* induction: SpyTag:  $6.7 \pm 0.9$  vs SunTag:  $4.4 \pm 1.3$ -fold, *NURR1* induction: SpyTag:  $3.3 \pm 0.1$  vs SunTag:  $3.1 \pm 0.1$ -fold).

### 5.2.2.2 Requirement of a new screening platform for SAM and VPR systems

While the above screenings were performed two promising new systems termed VPR [90] and SAM [91] were published. VPR-based gene induction of *NGN2* or *NEUROD1* in human iPS cells was found to induce neuronal differentiation suggesting a sufficient level of gene activation to influence cell fate [90]. Here, dCas9 is fused to the transactivating domains of 4 x VP16 (VP64), P65 and RTA (see illustration in Figure 4E). The SAM system utilizes a new strategy with two additional loops added to the gRNA that are bound by the Phage protein MS2. MS2 is expressed as a fusion protein with the transcriptional activators P65 and HSF1 which allows recruitment of MS2-P65-HSF1 to MS2 aptamers at the gRNA (see Figure 4F for further details). This system is co-expressed with dCas9 fusion proteins such as dCas9-VP64 which was reported to significantly improve gene induction compared to dCas9-VP64 alone [91]. In order to test these new systems luciferase assays were performed using VPR and SAM for *ASCL1* and *NURR1* induction (Figure 14).

Surprisingly, SAM and especially VPR seemed to inhibit the expression of both genes showing each a  $0.1 \pm 0.0$ -fold induction in Figure 14A. In the dual luciferase system used for these screenings the *firefly* luciferase activity (induced by successful generation of *ASCL1* or *NURR1*) was normalized to the activity of the constitutively expressed (*SV40* promoter driven) *renilla* luciferase. This should compensate for variations in transfection efficiency or pipetting errors. *Renilla* luciferase activity however, seemed to be strongly influenced by VPR ( $17.3 \pm 1.9$ -fold activation) and the *Tet-O* system ( $14.2 \pm 1.0$ -fold activation) as depicted in Figure 14B. This suggested an interaction of the transcriptional activators with the *SV40* promoter regulating *renilla* expression.

Figure 14C shows *firefly* activity without normalization to *renilla* and revealed the expected activating effects of the positive controls (*Tet-O-Ascl1*:  $6.8 \pm 0.6$ -fold, *Tet-O-Nurr1*:  $9.6 \pm 0.3$ -fold) but hardly an effect of SAM and VPR (both below two-fold activation). A closer look at the previously described screening experiments revealed that the so far used VP16 activation systems (including SpyTag and SunTag systems) did not influence *renilla* activity (data not shown). Nevertheless, the established luciferase assay platform was not suitable for further experiments using SAM or VPR systems. Most publications reporting CRISPR/Cas9 based gene induction show RT-qPCR data for quantification and comparative purposes [89-91, 110]. Further screenings were therefore performed by RT-qPCR to both omit the limitations of the luciferase assay system described above and to allow a better comparison with published data.

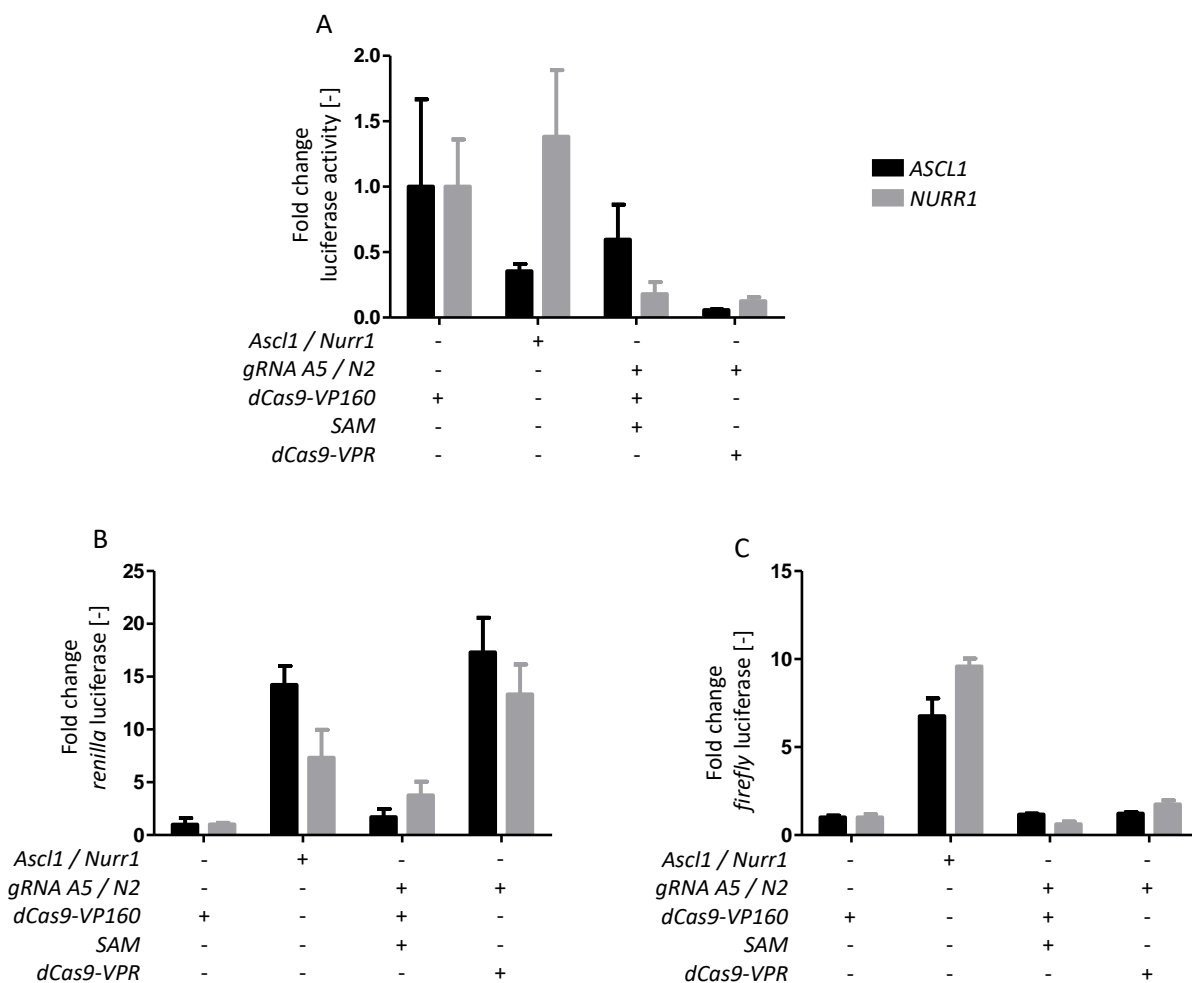


**Figure 14: Using VPR and *Tet-O*-systems influences *renilla* activity rendering this system unsuitable for screening purposes**

Luciferase assay measuring *ASCL1* and *NURR1* activity. **(A)** Firefly luciferase activity showing *ASCL1* and *NURR1* activation normalized to constitutively expressed *renilla*. Surprisingly, the use of the SAM and VPR systems seemed to have an inhibiting effect on the activity of both genes analyzed when *firefly* luciferase values were normalized to *renilla* luciferase activity. **(B)** Activity of the constitutively expressed *renilla* luciferase. Using the *Tet-O*-system and VPR had a strong activating effect on *renilla* luciferase activity rendering *renilla* luciferase activity unsuitable as control values for normalization. **(C)** Firefly luciferase activity showing *ASCL1* and *NURR1* activation without normalization to *renilla*. A clear activation upon overexpression of *ASCL1* and *NURR1* could be detected. Abbreviations: gRNA A5: gRNA targeting murine and human *Ascl1* promoters, gRNA N2: gRNA targeting murine and human *Nurr1* promoters, SAM: MS2-P65-HSF1 fusion protein, VP160: ten repeats of *Herpes simplex virus* protein VP16, VPR: VP64-P65-RTA fusion protein. Data was derived from one experiment. Error bars represent mean  $\pm$  SEM.

### 5.2.2.3 Increasing the number of gRNAs has a synergistic effect on gene induction

VPR and SAM systems were both reported to strongly induce gene expression in the original articles [90, 91]. However, this could not be confirmed in the luciferase assay shown in Figure 14C even without normalization to *renilla*. A difference in the experimental setup between his thesis and the article introducing the VPR system was the number and position of gRNAs used. While the above described experiments included a single gRNA (gRNA A5), Chavez *et al.*, 2015 used four gRNAs targeting the 900 bp upstream of the human *ASCL1* transcription start site (Figure 15A) [90]. In order to test the reproducibility RT-qPCR analysis was performed using the four published gRNAs targeting the human *ASCL1* promoter (*hA1* – *hA4*).

Interestingly, while single gRNAs only had a limited activating effect on *ASCL1* mRNA levels (each gRNA below 30-fold induction), combining three gRNAs ( $1.1 \pm 0.2 \times 10^3$ -fold induction) and especially four gRNAs ( $4.4 \pm 0.1 \times 10^3$ -fold induction) led to a synergistic activating effect as depicted in Figure 15B. The values for all four gRNAs closely resembled the findings of Chavez *et al.*, 2015 [90] thus proving the reproducibility of the system.

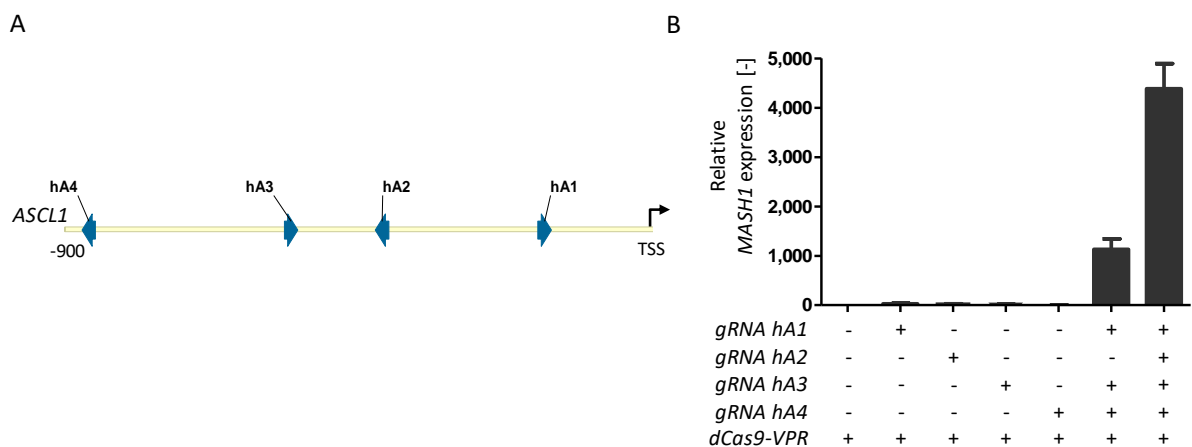


**Figure 15: Multiple gRNAs synergistically increase the activation of human *ASCL1* in HEK293 cells**  
**(A)** Position and orientation of gRNAs used by Chavez *et al.*, 2015 [90] for the induction of human *ASCL1* in HEK293 cells. **(B)** RT-qPCR analysis of *ASCL1* expression in HEK293 cells 48 h after transfection. While the activating effect of single gRNAs was low, combining three to four gRNAs had a synergistic activating effect on *ASCL1* expression. **Abbreviations:** gRNAs *hA1-hA4*: gRNAs A-D targeting the human *ASCL1* promoter, gRNA A5: gRNA targeting human and murine *ASCL1* promoters, VPR: VP64-P65-RTA fusion protein. Data was derived from one experiment. Error bars represent mean  $\pm$  SEM.

While single gRNAs have been successfully used for gene induction [91] and even direct reprogramming [108] other groups have reported similar findings of synergistic activating effects by increasing gRNA numbers [89, 106, 110, 113]. However, such a synergistic effect was not observed with the murine gRNAs tested earlier in this thesis (gRNAs *A5* and *N2*, see Figure 11). The goal of this project was to implement a CRISPR/Cas9 based system for gene induction and direct reprogramming *in vitro* which could then as a next step be analyzed in mouse models *in vivo*. Due to sequence differences in the human and murine *Ascl1* promoter region the human gRNAs (*hA1 – hA4*) do not bind to the murine promoter. It was therefore necessary to find new gRNAs targeting murine *Ascl1* that also offer the synergistic activating effect observed for the human gRNAs.

The initial murine gRNAs such as gRNA *A5* were designed based on high binding specificity meaning that the probability of binding off-targets was low (high off-target score). At this point a new online tool at <https://benchling.com/> also offered a so-called on-target score for gRNAs indicating gRNAs with a putatively high binding affinity based on an algorithm by Doench *et al.*, 2014 [135]. The three gRNAs with the highest on-target scores targeting the 250 bp upstream of the murine *Ascl1* transcription start site termed *mA1*, *mA2* and *mA3* (Figure 16A) were tested in a first RT-qPCR screen.

Figure 16B shows a strong synergistic effect on murine *Ascl1* mRNA levels when gRNAs *mA1*, *mA2* and *mA3* were combined reaching  $1.0 \pm 0.4 \times 10^4$ -fold induction. Interestingly, when adding the previously used gRNA *A5* the level of gene induction was reduced to  $4.9 \pm 0.4 \times 10^3$ -fold showing that not all combinations of gRNAs are suitable for high levels of gene induction. Screening different combinations of two or three gRNAs suggested a maximal activation of *Ascl1* when gRNAs *mA1* and *mA2* were used together as depicted in Figure 16C leading to  $1.8 \pm 0.2 \times 10^3$ -fold activation. Adding gRNA *mA3* did not further increase *Ascl1* expression ( $1.7 \pm 0.4 \times 10^3$ -fold activation). Differences observed for the absolute numbers of gene induction between experiments are based on the fact that fold change values were calculated relative to the control condition with no or very low *Ascl1* expression (Ct values between 33 and 36). Therefore, numbers can only be compared within an individual experiment.

Since an increase from three to four gRNAs had a positive effect in case of the human gRNAs in Figure 15B new murine gRNAs *mA4* and *mA5* were designed (see Figure 16A) to cover gaps between the previously tested gRNAs. However, Figure 16D shows that the additional gRNAs did not further increase *Ascl1* mRNA levels leaving *mA1* and *mA2* as the most promising combination.

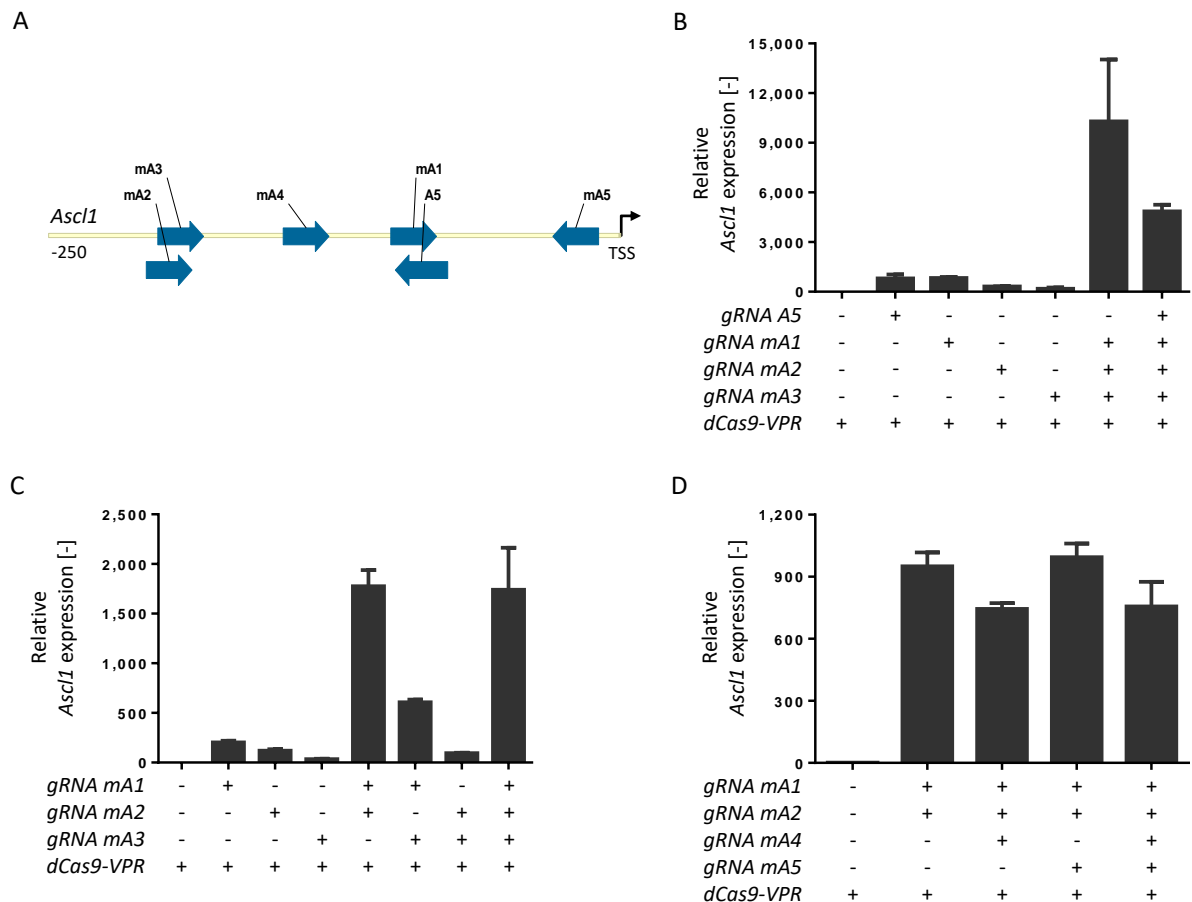


**Figure 16: Combining two gRNAs synergistically increases *Ascl1* induction in murine Neuro 2a cells** (A) Position and orientation of newly designed gRNAs targeting the murine *Ascl1* promoter region at -1 to -250 nt upstream of the transcription start site. (B) RT-qPCR analysis of *Ascl1* mRNA levels 48 h after transfection. While single gRNAs increased *Ascl1* mRNA levels only moderately, combining gRNAs *mA1*, *mA2* and *mA3* had a synergistic activating effect. (C) RT-qPCR analysis of *Ascl1* mRNA levels 48 h after transfection. Combining gRNAs *mA1* and *mA2* had the strongest activating effect which could not be further increased by the addition of gRNA *mA3*. (D) RT-qPCR analysis of *Ascl1* mRNA levels 48 h after transfection. The addition of gRNAs *mA4* and *mA5* did not further increase *Ascl1* expression when compared to gRNAs *mA1* and *mA2*. **Abbreviations:** gRNAs *mA1*-*mA5*: gRNAs targeting the murine *Ascl1* promoter, gRNA *A5*: gRNA targeting human and murine *Ascl1* promoters, VPR: VP64-P65-RTA fusion protein. Data was derived from one experiment, error bars represent mean  $\pm$  SEM.

#### 5.2.2.4 SAM and VPR systems are superior to SpyTag for *Ascl1* activation

Having established gRNAs *mA1* and *mA2* for murine *Ascl1* activation, the SpyTag, VPR and SAM systems were compared next. Figure 17A shows a significant increase in *Ascl1* mRNA levels when using VPR ( $423 \pm 144$ -fold) or SAM ( $1.4 \pm 0.1 \times 10^3$ -fold) compared to the SpyTag system ( $3.1 \pm 0.5$ -fold). These promising results raised the question whether a combination of SpyTag with SAM or VPR systems might improve the activating effect even further. The SAM system is based on recruitment of MS2-P65-HSF1 fusion proteins to MS2 aptamers at the gRNAs (see illustration in Figure 4) and co-expression of a dCas9 fusion protein. The idea therefore was to replace dCas9-VP160 by dCas9-12xSpyTag allowing recruitment of up to twelve VP160-SpyCatchers.

Surprisingly, the combination of SAM and dCas9-12x-SpyTag was less effective in *Ascl1* activation than SAM and dCas9-VP160 as depicted in Figure 17B ( $0.10 \pm 0.02 \times 10^3$  vs  $1.4 \pm 0.1 \times 10^3$ -fold induction). In order to test whether recruitment of multiple VPR activating complexes to a single dCas9 protein would be beneficial, VPR-SpyCatchers were developed at the institute by J. Truong. Here, VP160 activators fused to SpyCatchers were replaced by VPR. However, this exchange in activators did not significantly affect *Ascl1* induction as shown in Figure 17B (VP160-SpyCatchers:  $3.1 \pm 0.5$ -fold induction, VPR-SpyCatcher:  $23.1 \pm 5.3$ -fold induction). Furthermore, a combination of VPR-SpyCatchers and SAM was not beneficial for transcriptional activation as depicted in Figure 17B (SAM and VP160-SpyCatcher:  $101 \pm 25$ -fold, SAM and VPR-SpyCatcher:  $106 \pm 23$ -fold).

These data suggested an incompatibility of the SpyTag system with SAM and VPR possibly due to steric hindrances of the large activator complex being recruited to the SpyTag system.

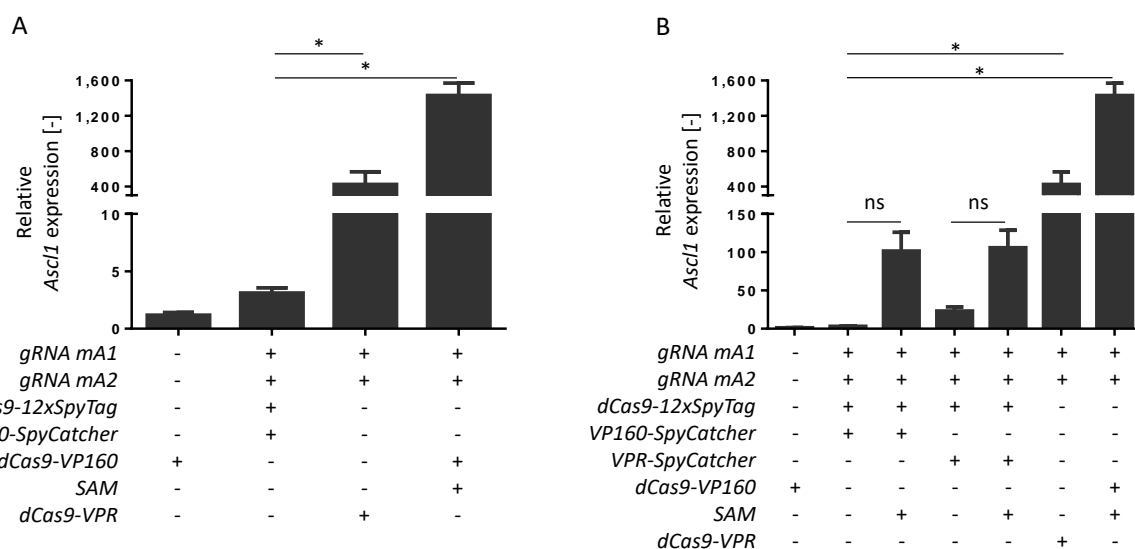


**Figure 17: VPR and especially SAM are superior to SpyTag for gene induction of *Ascl1* in Neuro 2a cells**

RT-qPCR analysis of *Ascl1* mRNA levels 48 h after transfection. **(A)** Using SAM and VPR for *Ascl1* gene induction significantly increased *Ascl1* mRNA levels when compared to the SpyTag system. **(B)** Combining SpyTag with SAM slightly increased *Ascl1* mRNA levels when compared to SpyTag alone but were lower than levels measured for SAM alone. Replacing VP160 of the SpyCatchers by VPR did not significantly increase *Ascl1* induction neither alone nor in combination with SAM. The use of SAM or VPR without the SpyTag technology had the strongest effect on *Ascl1* expression with best results obtained for SAM. Abbreviations: gRNAs *mA1*, *mA2*: gRNAs targeting the murine *Ascl1* promoter, SAM: MS2-P65-HSF1 fusion protein, VP160: ten repeats of *Herpes simplex virus* protein VP16, VPR: VP64-P65-RTA fusion protein. Data was derived from three independent experiments, error bars represent mean  $\pm$  SEM, Kruskal-Wallis test, Dunn's multiple comparison test, ns: not significant, \*P < 0.05.

### 5.2.2.5 Combining SAM and VPR systems has a synergistic effect on *Ascl1* expression

SAM and VPR were found to be the strongest activators tested in this project so far. It was therefore of interest whether it would be beneficial to combine these two systems without using the SpyTag system as illustrated in Figure 18A. Interestingly, the combination of SAM and VPR had a synergistic effect on *Ascl1* induction reaching  $7.3 \pm 0.8 \times 10^3$ -fold *Ascl1* expression while an additive effect would have been expected at approximately  $2.4 \times 10^3$ -fold ( $0.20 \pm 0.09 \times 10^3$ -fold VPR alone,  $2.2 \pm 0.2 \times 10^3$ -fold SAM alone). Although, this new combination of activators could not reach levels detected for direct *Ascl1* overexpression ( $4.1 \times 10^5 \pm 1.0 \times 10^5$ , Figure 18B) these results are very promising. Gene induction by the VPR system alone has already been shown to be sufficient to induce neuronal differentiation of iPS cells [90]. The significantly higher level of *Ascl1* mRNA by combining SAM and VPR systems therefore might be a valuable tool for direct conversion of somatic cells to neurons. Interestingly, this synergistic effect of SAM and VPR systems for gene induction has not been reported by others so far.

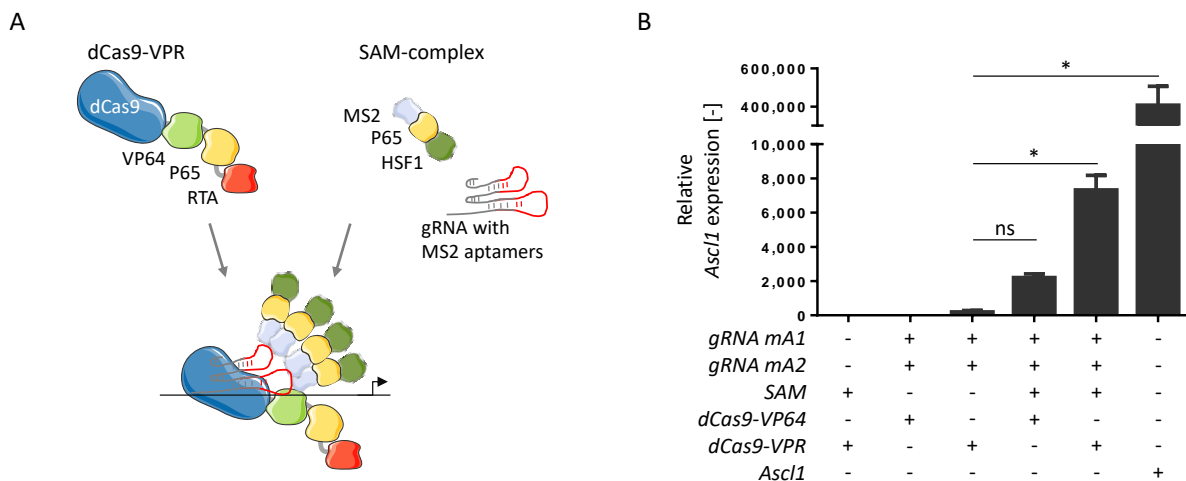


**Figure 18: Combining SAM and VPR synergistically increases *Ascl1* mRNA levels in Neuro 2a cells**  
**(A)** Schematic illustration combining activators of the VPR system fused to dCas9 and the SAM complex which binds MS2 aptamers of modified gRNAs. **(B)** RT-qPCR analysis of *Ascl1* mRNA levels 48 h after transfection. Combining SAM and VPR had a synergistic effect on *Ascl1* expression which reached  $7.3 \pm 0.8 \times 10^3$ -fold expression vs a calculated additive value of  $2.4 \times 10^3$ -fold ( $0.20 \pm 0.09 \times 10^3$ -fold VPR alone,  $2.2 \pm 0.2 \times 10^3$ -fold SAM alone). Direct overexpression of *Ascl1*, led to an increase of  $4.1 \times 10^5 \pm 1.0 \times 10^5$ -fold *Ascl1* mRNA levels. **Abbreviations:** gRNAs *mA1*, *mA2*: gRNAs targeting the murine *Ascl1* promoter, SAM: MS2-P65-HSF1 fusion protein, VP64: four repeats of *Herpes simplex virus* protein VP16, VPR: VP64-P65-RTA fusion protein. Data derived from six independent experiments (three independent experiments for *Ascl1* overexpression), error bars represent mean  $\pm$  SEM, Kruskal-Wallis test, Dunn's multiple comparison test, ns: not significant, \*P < 0.05. Asterisk indicates significant changes to dCas9-VPR alone.

Conversely, a recent article by Chavez *et al.*, 2016 comparing SAM, VPR and the SAM-VPR combination shows no synergistic effect of the two systems [110]. Here, the induction of several genes including *ASCL1* was analyzed in human HEK293 cells. These contradictory results could either be based on species differences (murine Neuro 2a cells vs human HEK293 cells) or differential effects of individual gRNAs used in the experiments.

In order to investigate this, gRNAs targeting the human *ASCL1* promoter were designed with comparable properties (protospacer sequence and distance between gRNA binding sites/ to the TSS) as the murine gRNAs *mA1* and *mA2*. Figure 19A shows an alignment of the 250 bp upstream of the transcription start sites of human and murine *Ascl1*. Large parts show sequence homologies including the binding site of gRNA *mA1* (yellow) which could therefore also be used for human *ASCL1* induction. gRNA *mA2* (dark blue) also bound in a homology area, however with one mismatch at the 5' end of the target sequence. Therefore, a new gRNA termed *seq. matched mA2* (grey) was designed targeting human *ASCL1* at an almost identical sequence as *mA2* with an adjusted 5' nucleotide. Due to additional nucleotides in the human *ASCL1* promoter between the two gRNA binding sites the distance between *mA1* and this new human *seq. matched mA2* gRNA was increased when compared with the original *mA1* and *mA2* gRNAs. To account for possible distance effects a second gRNA termed *dist. matched mA2* (green, Figure 19A) was designed targeting the human *ASCL1* promoter at the same distance to *mA1* as *mA2* did in the murine *Ascl1* promoter.

A comparative RT-qPCR analysis in Figure 19B revealed no significant differences of the sequence and distance matched gRNAs when used with either SAM or VPR systems alone in human HEK293 cells. Interestingly, when SAM and VPR were used together a trend towards higher activation was observed only with the sequence matched gRNA ( $3.9 \pm 0.3 \times 10^3$ -fold for SAM,  $4.9 \pm 0.4 \times 10^3$ -fold activation for SAM with VPR) but not for the distance matched gRNA. However, this effect was not as prominent as in murine Neuro 2a cells earlier. In order to determine whether the synergistic effect in Neuro 2a cells required the combination of both gRNAs (*mA1* and *mA2*), an additional RT-qPCR analysis was performed. Using gRNA *mA2* alone with SAM and VPR systems did not lead to a significant activation of *Ascl1* as shown Figure 19C. Interestingly, the combination of SAM and VPR had a synergistic effect when gRNA *mA1* was used alone (VPR:  $2.1 \pm 03$ , SAM:  $69.7 \pm 17.1$ , SAM and VPR:  $133.0 \pm 34.6$ ). However, the activating properties of gRNA *mA1* alone were limited when compared to the combination of gRNAs *mA1* and *mA2* reaching  $3.7 \pm 0.9 \times 10^3$ -fold induction (Figure 19C).

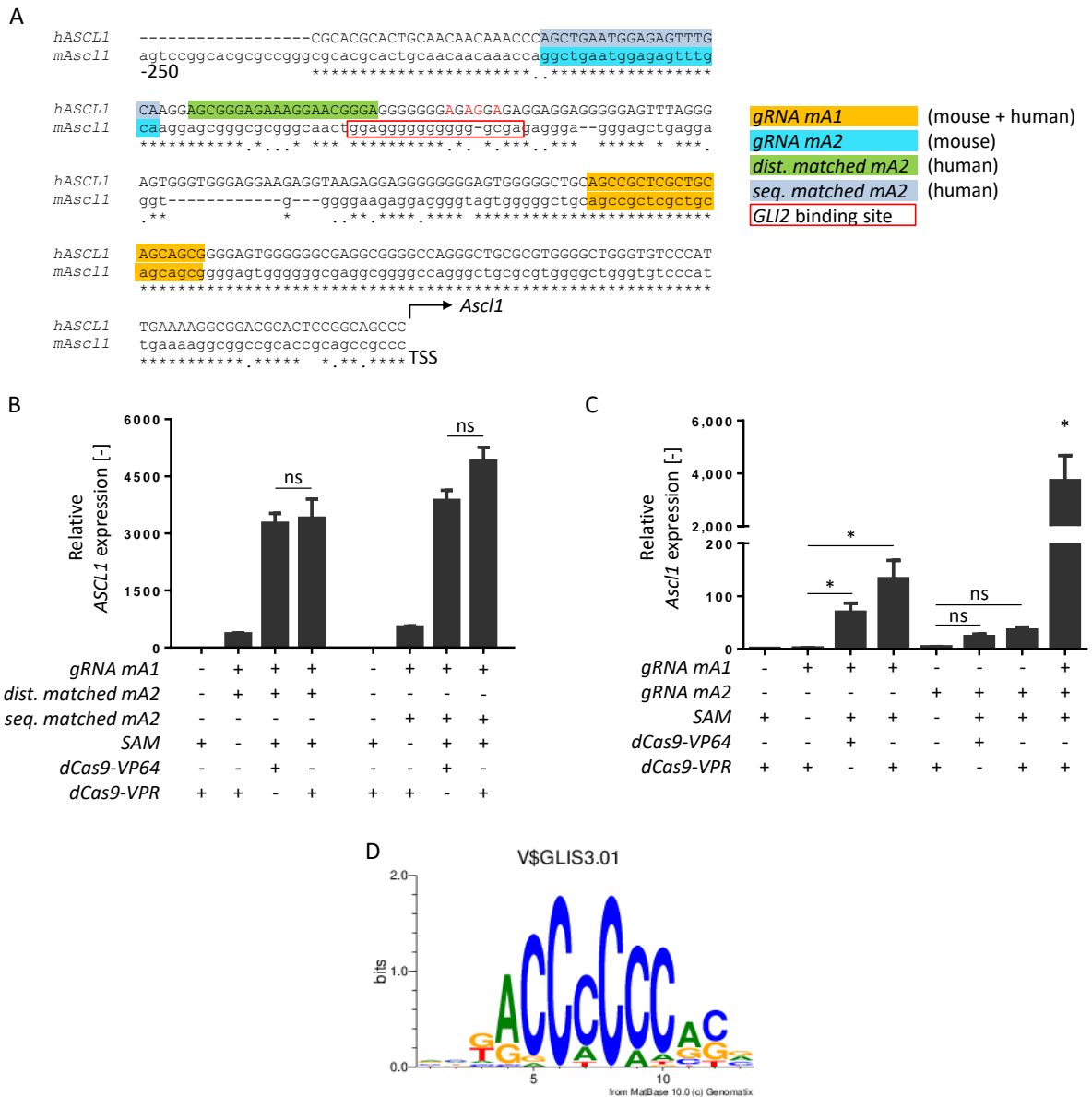


**Figure 19: The synergistic effect of SAM and VPR seems to be based on the gRNA sequence**

**(A)** Alignment of human *ASCL1* and murine *Ascl1* promoter regions 250 nt upstream of the transcription start sites. (\*) indicates sequence homology, (.) indicates a mismatch, (-) indicates a gap in the sequence. gRNA *mA1* (yellow) bound both sequences. For gRNA *mA2* (blue) a human equivalent termed *seq. matched mA2* (grey) was designed with an adjusted 5' nucleotide. The human gRNA *dist. Matched mA2* (green) was designed to compensate the additional nucleotides in the human *ASCL1* promoter thus allowing binding at the same distance to gRNA *mA1* as gRNA *mA2* did in case of murine *Ascl1*. A *Gli2* binding site (red rectangle) was identified adjacent to gRNA *mA2* by D. Trümbach using a Genomatix software tool. This *Gli2* binding site was not identified in the human *ASCL1* promoter due to single nucleotide mismatches (indicated in red). **(B)** RT-qPCR analysis detecting *ASCL1* induction in HEK293 cells 48 h after transfection performed by C. Bach (representative RT-qPCR run). No difference in activation was observed when gRNAs *dist. matched mA2* and *seq. matched mA2* were compared with SAM or VPR alone. When SAM and VPR were combined however, a trend towards higher activation was observed with gRNA *seq. matched* but not gRNA *dist. matched*. **(C)** RT-qPCR analysis of *Ascl1* induction 48 h after transfection of Neuro 2a cells. gRNA *mA1* seemed more powerful than gRNA *mA2* for the induction of *Ascl1*, with a synergistic effect when SAM and VPR were combined. Using both gRNAs with SAM and VPR together however again synergistically increased the level of induction. **(D)** Illustration of GLI protein family consensus binding site derived from Genomatix software by D. Trümbach. The larger a nucleotide symbol, the more conserved it is. **Abbreviations:** Gli: Glioma-associated oncogene family zinc finger, SAM: MS2-P65-HSF1 fusion protein, VP64: four repeats of *Herpes simplex virus* protein VP16, VPR: VP64-P65-RTA fusion protein. Data was derived from three independent experiments. Error bars represent mean  $\pm$  SEM, Kruskal-Wallis test, Dunn's multiple comparison test, ns: not significant, \*P < 0.05.

The role of the transactivation domains comprising SAM and VPR fusion proteins is the recruitment of the transcription machinery to the targeted promoter. The exact binding site of the dCas9 complex in relation to binding sites of transcriptional activators or inhibitors likely influences the transcriptional induction. Binding of dCas9 without any fused transcriptional activators to promoter regions was previously shown to silence gene expression [136]. This may be based on blocked binding sites of endogenous transcription factors or the transcription initiation complex. Conversely, when using dCas9 variants for gene induction it may be favorable to block binding sites of repressor proteins or to recruit endogenous transcription factors to their natural binding sites near the dCas9 complex.

A potential candidate for such a gain-of-function effect is Glioma-associated oncogene family zinc finger 2 (GLI2) which has been reported to bind and induce the murine *Ascl1* promoter [137]. A transcription factor binding site analysis by D. Trümbach revealed a *Gli2* binding site just downstream of gRNA *mA2* indicated in red brackets in Figure 19A. Recruitment of transcriptional activators to this *Gli2* binding site by SAM and VPR systems might therefore benefit *Ascl1* expression. Interestingly, this binding site is not conserved in the human *Ascl1* promoter due to single nucleotide exchanges (red nucleotides in Figure 19A, please note: GLI2 binds the reverse strand at the sequence indicated in Figure 19D). This may contribute to the differences in gene induction observed in human vs murine cells by SAM and VPR systems but has to be investigated in further detail.

Taken together, these data suggested that the choice of gRNAs and activator system are critical and that common rules for the prediction of a suitable system are difficult. Nevertheless, the SAM-VPR system described above seemed to be the most suitable for murine *Ascl1* induction and was therefore chosen for further experiments.

### **5.2.3 Design and generation of lentiviral vectors for SAM and dCas9-VPR delivery**

After having established a suitable system for *Ascl1* induction, an efficient delivery system was required for reprogramming experiments. Lentiviruses were chosen due to the high packaging capacity and transduction efficiency as well as the independency of cell replication for the integration into the host genome. Figure 20A shows the basic components of a third-generation lentiviral vector which allows delivery of up to 7 kb additional insert reaching a total length of 10 kb.

An Eukaryotic translation initiation factor 1A (*Ef1a*) promoter was chosen for the expression of the genes of interest due to its stable and high activity in a wide range of tissues including fibroblasts and neurons [120, 138] and common use in lentiviruses [91, 139].

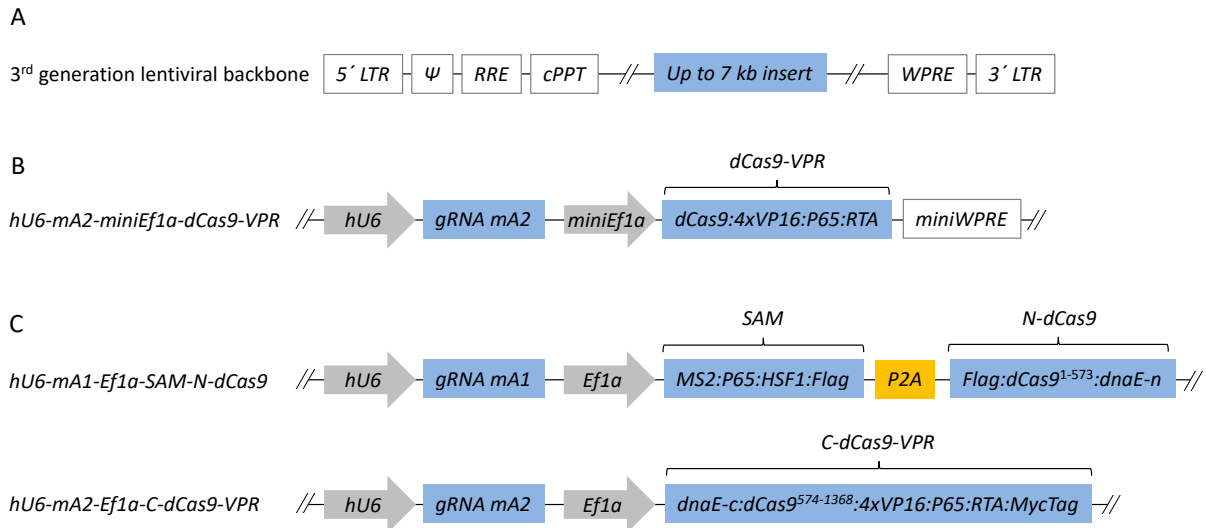


**Figure 20: Schematic illustrations of lentiviral vectors carrying gRNAs, dCas9 and activator components**

**(A)** Structure of a third generation lentiviral backbone flanked by *long terminal repeats (LTRs)*. Further important components are the packaging signal  $\Psi$ , the *rev response element (RRE)* that enables export of transcripts to the cytoplasm, the *central polypurine tract (cPPT)* which serves as recognition site for proviral DNA synthesis and the *woodchuck hepatitis virus post-transcriptional regulatory element (WPRE)* that supports mRNA export to the cytoplasm. Up to 7 kb of DNA including promoters can be added to the lentiviral vector for gene delivery. **(B)** Lentiviral vector carrying gRNA *mA2* and *dCas9-VPR* driven by an intronless *Ef1a* promoter. Furthermore, a shorter version of *WPRE* was used in order to stay below the packaging limit. **(C)** Illustration of the *SAM split dCas9-VPR* system. The two vectors contained all necessary components for gene induction of murine *Ascl1* by *SAM* and *VPR*. One vector carried gRNA *mA1*, *SAM* and *N-dCas9* fused to *N-intein (dnaE-n)*. The second vector contained gRNA *mA2* and a *C-intein-(dnaE-c)-C-dCas9-VPR* fusion. Upon interaction *N-intein* and *C-intein* splice themselves out and generate a seamless *dCas9-VPR* protein. Abbreviations: *C-dCas9*: C-terminal *dCas9* residues 574-1368, *dnaE-c*: C-terminal part of *DNA polymerase III subunit alpha (C-intein)*, *dnaE-n*: N-terminal part of *DNA polymerase III subunit alpha (N-intein)*, *Ef1a*: *Eukaryotic translation initiation factor 1A* promoter, *VP16*: *Herpes simplex virus protein vmw65*, *P65*: *P65* subunit of human *NF- $\kappa$ B*, *RTA*: Human herpesvirus 8 *Regulator of transcription activation*, *N-dCas9*: N-terminal *dCas9*-residues 1-573, *P2A*: *2A sequence of Porcine teschovirus-1*.

Furthermore, in contrast to the *Tet-O* system there would be no need to co-transduce cells with an additional lentivirus carrying the *rTTA2* activator. In chapter 5.1.1 disadvantages of using multiple viruses were described with only a fraction of cells being transduced by all viruses thus decreasing reprogramming efficiencies. Therefore, the goal was to deliver all components required (gRNAs *mA1* and *mA2*, *SAM* and *dCas9-VPR*) with the lowest possible number of viruses. However, the combination of one gRNA and *Ef1a-dCas9-VPR* already exceeds the lentiviral packaging capacity of 10 kb. This packaging limit is not clear-cut but titers decrease in a semi logarithmic fashion with increasing length [140]. Two strategies were therefore tested in order to decrease the length. First: reducing the size of the *Ef1a* promoter and the *WPRE* element in the lentiviral backbone and second: using an intein-mediated *dCas9-VPR* split version similar to the *split-Cas9* system previously established at the institute [141].

Figure 20B shows a lentiviral vector containing gRNA *mA2*, an intronless *Ef1a* promoter (nucleotides 233-1179 deleted) and a shortened *WPRE* element (*WPRE3*) [142]. This allows an overall reduction in size by 1.3 kb to 9.2 kb and thus below the packaging limit. The second strategy with a *split-dCas9-VPR* system is depicted in Figure 20C. Here, the N-terminal residues 1-573 of *dCas9* were fused to *dnaE-n* (*N-intein*) and the remaining C-terminal residues 574-1368 of *dCas9* were fused to *VPR* and *dnaE-c* (*C-intein*). This resulted in the generation of two fusion proteins of which N-intein and C-intein spliced themselves out upon interaction leaving a seamless *dCas9-VPR* protein [141, 143]. In this case *C-dCas9-VPR* was combined with gRNA *mA2* and *N-dCas9* with gRNA *mA1* and *SAM*. In order to simplify nomenclature this system is termed *SAM split-dCas9-VPR* in the following.

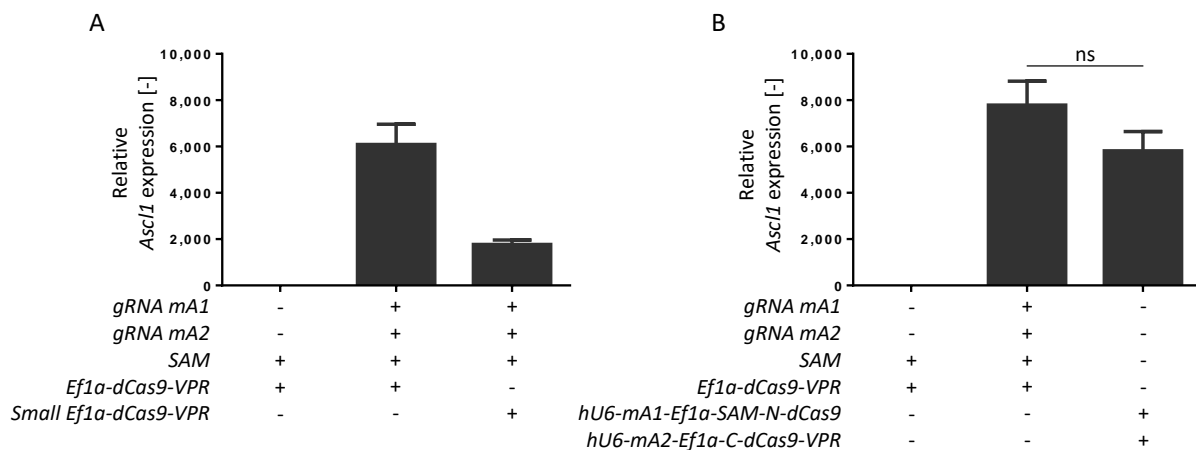


**Figure 21: The *SAM split-dCas9-VPR* system proves to be suitable for gene induction**

RT-qPCR analysis of *Ascl1* induction 48 h after transfection of Neuro 2a cells. **(A)** The use of an intronless *Ef1a* and shorter *WPRE* version was found to result in an approximately threefold reduction of *Ascl1* induction. Representative RT-qPCR run of two independent experiments. **(B)** The *SAM split-dCas9-VPR* system reached activation levels for *Ascl1* which were not significantly decreased when compared to the expression of *SAM* and *VPR* from individual vectors. Abbreviations: *C-dCas9*: C-terminal *dCas9* residues 574-1368, gRNAs *mA1*, *mA2*: gRNAs targeting the murine *Ascl1* promoter, *N-dCas9*: N-terminal *dCas9*-residues 1-573, *SAM*: MS2-P65-HSF1 fusion protein, *VPR*: VP64-P65-RTA fusion protein. Data was derived from three independent experiments. Mann-Whitney test, ns: not significant. Error bars represent mean  $\pm$  SEM.

Although 2A sequences are not cleaved completely as described in chapter 5.1.3 for the *ALN* vector, a P2A sequence was chosen to separate *SAM* and *N-dCas9*. As an alternative an *IRES* could have been used for the translation of *N-Cas9* from a bi-cistronic mRNA. However, the downstream gene of *IRES* is known to be expressed at lower levels [144, 145] perturbing stoichiometric expression levels of *N-dCas9* and *C-dCas9*. Furthermore, only one 2A sequence was used instead of two in the *ALN* construct (see Figure 6A) thus putatively reducing the overall effects of fusion proteins.

Last but not least, P2A has been shown to have the highest cleavage efficiency of commonly used 2A sequences in a variety of different cell types and was therefore chosen [119].

RT-qPCR analysis of the newly generated construct comprising an intronless *Ef1a* promoter and a short version of *WPRE* suggested a much lower level of *Ascl1* induction compared to the full-length version depicted in Figure 21A and was therefore not followed up any further ( $6.1 \pm 0.9$  vs  $1.8 \pm 0.2 \times 10^3$ -fold induction). The new *SAM split-dCas9-VPR* system was not significantly different to *SAM* and *dCas9-VPR* expressed from individual vectors although a slight decrease in activity from  $7.8 \pm 1.0 \times 10^3$  to  $5.8 \pm 0.9 \times 10^3$ -fold induction can be observed in Figure 21B. The *SAM split-dCas9-VPR* system was therefore used for further experiments and virus production since packaging limits were not exceeded and all components required for the induction of *Ascl1* could be carried by just two lentiviruses.

#### 5.2.4 Challenges in lentiviral Cas9 packaging

Having established the functionality of the newly generated *SAM split-dCas9-VPR* system by lipofection and RT-qPCR the next step was lentiviral production for reprogramming experiments. However, in several attempts lentiviral titers were low with only  $1 \times 10^5$  -  $1 \times 10^6$  total infectious particles per harvest whereas former harvests e.g. for *ALN* lentiviruses were in the range of  $1 \times 10^{10}$  -  $1 \times 10^{11}$  viral particles. With such a low titer a complete harvest ( $1.5 \times 10^5$  viral particles) would be required for a single well of a 24-well plate in order to transduce cells at a multiplicity of infection of three (MOI 3). Titers from colleagues also working with lentiviral *Ef1a-Cas9* vectors were comparably low suggesting possible adverse effects of the *dCas9* coding sequences or gRNA secondary structures for lentiviral packaging (personal communication). This was surprising, as similar designs have been published comprising e.g. an *Ef1a* promoter and *dCas9-VP64* [91]. However, in this publication selection markers were used to obtain a stable cell line where low numbers of transduced cells are not the limiting factor. Unfortunately, such a selection process is not suitable for reprogramming of primary cells (unpublished experimental data of collaborating group).

One alternative to viral delivery of *Cas9* would be lipofection which was utilized for the conversion of embryonic stem cells to extraembryonic lineages [106]. However, the efficiency of gene delivery in astrocytes was found to be  $\ll 1\%$  by lipofection (approximately  $70 \pm 20$  total cells 14 days after seeding  $5 \times 10^4$  cells, data not shown) compared to approximately 30 – 40% transduced cells by lentiviruses. This underlines the need for an efficient lentiviral delivery system.

Therefore, one idea was to invert the cassette including the gRNA sequence, *dCas9* components and activator complexes in order to prevent unintentional translation from the viral RNA during packaging or possible inhibitory effects due to secondary structures of the gRNA. However, a first RT-qPCR analysis suggested a strong decrease in *Asc11* induction from  $4.7 \pm 0.1 \times 10^3$  to  $0.30 \pm 0.02 \times 10^3$ -fold upon inversion of the cassette as depicted Figure 22A. This system was therefore not used for further tests. Another possible solution was the exchange of the *Ef1a* promoter as Black *et al.*, [107] report in a current article for the first time reprogramming of fibroblasts to neurons using *dCas9* expressed from lentiviruses by a human Ubiquitin C (*hUBC*) promoter. This was surprising as *hUBC* is a comparably weak promoter [120] and it was expected that high levels of expression would be beneficial for successful reprogramming (see Figure 8B and C). Nevertheless, sufficient lentiviral packaging must have been accomplished by Black *et al.*, [107].

Therefore, lentiviral production was repeated with a *hUBC* promoter and additionally a *Tet-O* promoter as an alternative known for its high levels of expression [120]. Interestingly, the replacement of the *Ef1a* promoter increased lentiviral titers to  $3 \times 10^8$  (*hUBC-Cas9*) and  $1 \times 10^9$  (*Tet-O-Cas9*) total viral particles per harvest. As expected, *Tet-O-Cas9* was expressed at much higher levels than *hUBC-Cas9* which was close to the detection limit of the immunocytochemistry analysis depicted in Figure 22C.

The *Tet-O* construct was chosen for further experiments due to its high level of expression and the possibility to influence timing and activity by adjusting the doxycycline concentration (see chapter 5.1.5). A RT-qPCR screen shown in Figure 22B comparing the *SAM split-dCas9-VPR* system using *Ef1a* or *Tet-O* promoters confirmed the functionality of the new *Tet-O* constructs. Western blot analysis in Figure 22D using a Cas9 antibody revealed successful generation of N-dCas9 at 80 kDa from newly generated viruses with comparable band patterns and intensities to transfected cells. A fraction of total N-dCas9 was found as a fusion protein with SAM at 130 kDa due to inefficient ribosome skipping at the P2A site separating SAM and N-dCas9. Upon addition of *C-dCas9-VPR* viruses a shift in size was observed indicating successful assembly of N- and C-dCas9 parts at 218 kDa.

These findings were confirmed by visualization of C-dCas9-VPR via a MycTag in a second western blot in Figure 22E. The newly generated *SAM split-dCas9-VPR* viruses were therefore successfully packaged and *dCas9-VPR* was able to assemble itself after transduction.

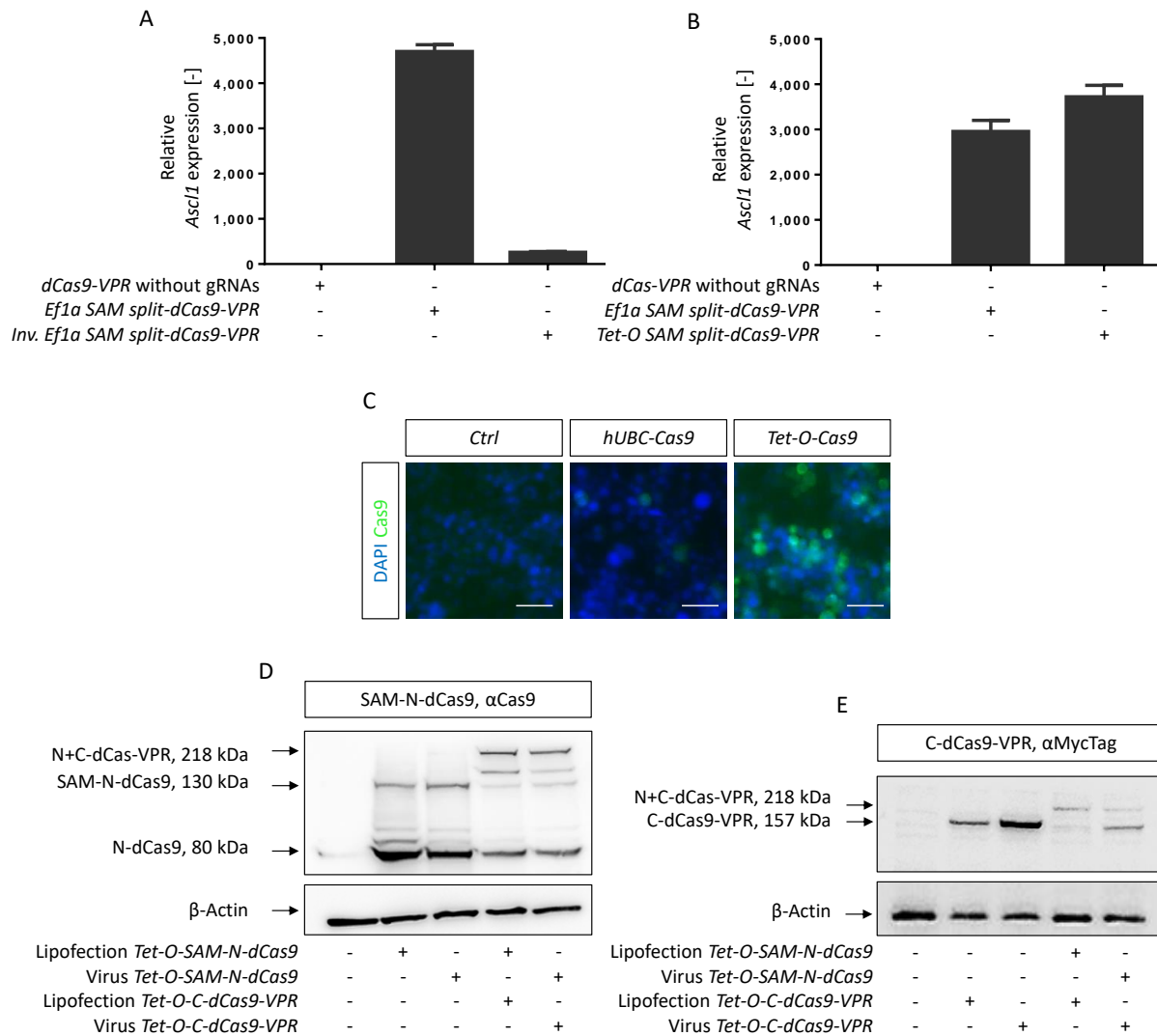


**Figure 22: Replacement of *Ef1a* by *Tet-O* or *hUBC* promoters enables lentiviral packaging of *dCas9***  
**(A)** RT-qPCR analysis of *Ascl1* induction in Neuro 2a cells 48 h after transfection. Inversion of the expression cassette of *split-dCas9-VPR* (*hU6-mA1-Ef1a-SAM-N-dCas9* + *hU6-mA2-Ef1a-C-dCas9-VPR*) resulted in a strong decrease in *Ascl1* expression. In this case, expression cassettes including promoters and gRNAs were inverted relative to the lentiviral backbone (see Figure 20C for comparison). **(B)** RT-qPCR of *Ascl1* induction comparing *split-dCas9-VPR* system with *Ef1a* or *Tet-O*-promoters revealed similar levels of activation for the two promoters. **(C)** Immunocytochemistry analysis of Cas9 in HEK293 cells 48 h after transduction by 0.5  $\mu$ l lentiviruses encoding *hUBC-Cas9* or *Tet-O-Cas9*. While the percentage of Cas9<sup>+</sup>/DAPI<sup>+</sup> cells was comparable the expression level in *hUBC-Cas9* transduced cells was much lower as suggested by the different intensities of the Cas9 signal. **(D)** Western blot analysis using an  $\alpha$ -Cas9 antibody detecting N-terminal Cas9 only. Viruses were functional as assessed by comparable bands of transfected and transduced cells. The P2A splicing between SAM and N-dCas9 was not complete as expected. However, with the majority of N-dCas9 correctly cleaved. Upon adding C-dCas9-VPR N- and C-parts assembled to dCas9-VPR at 218 kDa. **(E)** Western blot analysis using an  $\alpha$ -MycTag antibody for the detection of C-dCas9-VPR. The C-dCas9-VPR virus was functional with protein bands similar to transfected cells showing successful assembly of dCas9-VPR upon addition of N-dCas9. **Abbreviations:** C-dCas9: C-terminal dCas9 residues 574-1368, *Ef1a*: *Eukaryotic translation initiation factor 1A promoter*, N-dCas9: N-terminal dCas9-residues 1-573, SAM: MS2-P65-HSF1 fusion protein, *hUBC*: *human ubiquitin C promoter*, VPR: VP64-P65-RTA fusion protein. Scale bars: 50  $\mu$ m. Data was derived from one experiment. Error bars represent mean  $\pm$  SEM.

### 5.2.5 Direct reprogramming of astrocytes to neurons utilizing SAM and VPR

As a final step the reprogramming potential of the established SAM split-dCas9-VPR system was tested in primary cortical astrocytes isolated from CD1 mice at the age of five to six days. This system was chosen over MEFs as astrocytes are closer to a future *in vivo* situation where viruses should be injected into the mouse brain. Forskolin was again added to the differentiation medium (see Table 6) since conversion efficiency of astrocytes to neurons and their survival are increased upon induction of the forskolin target gene B-cell leukemia/ lymphoma 2 (*Bcl2*) [128, 146].

The disadvantage of primary cortical cells is the composition of the cell population which also includes neuronal precursors. In order to distinguish between newly reprogrammed neurons and those derived from precursors already present in the culture at the day of lentiviral transduction *dsRed* expressing lentivirus was added to control wells.

Figure 23A shows *dsRed*<sup>+</sup> cells at day 16 post transduction of which a fraction was also MAP2<sup>+</sup> indicating the basal level of neurons / neuronal precursors being transduced by lentiviruses. Immunocytochemistry analysis of cells transduced by *SAM split-dCas9-VPR* revealed FlagTag<sup>+</sup> cells (marker for N-dCas9 and SAM) which were also MAP2<sup>+</sup> suggesting putatively successful reprogramming of astrocytes to neurons in Figure 23A. Direct overexpression of *Ascl1* clearly resulted in an increase of MAP2<sup>+</sup> cells of which most seemed to be also ASCL1<sup>+</sup> (Figure 23A).

Figure 23B shows a quantification of MAP2<sup>+</sup> cells per DAPI with  $9.3 \pm 1.6\%$  neurons per DAPI in the control condition (*dsRed* virus). This percentage was doubled to  $18.5 \pm 3.6\%$  MAP2<sup>+</sup> cells in the *SAM split-dCas9-VPR* condition demonstrating successful reprogramming of astrocytes to neurons. The increase in neurons was not based on a higher transduction efficiency of *SAM split-dCas9-VPR* encoding lentiviruses as Figure 23C shows comparable transduction efficiencies of the lentiviruses used. When only looking at transduced cells (*dsRed*<sup>+</sup> or FlagTag<sup>+</sup>) the percentage of MAP2<sup>+</sup> cells slightly increased from  $13.4 \pm 2.4\%$  (*dsRed*) to  $18.7 \pm 2.2\%$  (*SAM split-dCas9-VPR*) in Figure 23D.

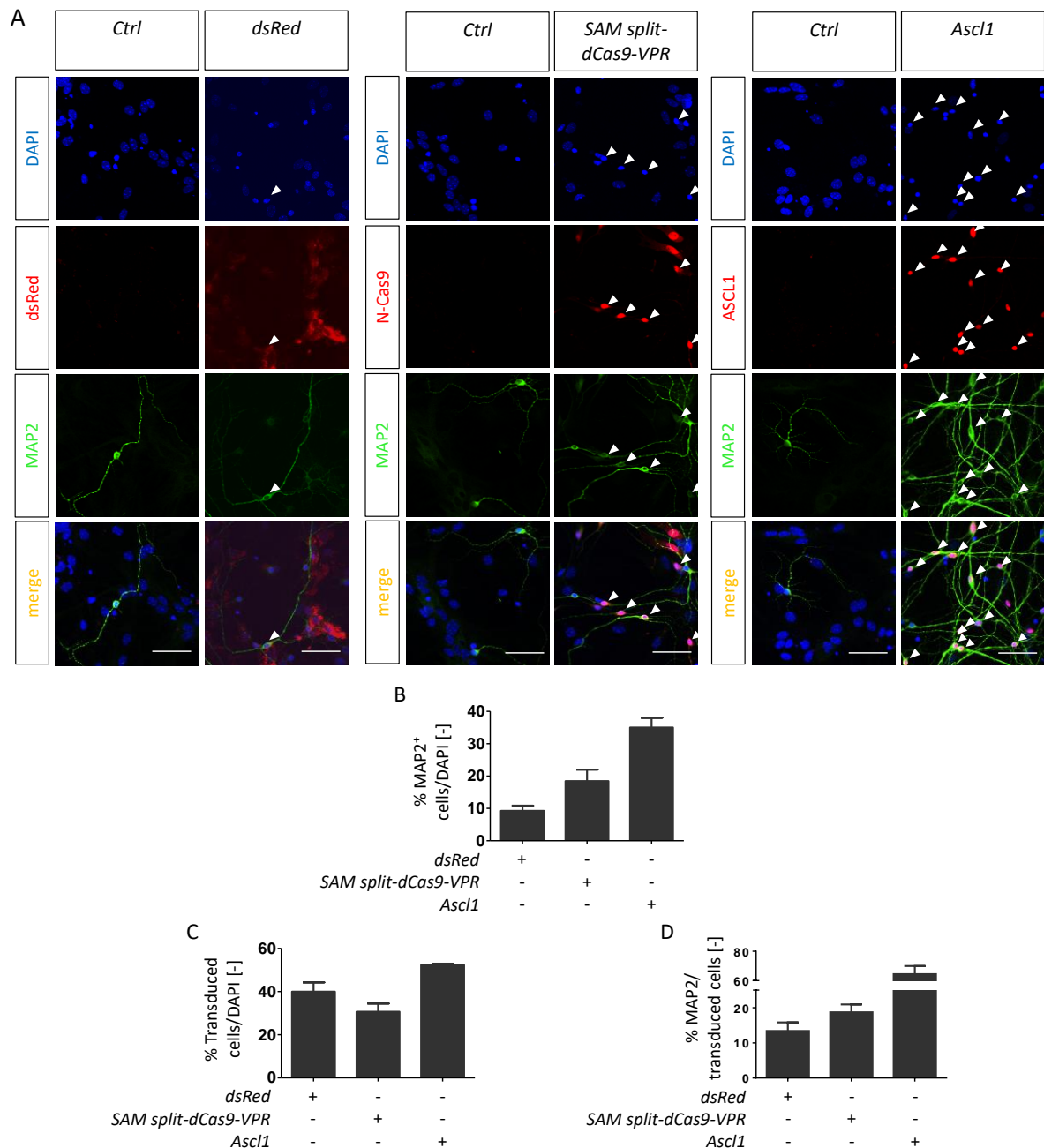


**Figure 23: Successful conversion of astrocytes to neurons utilizing the SAM split-dCas9-VPR system delivered by lentiviruses**

**(A)** Immunocytochemistry analysis of reprogrammed cells 16 days after transduction revealed successful reprogramming of astrocytes to neurons using the SAM split-dCas9-VPR system. *Tet-O-dsRed* lentivirus was used at MOI 1, *hU6-mA1-Ef1a-SAM-N-dCas9* at MOI 3, 0.5  $\mu$ l of *hU6-mA2-Ef1a-C-dCas9-VPR* virus were used due to difficulties in the detection of the MycTag for titer determination and *Tet-O-Ascl1* was used at MOI 1. **(B)** Quantification of MAP2<sup>+</sup> neurons/DAPI revealed an increase from  $9.3 \pm 1.6\%$  (*dsRed*) to  $18.5 \pm 3.6\%$  MAP2<sup>+</sup> cells for SAM split-dCas9-VPR and  $35.0 \pm 3.0\%$  (*Tet-O-Ascl1*) MAP2<sup>+</sup> cells suggesting successful reprogramming. **(C)** Quantification of transduced cells per DAPI. dsRed served as control for the transduction rate of neurons already present in the mixed culture at the day of transduction. The percentage of FlagTag<sup>+</sup> (detection of *N-dCas9* and SAM) and ASCL1<sup>+</sup> (detection of *Tet-O-Ascl1*) cells was comparable to dsRed. **(D)** Quantification of MAP2<sup>+</sup> neurons per transduced cells. Only dsRed<sup>+</sup>, FlagTag<sup>+</sup> or ASCL1<sup>+</sup> cells were checked for co-expression of MAP2.  $13.4 \pm 2.4\%$  of dsRed transduced cells were MAP2<sup>+</sup> indicating the basal fraction of neurons transduced by viruses. The use of SAM split-dCas9-VPR revealed a slight increase in MAP2<sup>+</sup>/FlagTag<sup>+</sup> cells to  $18.7 \pm 2.2\%$  indicating successful conversion of astrocytes to neurons.  $64.4 \pm 5.5\%$  of all ASCL1<sup>+</sup> cells were MAP2<sup>+</sup>. **Abbreviations:** MAP2: Microtubule-associated protein 2, SAM: MS2-P65-HSF1 fusion protein, TH: Tyrosine hydroxylase, VPR: VP64-P65-RTA fusion protein. Scale bars: 50  $\mu$ m. Data was derived from two independent experiments. Error bars represent mean  $\pm$  SEM.

These promising data indicated successful proof of concept experiments for the SAM split-dCas9-VPR system. Direct overexpression of *Ascl1* as a positive control ( $64.4 \pm 5.5\%$  MAP2<sup>+</sup> neurons / transduced cells) exceeded the effects of the SAM-VPR system putatively due to the higher expression level of *Tet-O-Ascl1* already observed in RT-qPCRs and also based on the fact that the split-Cas9 system required co-transduction and assembly of *N-dCas9* and *C-dCas9*. However, the CRISPR/Cas9 system is a promising new tool for direct conversion of somatic cells and might show its full potential when several genes have to be induced simultaneously e.g. for the generation DA neurons where common reprogramming strategies reach their limits.

RT-qPCR data revealed a synergistic effect when SAM and VPR systems were combined. In order to investigate a possibly similar effect for reprogramming different dCas9 versions were tested. At this point viruses carrying SAM or VPR alone were not available. DNA was therefore transferred using Lipofectamine LTX with Plus Reagent into astrocytes. Transfection efficiency of these primary cells was much lower than viral transduction ( $< 1\%$ ) and transiently expressed genes were hardly detectable by immunocytochemistry 16 days after transfection (data not shown). Therefore, *dsRed* which was still detectable at this time point was co-transfected with *dCas9* components. All *dsRed*<sup>+</sup> cells were analyzed for MAP2 expression and a neuronal morphology.

Figure 24A shows successfully reprogrammed cells for all dCas9 fusion proteins analyzed. Reprogramming efficiencies were quantified in Figure 24B showing successful reprogramming by SAM ( $15.2 \pm 0.9\%$  MAP2<sup>+</sup> cells per *dsRed*), VPR ( $9.8 \pm 2.9\%$  MAP2<sup>+</sup> cells per *dsRed*) or the combination of SAM and VPR (SAM split-dCas9-VPR,  $9.8 \pm 2.2\%$  MAP2<sup>+</sup> cells per *dsRed*). A synergistic effect of SAM and VPR however, could not be observed. This has to be analyzed in further experiments in detail.

Taken together, these reprogramming experiments for the first time show successful CRISPR/Cas9 based conversion of astrocytes to neurons. This is a very promising starting point for further optimizations of the system in order to increase reprogramming efficiencies and to investigate simultaneous activation of multiple genes.

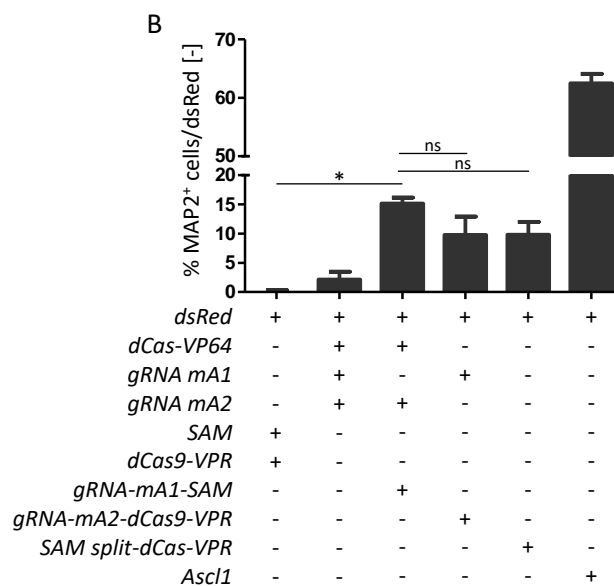
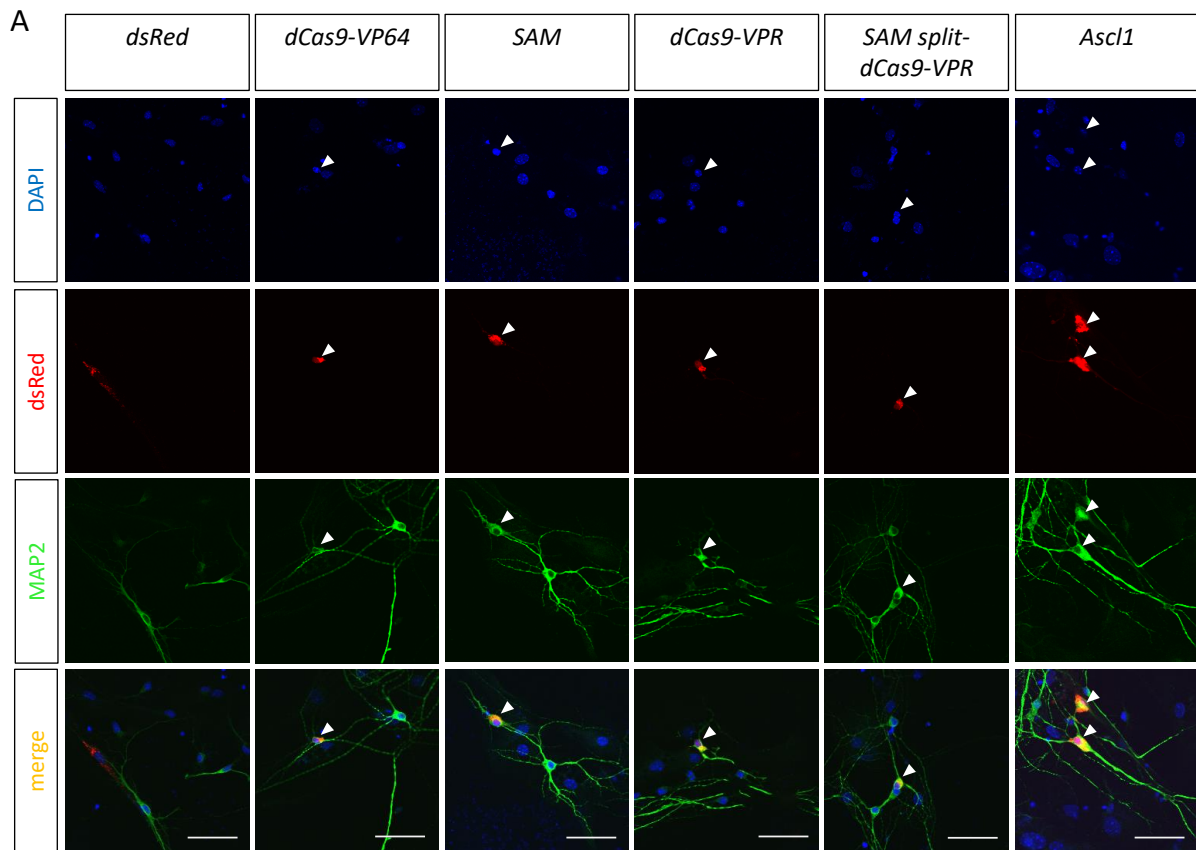


**Figure 24: The reprogramming potential of SAM or VPR alone is comparable to the SAM split-dCas9-VPR system in lipofection experiments**

(A) Immunocytochemistry analysis shows dsRed<sup>+</sup>/MAP2<sup>+</sup> cells indicating successful reprogramming 16 days after lipofectamine LTX transfection of astrocytes for all dCas9 variants tested. dsRed was co-transfected with all conditions in order to identify transfected cells. (B) Quantification of reprogrammed cells 16 days after lipofection. All dsRed<sup>+</sup> cells were checked for neuronal morphology and MAP2 expression. Due to different background levels of neurons in control wells, the percentage of dsRed<sup>+</sup> neurons in control wells was subtracted from all wells of an individual experiment. SAM alone seemed most potent for reprogramming but was not significantly different from dCas9-VPR or the combination of SAM and dCas9-VPR. Scale bars: 50 μm. Data was derived from three independent experiments, error bars represent mean ± SEM, Kruskal-Wallis test, Dunn's multiple comparison test, ns: not significant, \*P < 0.05.

## DISCUSSION

## 6 Discussion

### 6.1 Limitations of exogenous gene expression for direct reprogramming

#### 6.1.1 The requirement of co-transductions limits the reprogramming efficiency

Direct conversion of somatic cells such as fibroblasts to DA neurons is seen as a promising source for cell replacement therapies in PD. For this purpose, combinations of three to six different transcription factors are usually delivered by individual lenti- or retroviruses [32-37]. However, in chapter 5.1.1 of this thesis it was shown that co-transduction is already a limiting factor when analyzing the co-expression of just two factors (*Ascl1*, *Nurr1*). Here, only a fraction of cells was ASCL1<sup>+</sup>/NURR1<sup>+</sup> thus restricting the number of cells which could potentially be converted to DA neurons. In this case a multiplicity of infection of three (MOI 3) was used meaning that a threefold excess of viral particles was applied to cells.

One way to increase the transduction efficiency would be adding more viral particles. However, using *Ascl1*, *Lmx1a* and *Nurr1* (A+L+N) encoding lentiviruses each at MOI 10 reduced the reprogramming efficiency by 90% indicating adverse effects of high lentiviral concentrations (see appendix Figure 26). Therefore, increasing the number of lentiviral particles was not found to be an adequate option to improve reprogramming efficiencies.

#### 6.1.2 The high reprogramming efficiency of Caiazzo *et al.*, seems to be influenced by the reporter system

Caiazzo *et al.*, who originally described the A+L+N combination (unknown MOI) claimed a reprogramming efficiency of approximately 18% TH<sup>+</sup> DA neurons [37]. These numbers could neither be reproduced in this thesis (approximately 2% TH<sup>+</sup> cells, chapter 5.1.2) nor by others so far. A difference in the reprogramming protocols was the composition of the cell culture medium used during differentiation. While in the underlying thesis a 50:50 mixture of DMEM/F12 medium (addition of N2 supplement) and Neurobasal medium (addition of B27 supplement) was used (see Table 6 for further details), Caiazzo *et al.*, conducted their differentiation in DMEM/F12 medium with N2 supplement comprising the same constituents as N2 but at partially altered concentrations [37, 147]. This included a five-fold insulin concentration, 0.5-fold transferrin and 0.1-fold putrescine (see appendix, Figure 27 for details) – three factors important for cell proliferation in serum free media [148]. However, since B27 supplement also comprises these factors - although at unknown concentrations due to confidentiality reasons - it is unclear how individual concentrations in the mixed medium of this thesis compare to the medium of Caiazzo *et al.*

Therefore, reprogramming experiments were repeated with the cell culture medium of Caiazzo *et al.* with no significant effect on the number of reprogrammed cells (appendix, Figure 27). Thus, the medium composition was excluded as possible cause for the low reprogramming efficiency.

A factor that might influence the reprogramming efficiency is the origin of the MEFs utilized. In the underlying thesis MEFs were derived from *Pitx3<sup>GFP/+</sup>* mice [149] where TH expression has to be visualized by immunocytochemistry analysis. Caiazzo *et al.* utilized a transgene *Th-Gfp* reporter mouse line expressing *Gfp* under the control of the rat *Th* promoter [150] and GFP<sup>+</sup> cells were counted as successfully reprogrammed TH neurons. The GFP<sup>+</sup> domain in the respective mouse model however, was found to exceed the TH<sup>+</sup> population with only 60% of GFP<sup>+</sup> cells also expressing TH [150]. The numbers published by Caiazzo *et al.* may therefore overestimate the reprogramming efficiency. Taken together, co-transduction by multiple lentiviruses limits the reprogramming efficiency which could not be overcome by increasing the virus concentration or by changing the medium composition.

### 6.1.3 Forskolin treatment enables the generation of PITX3<sup>+</sup> DA neurons

In order to improve reprogramming efficiencies small molecules can be beneficial as an alternative to the addition of lineage specific transcription factors [121]. For example, forskolin (activator of cAMP signaling) together with dorsomorphin (inhibitor of bone morphogenic protein (BMP) signaling) has previously been shown to enable direct conversion of Neurogenin 2 transduced fibroblasts to cholinergic neurons, while Neurogenin 2 alone was not sufficient for direct reprogramming [121]. The authors did not investigate the underlying mechanisms of forskolin and dorsomorphin regarding the reprogramming process but it became clear that activating general pathways such as cAMP signaling can benefit neuronal differentiation.

In chapter 5.1.6 of this thesis, forskolin treatment of *A+L+N* transduced MEFs was found to result in a slight increase in the reprogramming efficiency to TH<sup>+</sup> DA neurons. Interestingly, forskolin does not affect *TH* expression but only the translation of *TH* mRNA via induction and binding of Poly(rC)-binding protein 2 (PCBP2) to the 3'-UTR of *TH* mRNA [126, 127]. The observed effect may therefore be based on higher levels of TH protein in low expressing cells which could now be detected by immunocytochemistry. Alternatively, the pro-survival effect of forskolin may play a role. Forskolin has previously been described to induce anti-apoptotic responses via upregulation of *Bcl2* and inhibition of *Caspase 3* and *Caspase 9* [128]. This protective effect of forskolin seems to be based on reduced lipid peroxidation which is a hallmark of ferroptosis [146, 151]. Nevertheless, a general effect on the survival of cells by forskolin treatment was not observed in this thesis as assessed by the number of DAPI<sup>+</sup> cells per mm<sup>2</sup>. This could be explained by the findings of Michel *et al.*, who report a

specific effect of increased cAMP signaling on the survival of mdDA neurons *in vitro* while e.g. GABAergic and serotonergic neurons showed a much lower dependency [152]. With approximately 1 – 2% of all cells being reprogrammed to TH<sup>+</sup> neurons these putatively cell type specific anti-apoptotic effects of forskolin therefore hardly affect the overall number of surviving cells but seem to be beneficial for the reprogrammed cells.

While several groups report direct conversion of fibroblasts to DA neurons, these cells often do not express the midbrain DA marker *Pitx3* [33-35, 37] meaning that these cells do not correspond to the DA subtype affected in PD [14]. Previous experiments at the institute confirmed that *A+L+N* overexpression is not sufficient for the generation of PITX3<sup>+</sup> DA neurons (dissertation F. Meier). This is somewhat surprising as both *Lmx1a* and *Nurr1* were found to directly activate *Pitx3* expression [52, 62]. A possible reason might be an inaccessibility of NURR1 and LMX1A binding sites in MEFs. In this thesis treatment of *A+L+N* transduced MEFs with the cAMP signaling activator forskolin was found to enable the generation of PITX3<sup>+</sup> DA neurons. This is a very promising result, as previous reprogramming protocols required co-delivery of five to six different transcription factors to a single cell for the generation of PITX3<sup>+</sup> DA neurons [32, 36].

Activation of cAMP signaling is known to support the differentiation of progenitor cells to mdDA neurons and is therefore commonly induced during terminal differentiation protocols of iPS cells, embryonic stem cells or ventral midbrain tissue [153-155]. A connection between forskolin and the direct reprogramming to DA neurons and *Pitx3* expression however, had not been made yet. One possible link between cAMP signaling and *Pitx3* expression could be Glial cell-line derived neurotrophic factor (GDNF). GDNF is a highly selective neurotrophic factor implicated in the survival of DA neurons [156] which has been shown to induce *Pitx3* expression [15]. The pro-survival effect of GDNF on DA neurons was found to be potentiated by cAMP signaling *in vitro* suggesting a crosstalk between cAMP and GDNF signaling pathways [157]. Whether forskolin indeed influences *Pitx3* expression via GDNF signaling however remains to be explored.

In conclusion, the addition of forskolin seems to support direct reprogramming of MEFs to DA neurons either via up-regulating *TH* translation or due to pro-survival effects. Furthermore, forskolin treatment of *A+L+N* transduced cells enabled the generation of ‘true’ mdDA neurons which is a promising starting point for further functional tests of these neurons *in vivo*.

#### 6.1.4 Inefficient ribosome skipping at 2A sites results in fusion proteins and cell death

In order to overcome the limitations of co-transduction, a tri-cistronic lentiviral vector encoding *Ascl1*, *Lmx1a* and *Nurr1* (*ALN*) was previously generated by F. Meier at the institute. Here, the three transcription factors were separated by 2A peptides (P2A, T2A) inducing ribosome skipping during protein biosynthesis and subsequent production of 'cleaved' ASCL1, LMX1A and NURR1 proteins. Surprisingly, reprogramming efficiencies with the tri-cistronic *ALN* vector were quite low (< 1% TH<sup>+</sup> cells). In this thesis, the generation of fusion proteins in large quantities could be shown in chapter 5.1.3 which likely accounts for the low reprogramming efficiency of the *ALN* construct.

While some reports claim almost complete separation of proteins at 2A peptides [158, 159] others have also reported the generation of fusion proteins [119]. P2A and T2A differ not only in their sequence but also in the efficiency of 'cleavage' which is strongly influenced by the cell type ranging from 50 – 90% for T2A and 80 – 95% for P2A [119]. Across a number of cell types P2A was found to have the highest efficiency in peptide separation of all tested 2A sequences [119]. Using only P2A due to the higher performance rate could be an option for DNA based gene delivery, but in lentiviruses repeat sequences bear the risk of recombination and thus deletions [160]. Therefore, P2A and T2A were used in the tri-cistronic *ALN* vector. Inefficient cleavage of P2A and T2A peptides added up generating a high proportion of fusion proteins consisting of two or three transcription factors. The low reprogramming efficiency of *ALN* may therefore be caused by fused and thus inactive transcription factors resulting in lower expression of their target genes.

However, incorrect or completely unfolded transcription factors can also trigger a process termed unfolded protein response [161]. This was observed in a conditional *Rosa26*<sup>CAG:ALN/+</sup> mouse line generated at the Helmholtz Zentrum München which carries the tri-cistronic *ALN* cassette [118]. These mice were crossed to *Tnap*<sup>TgCreER2/+</sup> and *Nestin-Cre* mice for *in vivo* analysis of the reprogramming potential in pericytes and neural stem/precursor cells, respectively [118]. Surprisingly, while TH<sup>+</sup> neurons were obtained *in vitro*, albeit at low numbers, *in vivo* reprogramming to DA neurons was completely absent. Further analysis *in vivo* revealed apoptosis in *ALN* expressing cells partially due to endoplasmic reticulum stress and unfolded protein response [118]. This was not investigated in detail *in vitro* but likely contributes to the reduced reprogramming efficiency of the tri-cistronic vector observed in this thesis.

Alternatives to 2A peptides could be internal promoters, *IRES* sequences or proteolytic processing e.g. by furins. However, when using multiple promoters transcriptional interference and promoter suppression have been reported especially in RNA viruses [162,

163]. Furthermore, the size of the vector would be significantly increased by additional promoters thus exceeding the lentiviral packaging limit. As mentioned earlier, *IRES* dependent expression usually reaches only 20 – 50% of the upstream gene thus preventing high levels of expression at equimolar ratios [144]. Finally, proteolytic processing by furins seems to be highly efficient [158] but can only be applied to secreted proteins as furins reside in the golgi apparatus [164]. Taken together, with all strategies having some drawbacks co-transduction by individual lentiviruses may be better suited than a tri-cistronic approach. However, several groups are working with up to six different transcription factors for the conversion of fibroblasts to DA neurons [32-34, 36]. In these publications reprogramming efficiencies were rather low in the range of 0.05 - 2.5% TH<sup>+</sup> cells certainly also due to the required co-transduction of up to six different viruses.

In conclusion, direct conversion of somatic cells by overexpression of exogenous factors has several downsides. When using single viruses to deliver the genes of interest, the efficiency of co-transductions is a limiting factor. By choosing a multi-cistronic vector the necessity of co-transduction can be overcome but the generation of fusion proteins leading to cell death and a decrease in the reprogramming efficiency was detected. It is therefore of interest to develop new tools circumventing these disadvantages. One promising system is the CRISPR/Cas9 technology which may show its full potential especially when a number of genes needs to be induced simultaneously by a pool of sequence specific gRNAs.

## **6.2 Utilizing CRISPR/Cas9 technology for gene induction and direct cell conversion**

### **6.2.1 The importance of gRNA screenings for transcriptional activation**

The design and selection of suitable gRNAs is crucial for any CRISPR/Cas9 based application in order to ensure specific and strong binding to target sites. Several factors should be considered including on- and off-target scores, position of the targeted sequence relative to the gene of interest and the combination of gRNAs. In this thesis, initially a single gRNA (gRNA A5) was found to efficiently induce the expression of *Ascl1* in Neuro2a and HEK293 cells (see chapter 5.2.1). Co-expression with other gRNAs did not result in synergistic effects. While this finding is in line with some reports [108, 109], by now most groups work with multiple gRNAs showing synergistic effects on gene induction [90, 106, 113, 165].

It was therefore of interest to find gRNAs providing such a beneficial synergistic effect as direct conversion of cells seems to require high levels of expression [166]. While gRNA A5 was chosen due to a low off-target score, the second generation of gRNAs targeting the

murine *Ascl1* promoter (*mA1* - *mA5*) was chosen due to high on-target scores suggesting improved binding to DNA. gRNAs *mA1* and *mA2* were identified as top ranked gRNAs binding the *Ascl1* promoter with on-target scores of 57 and 61 out of 100, respectively. Indeed, these new gRNAs showed a synergistic effect when applied together. Interestingly, the level of gene induction could not be further increased by adding additional gRNAs *mA3*, *mA4* or *mA5* (on-target scores of 61, 30, 41, respectively). The total number of gRNAs required for a maximum effect seems to be highly gene and locus dependent ranging mostly from one to four gRNAs [89, 108, 165]. Interestingly, replacement of *mA2* by *mA3* resulted in a much lower *Ascl1* expression level although binding sites (shift by five nucleotides) and on-target scores (both 61) were almost identical. Chromatin accessibility was found not to influence CRISPR/Cas9 based gene induction [113]. It has therefore been speculated that differential effects of gRNAs with comparable properties could be due to competitive binding events with endogenous transcription factors [108, 113]. This suggests that the on-target score can be suitable to identify gRNAs with excellent binding properties but does not necessarily predict gene induction potential.

When thinking ahead to possible *in vivo* applications of CRISPR/Cas9-based gene induction the risk of off-target effects should be addressed. gRNAs were previously found to partially bind off-target sequences despite mismatches [167]. In case of wt Cas9 nucleases off-target effects can have severe consequences due to unwanted double-strands breaks and subsequent frame-shift mutations [168]. For gene induction however, off-target effects only play a minor role. The requirement to bind near a transcription start site (ideally within the first 250 nt upstream of TSS [89, 91, 106]) in order to induce gene expression already decreases the number of loci that could be affected. Furthermore, the observed synergistic effect of multiple gRNAs also plays a protective role as co-binding of several gRNAs to a single off-target promoter seems even less likely. This is supported by the findings of Perez-Pinera *et al.*, who report no detectable off-target effects of CRISPR/Cas9-based gene induction in a RNA-seq analysis [113].

To conclude this part, although tools are available to predict binding properties of gRNAs, screenings are still required to identify an optimal set of gRNAs to induce the expression of target genes at high levels.

## 6.2.2 Screenings of dCas9 fusion proteins for an efficient gene induction

Besides identifying a set of gRNAs the choice of a suitable dCas9 system for gene induction is just as important. In this thesis, several dCas9-fusion proteins were analyzed regarding their potential for gene induction with the aim to identify the system with the highest activation effect. An increase in VP16 repeats was found to benefit transcriptional activation when comparing dCas9-VP160 with the SpyTag system (up to 12 x VP160 repeats) and the

SunTag system (up to 24 x VP64 repeats) [100] in chapter 5.2.2.1. The role of the fused VP16 transactivation domains is the recruitment of factors involved in the formation of the transcription initiation complex such as the general transcription factor TFIIB [96, 97]. Besides simply offering an increased number of VP16 repeats the success of SpyTag and SunTag systems may also be based on a wider coverage of putative DNA binding sites for transcriptional activators due to the extended geometry of the fusion proteins. Without knowing where exactly binding of the transcription complex is required at the promoter of a particular gene, an increased coverage of the genomic DNA by VP16 copies could be helpful. Although the total number of VP16 repeats is even higher in case of SunTag, the SpyTag system seemed at least as powerful. This may be based on the underlying molecular mechanisms of VP16 recruitment. Interaction of SpyTag and SpyCatcher results in the formation of a permanent isopeptide bond and thus a lasting fusion of VP160-SpyCatchers with the dCas9-SpyTag protein [98, 99]. In the SunTag system, VP64-repeats are fused to scFv antibodies which bind SunTag arrays at the C-terminus of dCas9 resulting in a binding equilibrium. For a maximum effect 24 scFv-VP64 fusion proteins have to bind to a single dCas9 at any given time which may be a limiting factor.

VPR and especially SAM systems [90, 91] were found in chapter 5.2.2.4 to induce *Ascl1* expression at significantly higher levels than the SpyTag system with gRNAs *mA1* and *mA2*. This seems to be based on the additional transactivation domains (P65 and HSF1 for SAM, P65 and RTA for VPR) allowing the recruitment of further cell-intrinsic components of transcription complexes. Amongst them are well known factors implicated in the regulation of gene expression such as the TATA-box binding protein, CREB which acts downstream of cAMP signaling and chromatin remodelers of the SWI/SNF family [101, 103, 105]. A recent publication [110] comparing SAM, VPR and SunTag systems in HEK293 cells reports similar findings confirming the results obtained in murine Neuro2a cells. Surprisingly, combining either SAM or VPR with the SpyTag system was not beneficial. A possible explanation could be steric hindrance. The SAM complex binds hairpin aptamers at the gRNA and was published in combination with dCas9-VP64 [91]. Upon binding of up to twelve VP160-Spycatchers to dCas9-SpyTag the interaction of SAM and gRNA aptamers might be impaired. This would explain why the level of activation by SAM plus SpyTag system dropped even below the values measured for SAM with d-Cas9-VP64. This could not be overcome by replacing the 12xSpyTag by a smaller 4xSpyTag version (see appendix, Figure 28). Similarly, substituting VP160 of the SpyTags by VPR did not seem to be an advantage possibly also due to steric hindrances by the increased size of VP64-P65-RTA vs VP160. To address this point, peptide linker sizes between dCas9 and the SpyTag array as well as in-between individual SpyTags (currently GSGGKGGSG linker) could be increased

allowing a putatively improved accessibility. An alternative would be the commonly used and highly flexible (GGGGS)<sub>n</sub>-linker which can be used as tandem repeats [169].

*Ascl1* mRNA levels obtained by direct overexpression of *Ascl1* (*Tet-O-Ascl1* vector) exceeded the levels observed for CRISPR/Cas9 based gene induction in RT-qPCR analysis. However, this was not surprising as a single cell receives several copies of each plasmid and *Ascl1* can be expressed from all *Tet-O-Ascl1* constructs simultaneously [170]. Furthermore, *Tet-O* is a rather strong promoter system [120]. In case of the CRISPR/Cas9 system *Ascl1* can only be expressed from the endogenous *Ascl1* promoter. A quantitative comparison is therefore difficult and *Tet-O-Ascl1* values should only be treated as a qualitative positive control showing the functionality of the system. In any case, the aim was not to compete with transcriptional levels obtained by direct overexpression but to induce endogenous *Ascl1* expression to more closely resemble physiological processes and to take advantage of epigenetic remodeling of targeted loci [107].

Taken together, offering a variety of different transactivators fused to dCas9 improves the gene induction potential compared to multiple repeats of VP16. However, not all systems seem to be compatible with each other.

### 6.2.3 Synergistic activating effect of SAM and VPR systems

While a combination of SpyTag with SAM or VPR systems was not successful, co-expression of SAM and dCas9-VPR was found to result in a synergistic activation of *Ascl1* expression in Neuro2a cells using gRNAs *mA1* and *mA2* (see chapter 5.2.2.5). With SAM being described as one of the most powerful activating systems so far [110], a further increase in transcriptional induction by combining two systems is very promising for later reprogramming experiments where high levels of expression seem to be required [166]. However, in a recent article Chavez *et al.*, 2016 [110] also compared SAM, VPR and the combination of both systems. Surprisingly, no beneficial effect was reported upon combining these two systems for *ASCL1* and three other genes in HEK293 cells [110].

These contradictory results for *ASCL1* induction may be based on experimental differences regarding gRNAs and cell types utilized. A general Neuro 2a specific effect was excluded as SAM and VPR did not show such a synergistic effect when other genes were induced in these cells (J. Schwab, data not shown). Chavez *et al.*, 2016 used four gRNAs (*hA1 – hA4*) targeting 1 kb upstream of the human *ASCL1* TSS in HEK293 cells. In this thesis two gRNAs (*mA1*, *mA2*) binding within the first 250 bp upstream of the murine *Ascl1* TSS were tested in Neuro 2a cells. The question therefore was whether the synergistic effect of SAM and VPR systems observed in Neuro 2a cells could be reproduced in human HEK293 cells with gRNAs closely resembling *mA1* and *mA2*. Therefore, two new gRNAs termed *dist. matched*

*mA2* (identical distance between targeting sequences as in case of murine *mA1* and *mA2*) and *seq. matched mA2* (except for 5' nucleotide identical protospacer sequence as *mA2* but increased distance to *mA1* by 23 nt) were designed. Interestingly, when using the *dist. matched mA2* gRNA there was no difference in activation when using the SAM system alone or in combination with VPR. This indicated that the synergistic effect observed in Neuro 2a cells was not based on the distance of the activation systems relative to each other or the TSS of *Ascl1*.

However, in case of the *seq. matched mA2* gRNA a trend towards increased *ASCL1* expression but not a synergistic effect as in murine cells was observed in HEK293 cells for SAM plus VPR when compared to SAM alone. This effect therefore seems to be sequence specific and possibly based on interactions of the fused transactivation domains with endogenous factors regulating *Ascl1* expression. It has to be analyzed in further detail whether e.g. *GLI2* plays a role here. *GLI2* is a known activator of *Ascl1* [137] and a *GLI2* binding site was found just downstream of gRNA *mA2* in a Genomatix promoter analysis. Recruitment of transcriptional activators to this *GLI2* binding site by SAM and VPR systems might therefore benefit *Ascl1* expression. Interestingly, during the gRNA screening process in chapter 5.2.2.3 the addition of gRNA *mA4* to gRNAs *mA1* and *mA2* resulted in a reduced level of *Ascl1* induction. *mA4* binds just six nucleotides downstream of the *GLI2* binding site thus possibly perturbing its binding. Furthermore, the *GLI2* binding site is not conserved in the human *ASCL1* promoter due to nucleotide mismatches and therefore not recognized by the Genomatix software. This may contribute to the differences in gene induction observed in human vs murine cells by SAM and VPR systems but has to be investigated in further detail.

Interestingly, Chavez *et al.*, 2016 also report differences in the activation potential of individual dCas9 fusion proteins depending on target gene and cell type [110]. For example, SAM was found to be more potent than the VPR system for the induction of Hemoglobin subunit gamma 1 (*HBG1*) in HeLa cells whereas the opposite effect was observed in the MCF-7 breast cancer cell line [110]. For the induction of Titin (*TTN*) however, the SunTag system seemed to be more suitable than SAM or VPR [110]. These data suggest that for an efficient induction of a specific gene not only gRNAs have to be screened but also compatible dCas9 fusion proteins.

Taken together, several factors including the interaction of gRNAs and activator system as well as the respectively targeted locus influence the level of gene induction. Here, a seemingly unique synergistic effect of *Ascl1* induction by SAM and VPR systems was found in Neuro 2a cells by using gRNAs *mA1* and *mA2*. So far analysis of transcription factor binding sites is not included in the gRNA design but may be a valuable tool for future applications.

### 6.2.4 Challenges in lentiviral delivery of dCas9 systems

In this thesis, *SAM split-dCas9-VPR* vectors were generated to efficiently transduce astrocytes by lentiviruses each carrying one gRNA and either SAM and N-dCas9 or C-dCas9-VPR. The intein-mediated assembly of N- and C-dCas9 was found not to be impaired by the fusion of VPR to C-dCas9 thus increasing the field of applications for the split-Cas9 system originally published for wt Cas9 [141]. Surprisingly, lentiviral production of the *SAM split-dCas9-VPR* system repeatedly resulted in very low titers ( $1 \times 10^5$ -fold lower than for co-produced *Tet-O-Ascl1* virus). This suggested negative effects of the expression cassette on lentiviral packaging. Interestingly, in the original publications of VPR, SAM and SunTag systems stable cell lines expressing dCas9 fusion proteins were used thus omitting the need for efficient lentiviral *dCas9* delivery [90, 91, 100]. However, this is not suitable for the direct conversion of primary cells such as MEFs or astrocytes which stop proliferation after few passages and can therefore not undergo lengthy selection processes for successful transgene expression [34, 171]. So far, direct conversion of somatic cells based on lentiviral delivery of *dCas9* was achieved in only two reports where *dCas9* was expressed under the control of either *Tet-O* or *hUBC* promoters [107, 108]. Indeed, lentiviral delivery of *Cas9* was successful in this thesis when the *Ef1a* promoter was replaced by *Tet-O* or *hUBC* promoters in chapter 5.2.4. This was surprising as *Ef1a* is a commonly used promoter also in lentiviral vectors [91, 172].

The underlying mechanism was not further investigated but one explanation could be the loss of the large intronic sequence of the *Ef1a* promoter due to splicing events during packaging of the virus [173]. This results in an intron-less *Ef1a* promoter comparable to the *small Ef1a-dCas9-VPR* construct which was found in this thesis to induce only low levels of gene expression. Expression levels close to the detection limit of immunocytochemistry could be a limiting factor during titer analysis. However, such an intronic loss was not observed by Cooper *et al.*, where *Ef1a* was used to drive *Gfp* expression in a lentiviral vector [173]. This indicates a specific interaction between *Ef1a* promoter and gRNA or *Cas9* sequences adversely affecting lentiviral packaging or expression. Interestingly, for the *hUBC* promoter Cooper *et al.*, reported splicing events during lentiviral packaging and subsequently a fourfold reduction in expression [173]. Since *hUBC* is a weak promoter even without splicing [120] the *Tet-O* system was chosen to replace the *Ef1a* promoter as the aim of this thesis was to find a dCas9-based system allowing the highest possible induction of target genes.

In conclusion, the split-Cas9 strategy is also suitable for gene induction and the combination of promoter and coding sequence can significantly affect the efficiency of lentiviral delivery.

### 6.2.5 Direct conversion of astrocytes to neurons utilizing VPR and SAM

Using the SAM split-dCas9-VPR system astrocytes were successfully converted to neurons in chapter 5.2.5. These results are very promising as direct conversion of somatic cells had not been achieved with SAM or VPR systems before. Furthermore, astrocytes have not been directly converted with any CRISPR/Cas9 based system up to now. Therefore, these results act as proof-of-principle for the SAM split-dCas9-VPR system. It was not surprising that direct overexpression of *Ascl1* resulted in a higher reprogramming efficiency than the CRISPR/Cas9-based approach. When inducing just a single gene the CRISPR/Cas9 based approach has some downsides including the limiting effect of the required co-transduction by two viruses (*SAM-N-dCas9* and *C-dCas9-VPR* vs *Tet-O-Ascl1*). This means that only a fraction of FlagTag<sup>+</sup> (N-dCas9<sup>+</sup>) cells were also co-transduced by a *C-dCas9-VPR* encoding lentivirus similar to the findings for *Ascl1* and *Nurr1* at the beginning of this thesis in chapter 5.1.1. Therefore, the percentage of MAP2<sup>+</sup> cells per FlagTag<sup>+</sup> cells underestimates the reprogramming potential of SAM split-dCas9-VPR.

Furthermore, N-dCas9 and C-dCas9-VPR have to assemble in order to become a functional dCas9-VPR protein. Finally, protein separation at P2A, which was used to separate SAM and N-dCas9 is also a limiting factor. However, these calculated downsides of the SAM split-dCas9-VPR system should only be prominent when a single gene is induced. The underlying idea to generate this new system was based on the simultaneous induction of several genes where this new technology may show its full potential. In this case, direct overexpression of multiple transcription factors would require co-transduction of several viruses whereas gRNA multiplexing can still be applied to express all required gRNAs from the two established vectors *SAM-N-dCas9* and *C-dCas9-VPR* due to the small size of gRNA expression cassettes.

Indeed, in a recent article Black *et al.*, report a twofold increase in reprogrammed neurons when inducing the expression of endogenous genes *Brn2*, *Ascl1* and *Myt1l* in MEFs by VP64-dCas9-VP64 compared to direct overexpression of the three transcription factors [107]. So far, this is the only report of directly converted somatic cells to neurons by dCas9 mediated gene induction. Naturally, the performance of this system was compared to the SAM-VPR system. RT-qPCR analysis revealed no significant activation of *Ascl1* expression when using VP64-dCas9-VP64 with gRNAs *mA1* and *mA2* (appendix, Figure 29). This reflects earlier findings of this thesis which suggested that a single kind of transcriptional activator (VP16) and the relatively weak *hUBC* promoter are not suited for a strong transcriptional induction (chapters 5.2.2.4 and 5.2.4). It could be argued that this is mainly based on the different performance of promoters used (weak *hUBC* for *VP64-dCas9-VP64* versus strong *Tet-O* for *SAM split-dCas9-VPR*). However, Chavez *et al.*, 2016 came to a

similar solution comparing *Tet-O-VP64-dCas9-BFP-VP64* with *Ef1a-SAM* or *CMV-VPR* systems [110]. The latter three promoters reach comparable levels of expression [120] confirming actual differences in the activation potential of the tested systems. Here, gene induction by VPR and *VP64-dCas9-BFP-VP64* were comparable for human *ASCL1* and *NEUROD1* but SAM performed approximately ten-fold stronger in both cases [110].

Along these lines, when testing the *hUBC-VP64-dCas9-VP64* system with gRNAs *mA1* and *mA2* for reprogramming of astrocytes to neurons no significant increase in reprogrammed cells was observed (transfer by lipofection, appendix Figure 30). Besides the weak *hUBC* promoter the combination of specific gRNAs and the transcriptional activator system also seems to play a role. This was already suggested by the results regarding the synergistic effect of SAM and VPR systems for *Ascl1* induction and the findings of Chavez *et al.* 2016, [110] who reported differential gene induction properties of dCas9 fusion proteins depending on gene and cell type. This might also explain the missing synergistic effect in the reprogramming potentials of SAM and VPR when used alone or in combination in lipofection based reprogramming experiments. However, the underlying mechanisms in astrocytes have to be analyzed in more detail before a final conclusion can be drawn.

Taken together, the successful conversion of astrocytes to neurons by CRISPR/Cas9 based gene induction of *Ascl1* demonstrates the suitability of this system for the direct reprogramming of cells. It is therefore a promising starting point for further tests including simultaneous induction of multiple genes and *in vivo* experiments to analyze the functionality of reprogrammed cells. *In vivo*, CRISPR/Cas9-based gene induction may have further advantages by modifying the epigenetic landscape of targeted promoters thus resembling natural gene expression [107]. This was found to result in sustained levels of gene expression even when using transient expression systems [107]. This system may therefore be helpful to overcome the limitations of exogenous transcription factor expression as described in this thesis and by Theodorou and Rauser *et al.*, [118].

CONCLUSION

AND FUTURE PERSPECTIVES

## 7 Conclusion and future perspectives

In this thesis limitations of exogenous gene expression for direct reprogramming were shown due to low efficiencies of co-transduction and the generation of fusion proteins. Promisingly, forskolin was found to support the direct conversion of *Ascl1*, *Lmx1a* and *Nurr1* transduced MEFs to dopaminergic neurons and enabled the generation of TH<sup>+</sup>/PITX3<sup>+</sup> midbrain dopaminergic neurons. These findings are highly promising as overexpression of *Ascl1*, *Lmx1a* and *Nurr1* alone was not sufficient to generate PITX3<sup>+</sup> mdDA neurons which therefore do not resemble the DA neuron subtype affected in PD. As next steps, the functionality of these neurons should be further characterized by electrophysiology and finally transplantation in lesioned mouse models to investigate the therapeutic benefits.

As an alternative to exogenous gene expression a combination of SAM and dCas9-VPR was found to strongly induce endogenous *Ascl1* levels in murine Neuro 2a cells. Interestingly, the newly observed synergistic effect of these two systems seemed to depend on the chosen set of gRNAs and was specific for *Ascl1* and the murine cell system used. For the first time SAM and VPR systems were utilized in this thesis to directly convert astrocytes to neurons. These promising data are a basis for further improvements in order to further increase the reprogramming efficiency and also guide reprogrammed cells towards a specific neuronal subtype such as mdDA neurons.

Currently, optimized versions are tested such as a *SAM split-dCas9-VPR* system driven by a *GFAP* promoter which restricts expression to astrocytes. This should help simplifying the quantitative analysis where newly converted neurons must be distinguished from neurons already present at the beginning of the primary cortical cell population. One central task for the future will be the simultaneous induction of multiple genes in order to generate specific neuronal subtypes. For this, multiplexing is required which allows expression of several gRNAs from a single vector.

Finally, the developed system will be tested *in vivo* by injecting the SAM dCas9-VPR system into the murine cortex to analyze the reprogramming and rescue potential in disease models such as 6-OHDA treated mice.

Taken together, in this thesis successful proof-of-principle experiments show the highly promising potential of the CRISPR/Cas9 technology for the direct conversion of somatic cells which will now be a basis for further developments.

## MATERIAL AND METHODS

## 8 Material and methods

### 8.1 Material

**Table 2: Equipment**

<b>Description</b>	<b>Supplier</b>
<b>ABI Prism 7900 HT Real-Time PCR System</b>	Applied Biosystems, USA
<b>AxioCam HRc camera</b>	Zeiss, Germany
<b>Axioplan 2 microscope</b>	Zeiss, Germany
<b>Branson Sonifier cell disruptor B15</b>	Branson, USA
<b>CellInsight NXT High Content Screening Platform</b>	ThermoFisher Scientific, Germany
<b>Centrifuge Avanti J-30I; JA-30.50 Ti Rotor</b>	Beckman Coulter, Germany
<b>Centro LB 960 luminometer</b>	Berthold Technologies, Germany
<b>ChemiDoc MP imaging system</b>	BioRad, Germany
<b>Fusion SL imaging system</b>	Vilber, Germany
<b>Gel-Documentation system E.A.S.Y Win32</b>	Herolab, Germany
<b>LightCycler 480</b>	Roche, Germany
<b>NanoDrop® Spectrophotometer ND-1000</b>	Peqlab, Germany
<b>Olympus IX81</b>	Olympus, Germany
<b>PCR Gelelectrophoresis chambers</b>	Peqlab, Germany
<b>Thermo cycler Mastercycler pro</b>	Eppendorf, Germany
<b>Transilluminator</b>	Herolab, Germany
<b>Western Blot chambers Novex® Mini-Cell</b>	ThermoFisher Scientific, Germany

**Table 3: General consumables**

<b>Description</b>	<b>Catalogue number</b>	<b>Supplier</b>
<b>50 ml syringe</b>	300865	BD Plastipak, USA
<b>AceGlow Luminol Enhancer Solution</b>	37-3420	Peqlab, Germany
<b>Adhesive Seal Sheets</b>	AB-1170	ThermoFisher Scientific, Germany
<b>AquaPolyMount</b>	18606	Polysciences, USA
<b>Blotting-grade Blocker, nonfat milk</b>	170-6404	Biorad, Germany
<b>Cell strainer, 70 µm</b>	352350	BD Falcon, USA
<b>Centrifugation tube for Avanti J-30I</b>	357003	Beckman Coulter, Germany
<b>Cover slips</b>	1001/14	Karl Hecht, Germany
<b>EasYFlask 225 cm<sup>2</sup></b>	159934	ThermoFisher Scientific, Germany

<b>EasYFlask 75 cm<sup>2</sup></b>	156499	ThermoFisher Scientific, Germany
<b>Framestar 384</b>	4ti-0384/C	4titude, United Kingdom
<b>GeneRuler 100 bp DNA Ladder</b>	SM0243	ThermoFisher Scientific, Germany
<b>GeneRuler 1kb DNA Ladder</b>	SM0311	ThermoFisher Scientific, Germany
<b>Immobilion P Transfer Membrane</b>	IPVH00010	Merck Millipore, Germany
<b>Nunc multidish 24</b>	142475	ThermoFisher Scientific, Germany
<b>Nunclon Delta Surface 96 well plate</b>	13610	ThermoFisher Scientific, Germany
<b>NuPAGE 4-12% Bis-Tris Gel</b>	NP0321	ThermoFisher Scientific, Germany
<b>NuPAGE® LDS Sample Buffer (4x)</b>	NP0007	ThermoFisher Scientific, Germany
<b>NuPAGE® MOPS SDS Running Buffer (20x)</b>	NP0001	ThermoFisher Scientific, Germany
<b>NuPAGE® Transfer Buffer (20x)</b>	NP0006-1	ThermoFisher Scientific, Germany
<b>Page Ruler Plus Prestained</b>	26619	ThermoFisher Scientific, Germany
<b>Phosphatase inhibitor cocktail</b>	04906837001	Roche, Germany
<b>Protease inhibitor cocktail</b>	11836170001	Roche, Germany
<b>SuperFrost™ Plus glas slides</b>	4951PLUS4	ThermoFisher Scientific, Germany
<b>Syringe 0.22 µm PES filter</b>	SLGP033RS	Merck Millipore, Germany
<b>Syringe 0.45 µm PES filter</b>	SLHP033RS	Merck Millipore, Germany
<b>TaqMan Universal PCR MasterMix</b>	5000991	ThermoFisher Scientific, Germany
<b>Whatman paper</b>	3030-931	Sigma-Aldrich, Germany

Table 4: Chemicals

<b>Description</b>	<b>Catalogue number</b>	<b>Supplier</b>
<b>2-Mercaptoethanol</b>	M7522	Sigma-Aldrich, Germany
<b>Agarose</b>	870055	Biozym, Germany
<b>Ampicilline</b>	11593-027	ThermoFisher Scientific, Germany
<b>Ampuwa</b>	B230673	Fresenius Kabi, France
<b>Bovine serum albumin</b>	A3059	Sigma-Aldrich, Germany
<b>D-(+)-glucose</b>	G8270	Sigma-Aldrich, Germany

<b>Dimethyl sulfoxide</b>	D5879	Sigma-Aldrich, Germany
<b>EDTA</b>	E5134	Sigma-Aldrich, Germany
<b>Ethanol</b>	1.00983.2500	Merck Millipore, Germany
<b>Ethidiumbromide</b>	2218.2	Carl Roth GmbH, Germany
<b>Formalin, 10%</b>	F5554	Sigma-Aldrich, Germany
<b>Isopropanol</b>	109634	Merck KGaA, Germany
<b>KCl cell culture grade</b>	P5405	Sigma-Aldrich, Germany
<b>Methanol</b>	1.06009.2500	Merck Millipore, Germany
<b>MgCl<sub>2</sub> cell culture grade</b>	M4880	Sigma-Aldrich, Germany
<b>Milk powder</b>	170-6404	Biorad, Germany
<b>NaCl cell culture grade</b>	S5886	Sigma-Aldrich, Germany
<b>Sodium Chloride</b>	106404	Merck KGaA, Germany
<b>Triton X 100</b>	T9284	Sigma-Aldrich, Germany
<b>Trizma cell culture grade</b>	T2319	Sigma-Aldrich, Germany
<b>Tween 20</b>	P1379	Sigma-Aldrich, Germany

Table 5: Cell culture media and supplements

<b>Description</b>	<b>Catalogue number</b>	<b>Supplier</b>
<b>B27 Serum-Free-Supplement</b>	17504044	ThermoFisher Scientific, Germany
<b>B-27 Supplement Minus Vitamin A</b>	12587010	ThermoFisher Scientific, Germany
<b>BDNF</b>	203702	Merck Millipore, Germany
<b>bFGF</b>	13256029	ThermoFisher Scientific, Germany
<b>DAPI</b>	D8417	Sigma-Aldrich, Germany
<b>DMEM</b>	21969	ThermoFisher Scientific, Germany
<b>DMEM/F12 GlutaMAX™-I</b>	31331	ThermoFisher Scientific, Germany
<b>Doxycycline</b>	44577	Sigma-Aldrich, Germany
<b>DPBS</b>	14190	Sigma-Aldrich, Germany
<b>EGF</b>	E4127	Sigma-Aldrich, Germany
<b>Fetal Bovine Serum</b>	A2153	ThermoFisher Scientific, Germany
<b>FGF-basic recombinant mouse</b>	PMG0034	ThermoFisher Scientific, Germany
<b>Forskolin</b>	F3917	Sigma-Aldrich, Germany
<b>Hanks balanced salt solution, Mg<sup>2+</sup>/Ca<sup>2+</sup> free</b>	14175-053	ThermoFisher Scientific, Germany
<b>Horse serum</b>	16050-122	ThermoFisher Scientific, Germany

<b>L-ascorbic acid</b>	A4034100G	Sigma Genosys, Germany
<b>L-glutamine</b>	16285	Roche, Germany
<b>Lipofectamine 2000</b>	11668-019	ThermoFisher Scientific, Germany
<b>Lipofectamine® LTX with Plus™ Reagent</b>	15338100	ThermoFisher Scientific, Germany
<b>N2 Supplement-A</b>	07152	Lab Life, Germany
<b>Neurobasal medium</b>	21103-049	ThermoFisher Scientific, Germany
<b>Opti-MEM I</b>	31985-047	ThermoFisher Scientific, Germany
<b>Penicillin/Streptomycin</b>	15070063	ThermoFisher Scientific, Germany
<b>Poly-D-lysine</b>	A-003-E	Merck Millipore, Germany
<b>Trypsin-EDTA Solution (0.05%)</b>	25300054	ThermoFisher Scientific, Germany
<b>Trypsin-EDTA Solution (0.25%)</b>	25200056	ThermoFisher Scientific, Germany

**Table 6: Composition of buffers and cell culture media**

<b>Description</b>	<b>Constituents</b>
<b>Agar plates</b>	10 g tryptone 5 g yeast extract 10 g NaCl 15 g agar Add water to 1 L pH 7
<b>Astrocyte dissection medium</b>	HBSS buffer 1% penicillin/streptomycin
<b>Astrocyte plating medium</b>	DMEM/F12 GlutaMAX™-I 10% FCS 5% horse serum 45 mg/ml glucose additionally 1x B27 supplement 10 ng/ml EGF 10 ng/ml bFGF 1% penicillin/streptomycin
<b>Astrocyte reprogramming medium</b>	DMEM/F12 GlutaMAX™-I 45 mg/ml glucose additionally 1x B27 supplement 1% penicillin/streptomycin 25 µM forskolin 20 ng/ml BDNF every fourth day
<b>DMEM medium for HEK293, Lenti-X 293T, N2A cells</b>	DMEM 10% FCS 1% L-glutamine

<b>Immunocytochemistry blocking buffer</b>	PBS 1% BSA 0.5% Triton-X100
<b>LB medium</b>	10 g tryptone 5 g yeast extract 10 g NaCl Add water to 1 L pH 7
<b>MEF medium (Fibroblast cultivation medium)</b>	DMEM 10% FCS 1% L-glutamine 1% penicillin/streptomycin
<b>N2-B27 medium (Fibroblast reprogramming medium)</b>	50% DMEM/F12 GlutaMAX™-I 50% Neurobasal 0.5x B27 supplement minus vitamin A 0.5x N2 supplement 100 µM ascorbic acid 0.5% L-glutamine 20 ng/ml BDNF 1% penicillin/streptomycin
<b>RIPA buffer</b>	50 mM Tris-HCl 150 mM NaCl 1% Triton-X100 0.5% Na-Deoxycholate 0.1% SDS 3 mM EDTA Addition of protease/phosphatase inhibitors
<b>TAE buffer</b>	40 mM Tris 20 mM acetic acid 1 mM EDTA
<b>TBS-5 buffer</b>	50 mM Tris-HCl, pH7.8 0.13 mM NaCl 10 mM KCl 5 mM MgCl <sub>2</sub>
<b>TBS-T buffer</b>	20 mM Tris-HCl, pH 7.5 136 mM NaCl 0.1% Tween 20
<b>TE buffer</b>	10 mM Tris-HCl 1 mM disodium EDTA pH 8.0
<b>Western blot blocking buffer</b>	TBS-T buffer 5% non-fat milk powder (5% BSA for ASCL1)

Table 7: Kits

Description	Catalogue number	Supplier
Dual-Luciferase® Reporter Assay System	E1910	Promega, USA
NEBuilder HiFi DNA Assembly Cloning Kit	E5520	New England Biolabs, Germany
Pierce BCA Protein Assay Kit	23225	ThermoFisher Scientific, Germany
PureLink® HiPure Plasmid Filter Maxiprep Kit	K210016	ThermoFisher Scientific, Germany
QIAprep Spin Maxiprep Kit	12162	Qiagen, Germany
QIAprep Spin Miniprep Kit	27104	Qiagen, Germany
QIAquick Gel Extraction Kit	28704	Qiagen, Germany
QIAquick PCR Purification Kit	28104	Qiagen, Germany
QuikChange Lightning Site-Directed Mutagenesis Kit	210518	Agilent, Germany
Rapid DNA Dephos & Ligation Kit	04898117001	Roche, Germany
RNeasy plus Mini Kit	74134	Qiagen, Germany
StrataClone PCR Cloning Kit	240205	Agilent, Germany
SuperScript® VILO cDNA Synthesis Kit	11755050	ThermoFisher Scientific, Germany
TOPO TA Cloning Kit	45-0640	ThermoFisher Scientific, Germany

Table 8: Enzymes

Description	Catalogue number	Supplier
BamHI	R3136	New England Biolabs, Germany
BbsI	R0539	New England Biolabs, Germany
BsiWI	R0553	New England Biolabs, Germany
BsmBI	R0580	New England Biolabs, Germany
EcoRI	R0101	New England Biolabs, Germany
EcoRI-HF	R3101	New England Biolabs, Germany
KAPA HiFi DNA polymerase	07-KK2100-01	VWR, Germany
NotI	R0189	New England Biolabs, Germany
NotI-HF	R3189	New England Biolabs, Germany
Q5 High-Fidelity 2X Master Mix	M0492	New England Biolabs, Germany
REDTaq ReadyMix PCR Reaction Mix	R2523	Sigma-Aldrich, Germany
RsrII	R0501	New England Biolabs, Germany
SbfI-HF	R3642	New England Biolabs, Germany

**Table 9: Primary antibodies**

Target	Host	Dilution	Catalogue #	Supplier
<b>ASCL1</b>	Mouse	ICC: 1:1000 WB: 1:250, 5% BSA for blocking	556604	BD Biosciences, USA
<b>Cas9</b>	Mouse	ICC: 1:500	A-9000	EpiGentek, USA
<b>FlagTag</b>	Mouse	ICC: 1:1000, 10% NGS serum	F1804	Sigma-Aldrich, Germany
<b>GFP</b>	Chicken	ICC: 1:1000	PA1-9533	AVES, USA
<b>GFP</b>	Mouse	ICC: 1:1000	11814460001	Roche, Germany
<b>LMX1A</b>	Rabbit	WB: 1:2000	ab10533	Merck-Millipore, Germany
<b>MAP2</b>	Rabbit	ICC: 1:1000	AB5622	Merck-Millipore, Germany
<b>MycTag</b>	Goat	ICC: 1:2000	ab9132	Abcam, Germany
<b>MycTag</b>	Mouse	ICC: 1:1000	M4439	Sigma-Aldrich, Germany
<b>NURR1</b>	Rabbit	ICC: 1:2000 WB: 1:100	sc-990	Santa Cruz, USA
<b>PITX3</b>	Rabbit	ICC: 1:300	38-2850	ThermoFisher Scientific, Germany
<b>TH</b>	Mouse	IHC: 1:600 ICC: 1:600	MAB318	Merck-Millipore, Germany
<b>TH</b>	Rabbit	ICC: 1:1000	AB152	Merck-Millipore, Germany
<b>TUJ1</b>	Rabbit	ICC: 1:500	ab18207	Abcam, Germany
<b><math>\beta</math>-actin</b>	Mouse	WB: 1:10000	ab6276	Abcam, Germany

**Table 10: Secondary antibodies**

Target	Conjugate	Host	Dilution	Catalogue #	Supplier
<b>Chicken IgG</b>	Cy2	Rabbit	ICC: 1:250	703225155	Dianova, Germany
<b>Goat IgG</b>	Alexa 488	Donkey	ICC: 1:500	A-11055	ThermoFisher Scientific, Germany
<b>Goat IgG</b>	Alexa 594	Donkey	ICC: 1:500	A-11058	ThermoFisher Scientific, Germany
<b>Mouse IgG</b>	Alexa 350	Donkey	ICC: 1:250	A10035	ThermoFisher Scientific, Germany
<b>Mouse IgG</b>	HRP	Goat	WB: 1:5000	115-035-003	Dianova, Germany

<b>Mouse IgG</b>	Alexa 488	Donkey	ICC: 1:500	A21202	ThermoFisher Scientific, Germany
<b>Mouse IgG</b>	Alexa 594	Donkey	ICC: 1:500	A21203	ThermoFisher Scientific, Germany
<b>Rabbit IgG</b>	Alexa 488	Donkey	ICC: 1:500	A-21206	ThermoFisher Scientific, Germany
<b>Rabbit IgG</b>	DyLight647	Donkey	ICC: 1:250	711495152	Dianova, Germany
<b>Rabbit IgG</b>	HRP	Goat	WB: 1:5000	111-035-003	Dianova, Germany
<b>Rabbit IgG</b>	Alexa 594	Donkey	ICC: 1:500	A-21207	ThermoFisher Scientific, Germany
<b>Rat IgG</b>	Alexa 488	Donkey	ICC: 1:500	A21208	ThermoFisher Scientific, Germany

**Table 11: Primers for amplification and sequencing**

<b>Description</b>	<b>Sequence 5' – 3'</b>
<b>BsiWI-del-F</b>	gcttagtaaggacacgtatgatgacgatctcgacaat
<b>C-Cas-BsiWI-F</b>	ggactatcgtacgccaccatgataaagattgccaccagaaagtatctg
<b>C-Cas-Sbfl-R</b>	ggactatcctgcaggtcagaggtcctcctcgaaatcaactc
<b>dCasVP64-BsiWI-F</b>	ggactatcgtacggccaccatggataaaaagtattctattg
<b>dCasVP64-Sbfl-R</b>	ggactatcctgcaggtcataacatatcgagatcgaaatcgccagagcatc
<b>Flag-Oligo-F</b>	gtacagactacaaggacgacgacgataaagttag
<b>Flag-Oligo-R</b>	aattctcacttatcgtcgtcgtcctgtagtct
<b>gBlock-Flag-P2A</b>	ctcccaaagccaaggaccccactgtctcctgtacagactacaaggacgacgacgataagggagcgg agccacaaacttctctctgctcaagcaggcaggcagctggaggaaaacctggaccaatgggaccta agaaaaagaggaaggtggcggcctgactacaaggatgacgacgataaagacaagaagtagcagca tcggcctggccatcggcaccactctgtgggctgggccc
<b>hUBC-ampl-F</b>	ggactatggatcccggaccgtaagggtgcagcggcctc
<b>hUBC-ampl-R</b>	ggactatgaattcccctgcagggtactgtatcgtacggtattagcagcccaagctcgtctaaca
<b>Int-C-Cas-Fw</b>	tctccattcaggtgtcgtgatgtacactgctaaccatgttcatgcctc
<b>Int-C-Cas-Rev</b>	gaggttgattaccgataagcttgatatcgaattctcaaacagagatgtgtcgaagatg
<b>N-Cas-BsiWI-F</b>	ggactatcgtacgccaccatggctcaaaacttactcagttcg
<b>N-Cas-Int F</b>	gaagtacagcatcggcctggc
<b>N-Cas-Int R</b>	agcttgatatcgaattctcagttggcaggtgtccacc
<b>N-Cas-Sbfl-R</b>	ggactatcctgcaggtcagttggcaggtgtccac
<b>SAM-Sbfl-R</b>	ggactatcctgcaggtcacttatcgtcgtcctgtagtctgtac
<b>TRE-ampl-F</b>	ggactatggatcccggaccgctcaggttaccactccctatcagtgatagag
<b>TRE-ampl-R</b>	ggactatgaattcccctgcagggtactgtatcgtacgccctagagtgagtcgtattaccgaggcggatcgg

<b>VP64-Cas-VP64-Fw</b>	ggactatcgtagccaccatggactacaaagaccatgacg
<b>VP64-Cas-VP64-Rw</b>	ggactatcctgcagggtcactgtacagctcgccatgccg
<b>VPR-BsiWI-F</b>	ggactatcgtagccaccatggacaagaagtactccattgg
<b>VPR-Sbfl-del-F</b>	agaatcggatctgctacctacaggagatcttagtaatg
<b>VPR-Sbfl-R</b>	ggactatcctgcagggtcaaacagagatgtgtcgaagatggacagtc

Table 12: gRNA targeting sequences

Description	Sequence 5' – 3' without PAM	Position to TSS	Score
<b>gRNA A1, murine Ascl1</b>	GTTGTTGCAGTGCGTGCGCC	-230 / anti-sense	On-target: Off-target: 94
<b>gRNA A2, murine Ascl1</b>	CGGTGCGGCCGCCTTTTCAA	-25 / anti-sense	On-target: N/A Off-target: 93
<b>gRNA A3, murine Ascl1</b>	GAGTTTGCAAGGAGCGGGCG	-179 / sense	On-target: N/A Off-target: 42
<b>gRNA A4, murine Ascl1</b>	GCGGGGCCAGGGCTGCGCGT	-47 / sense	On-target: N/A Off-target: 77
<b>gRNA A5, murine Ascl1</b>	CTCCCCGCTGCTGCAGCGAG	-92 / anti-sense	On-target: N/A Off-target: 71
<b>gRNA A6, murine Ascl1</b>	ACGCACTGCAACAACAAACC	-211 / sense	On-target: N/A Off-target: 70
<b>gRNA A7, murine Ascl1</b>	CCCAGCCCCACGCGCAGCCC	-52 /anti-sense	On-target: N/A Off-target: 59
<b>gRNA A8, murine Ascl1</b>	CGCGGGCAACTGGAGGGGGG	-161 / sense	On-target: N/A Off-target: 57
<b>gRNA dist. matched mA2, human ASCL1</b>	AGCGGGAGAAAGGAACGGGA	-185 /sense	On-target: 55 Off-target: 57
<b>gRNA hA1, human Ascl1</b>	CGGGAGAAAGGAACGGGAGG	-196 / sense	On-target: 30 Off-target: 51
<b>gRNA hA2, human Ascl1</b>	AAGAACTTGAAGCAAAGCGC	-451 /anti-sense	On-target: 50 Off-target: 74
<b>gRNA hA3, human Ascl1</b>	TCCAATTTCTAGGGTCACCG	-572 /sense	On-target: 68 Off-target: 82
<b>gRNA hA4, human Ascl1</b>	GTTGTGAGCCGTCTGTAGG	-886 /anti-sense	On-target: 57 Off-target: 83
<b>gRNA mA1, murine Ascl1</b>	AGCCGCTCGCTGCAGCAGCG	-83 / sense	On-target: 57 Off-target: 43
<b>gRNA mA2, murine Ascl1</b>	GGCTGAATGGAGAGTTTGCA	-190 / sense	On-target: 61 Off-target: 36
<b>gRNA mA3, murine Ascl1</b>	AATGGAGAGTTTGCAAGGAG	-185 / sense	On-target: 61 Off-target: 35

<b>gRNA mA4, murine Ascl1</b>	GGAGGGAGCTGAGGAGGTGG	-130 / sense	On-target: 30 Off-target: 33
<b>gRNA mA5, murine Ascl1</b>	ATTGAAAAGGCGGCCGCACC	-26 / anti-sense	On-target: 41 Off-target: 48
<b>gRNA N1, murine Nurr1</b>	TCCGACCTGACGTCACGACT	-48 / anti-sense	On-target: N/A Off-target: 95
<b>gRNA N2, murine Nurr1</b>	TACCAAAGCGAGCGCGGGCC	-10 / sense	On-target: N/A Off-target: 94
<b>gRNA N3, murine Nurr1</b>	AAGGTGGGAACGGTTCACCT	-80 / anti-sense	On-target: N/A Off-target: 84
<b>gRNA N4, murine Nurr1</b>	CGTGTGAGGACGCAAGGTCT	-198 / sense	On-target: N/A Off-target: 83
<b>gRNA N5, murine Nurr1</b>	CTCCTGGCCCGCGCTCGCTT	-19 / anti-sense	On-target: N/A Off-target: 80
<b>gRNA N6, murine Nurr1</b>	TCCACCCAAGTGGGCTACCA	-86 / sense	On-target: N/A Off-target: 77
<b>gRNA N7, murine Nurr1</b>	TAGCATCACCACGGACTTCA	-152 / sense	On-target: N/A Off-target: 74
<b>gRNA N8, murine Nurr1</b>	AAGTGTGACTTCTGCAACCC	-139 / anti-sense	On-target: N/A Off-target: 53
<b>gRNA seq. matched mA2, human ASCL1</b>	AGCTGAATGGAGAGTTTGCA	-208 / sense	On-target: 61 Off-target: 35

Table 13: Taqman probes

<b>Description</b>	<b>Catalogue number</b>	<b>Supplier</b>
<b>ACTB, human</b>	Hs99999903_m1	ThermoFisher Scientific, Germany
<b>Actb, mouse</b>	Mm00607939_s1	ThermoFisher Scientific, Germany
<b>ASCL1, human</b>	Hs04187546_g1	ThermoFisher Scientific, Germany
<b>Ascl1, mouse</b>	Mm03058063_m1	ThermoFisher Scientific, Germany
<b>Gapdh, mouse</b>	Mm99999915_g1	ThermoFisher Scientific, Germany

Table 14: DNA Vectors

Description	Catalogue number	Supplier/reference/producer
dSpCas9(D10A,H840A)_12xSpyTag	N/A	Available at the IDG; generated by J. Truong
dSpCas9(D10A,H840A)_4xSpyTag	N/A	Available at the IDG; generated by J. Truong
dSpCas9(D10A,H840A)_8xSpyTag	N/A	Available at the IDG; generated by J. Truong
dSpCas9_VP160 (SpCas9 <sup>2-573</sup> ) and C-Cas9 (SpCas9 <sup>574-1368</sup> )	N/A	Available at the IDG; generated by J. Truong
hU6-mA1-Ef1a-SAM	N/A	Generated in this thesis
hU6-mA1-Ef1a-SAM-N-dCas9 (D10A-SpCas9 <sup>2-573</sup> )	N/A	Generated in this thesis
hU6-mA1-Tet-O-SAM	N/A	Generated in this thesis
hU6-mA1-Tet-O-SAM-N-dCas9 (D10A-SpCas9 <sup>2-573</sup> )	N/A	Generated in this thesis
hU6-mA2-Ef1a-C-dCas9-VPR (H840A-SpCas9 <sup>574-1368</sup> )	N/A	Generated in this thesis
hU6-mA2-Tet-O-C-dCas9-VPR (H840A-SpCas9 <sup>574-1368</sup> )	N/A	Generated in this thesis
hU6-mA2-Tet-O-dCas9-VPR	N/A	Generated in this thesis
lenti dCAS-VP64_Blast	61425	Addgene, USA / [91]
lenti MS2-P65-HSF1_Hygro (SAM)	61426	Addgene, USA / [91]
lenti sgRNA(MS2)_zeo backbone (SAM gRNA)	61427	Addgene, USA / [91]
Luciferase reporter: Ascl1((E1)6-Luc)	N/A	Castro <i>et al.</i> , 2006 [134]
Luciferase reporter: Lmx1a (Pitx3 promoter)	N/A	Available at the IDG; generated by C. Peng [15]
Luciferase reporter: Nurr1 (DeltaM-Luc)	N/A	Castro <i>et al.</i> , 2006 [134]
Npu-DnaE-C-Intein_C-SpCas9(574-1368)	N/A	Available at the IDG, [141]
N-SpCas9(2-573)_Npu-DnaE-N-Intein	N/A	Available at the IDG, [141]
pBS-U6-chimaeric-F+E	N/A	Available at the IDG
pCAG-Cas9v2_Intein_C-Part_v1_new	N/A	Available at the IDG; generated by J. Truong
pCCLsin.PPT.hPGK.rtTAm2 (rTTA)	N/A	Caiazza <i>et al.</i> 2011, [37]
pcDNA3.1 (+)	V79020	Thermo Fisher, Germany
pHRdSV40-dCas9-10xGCN4_v4-P2A-BFP (SunTag)	60904	Addgene, USA / [100]
pHRdSV40-NLS-dCas9-24xGCN4_v4-NLS-P2A-BFP-dWPRES (activators for SunTag)	60910	Addgene, USA / [100]
pKLV-U6gRNA(BbsI)-PGKpuro2ABFP	50946	Addgene, USA / [174]
pLV hUbc-dCas9 VP64-T2A-GFP	53192	Addgene, USA / [175]
pLV hUbc-VP64 dCas9 VP64-T2A-GFP	59791	Addgene, USA / [175]

<b>pMD2.G</b>	12259	Addgene, USA / gift from Didier Trono
<b>pMDLg/pRRE</b>	12251	Addgene, USA / [176]
<b>pRL-SV40 Vector</b>	E2231	Promega, USA
<b>pRSV-Rev</b>	12253	Addgene, USA / [176]
<b>pSC-B-amp/kan</b>	240207	Agilent Technologies, USA
<b>SP-dCas9-VPR</b>	63798	Addgene, USA / [90]
<b>Sso7d_dSpCas9(D10A,H840A)_12xSpyTag</b>	N/A	Available at the IDG; generated by J. Truong
<b>Sso7d_dSpCas9(D10A,H840A)_4xSpyTag</b>	N/A	Available at the IDG; generated by J. Truong
<b>Sso7d_dSpCas9(D10A,H840A)_8xSpyTag</b>	N/A	Available at the IDG; generated by J. Truong
<b>Sso7d_dSpCas9_VP160</b>	N/A	Available at the IDG; generated by J. Truong
<b>Tet-O-ALN (Ascl1-T2A-Lmx1a-P2A-Nurr1)</b>	N/A	Available at the IDG; generated by J. Zhang
<b>Tet-O-Ascl1</b>	N/A	Caiazzo <i>et al.</i> 2011, [37]
<b>Tet-O-FUW</b>	N/A	Caiazzo <i>et al.</i> 2011, [37]
<b>Tet-O-Lmx1a</b>	N/A	Caiazzo <i>et al.</i> 2011, [37]
<b>Tet-O-Nurr1</b>	N/A	Caiazzo <i>et al.</i> 2011, [37]
<b>Tet-O-Smarca1</b>	N/A	Available at the IDG; generated by B. Rauser
<b>Tet-O-T2A-dsRed</b>	N/A	Available at the IDG
<b>VP160_SpyCatcher</b>	N/A	Available at the IDG; generated by J. Truong

Table 15: Cell lines

<b>Description</b>	<b>Catalogue number</b>	<b>Supplier</b>
<b>HEK293</b>	CRL-1573	ATCC, USA
<b>Neuro-2a</b>	CCL-131	ATCC, USA
<b>Lenti-X™ 293T</b>	632180	Takara Bio, USA

Table 16: Bacterial strains

<b>Description</b>	<b>Catalogue number</b>	<b>Supplier</b>
<b>DH5α</b>	18265017	Thermo-Fischer Scientific, USA
<b>XL10-Gold Ultracompetent Cells</b>	200315	Agilent Technologies, USA
<b>One Shot® TOP10</b>	C404010	Thermo-Fischer Scientific, USA

**Table 17: Mouse strains**

Description	Supplier
C67BI6/N	Charles River; Germany
CD-1	Charles River; Germany
Pitx3 <sup>GFP/GFP</sup>	Zhao <i>et al.</i> 2004, [149]

**Table 18: Software**

Description	Supplier
CellInsight NXT	Thermo Scientific, Germany
GraphPad Prism 5.01	Graphpad Software, Inc., USA
Stereo Investigator 5.05.4	MBF Bioscience, USA
Fluoview 2.0b	Olympus, Germany
SDS 2.4.1	Applichem, Germany
MicroWin32 5.0.249	HeroLab, Germany
Vector NTI® Advance 11.5.2	Invitrogen, Germany

## 8.2 Methods

### 8.2.1 Isolation and culture of primary cells and established cell lines

All experiments in cell culture were performed under sterile conditions. Primary cells were incubated at 37°C, 5% CO<sub>2</sub>. Established cell lines were cultured at 37°C, 7% CO<sub>2</sub>.

#### 8.2.1.1 Storage and culture of stable cell lines

HEK293, Lenti-X 293T and N2A cell lines were stored in liquid nitrogen in 10% DMSO/DMEM medium (Table 6). Cells were thawed at 37°C in a water bath and diluted in 10 ml DMEM medium before centrifugation at 200 x g for 3 min. The cell pellet was resuspended in fresh DMEM medium and cells were cultured in T75 flasks with 20 ml DMEM medium. Upon reaching a confluency of approximately 90% cells were passaged by washing the cells with sterile Dulbecco's Phosphate-Buffered Saline (DPBS) and subsequent trypsinization using 0.25% Trypsin/EDTA. After centrifugation for 2 min at 200 x g supernatant was removed and the cell pellet was resuspended in fresh DMEM medium. Cells were then seeded in a fresh flask in a 1:10 dilution.

#### 8.2.1.2 Isolation and culture of primary fibroblasts

Primary mouse embryonic fibroblasts (MEFs) were isolated from E14.5 CD1 or *Pitx3*<sup>GFP/+</sup> mouse embryos. Head, viscera, extremities and spinal cord were removed in cold PBS containing 1% penicillin/streptomycin. The remaining tissue was chopped into pieces and incubated in 0.05% Trypsin/EDTA at 37°C for 10 min. Afterwards, trypsin was inactivated by the addition of MEF medium (Table 6) and the suspension was filtered using 70 µm cell strainers in order to obtain a single cell suspension. Cells were centrifuged at 200 x g for

4 min and resuspended in fresh MEF medium. Centrifugation was repeated twice before  $5 \times 10^6$  cells were seeded in a T75 flask containing 20 ml MEF medium. Upon reaching 80% confluency cells were trypsinized and stored in liquid nitrogen using 10% DMSO/MEF medium. These cells were considered passage one MEFs.

### **8.2.1.3 Isolation and culture of primary astrocytes**

Primary cortical astrocytes were obtained from postnatal (p5 – p6) CD1 mice as described by Heinrich *et al.*, 2011 [49]. Shortly, the brain was collected; cerebellum and optic chiasm were removed in cold astrocyte dissection buffer (Table 6). Afterwards the two hemispheres were separated by a longitudinal cut. Diencephalon and hippocampal formation were discarded leaving the cortex. Meninges were cleared away carefully and the remaining tissue was transferred to a tube containing cold astrocyte dissection buffer. The cortexes of three animals were pooled. Dissection buffer was removed under sterile conditions and 5 ml astrocyte plating medium (Table 6) were added. A 200  $\mu$ l pipette tip was stuck on the tip of a 10 ml pipette and the medium containing the tissue was carefully pipetted up and down three times in order to break down the cortexes. Afterwards, the cell suspension was pipetted into a T75 flask and additional 15 ml of astrocyte plating medium were added. Cells were incubated for four days at 37°C. Flasks were tapped vigorously to loosen tissue chunks and loose cells such as oligodendrocytes or microglia. Then, medium was replaced by fresh astrocyte medium and cells were incubated for another six days. At this point astrocytes were trypsinized and directly used for experiments.

### **8.2.1.4 Coating of cover slips for cell attachment**

In order to allow a qualitative and quantitative analysis of cell culture experiments after immunocytochemistry cells were seeded on glass coverslips in 24-well plates. These cover slips required coating by poly-D-lysine to enable cell attachment. Prior to coating the coverslips were autoclaved and placed in individual wells containing sterile water. The water was replaced by 500  $\mu$ l 5% poly-D-lysine/PBS solution and the plates were incubated at 37°C overnight. The cover slips were washed three times with sterile water and dried at room temperature (RT) under sterile conditions. Plates were stored at 4°C for up to one week.

### **8.2.1.5 Lipofection**

Lipofection of HEK293, Lenti-X™ 293T and N2A cells was performed using Lipofectamine2000 according to the manufacturer's instructions. Shortly, Lipofectamine 2000 was diluted in serum free OPTI-MEM and incubated for 5 min. Afterwards, pre-diluted DNA in OPTI-MEM medium was added and the mix was incubated at RT for 20 min. The DNA/Lipofectamine 2000 mix was added dropwise to the cells. After 6 h medium was replaced by fresh medium. In order to enable a quantitative comparison of transcriptional activators by luciferase assays or RT-qPCR, plasmids with different sizes were adjusted on

the molar level. Within individual experiments the total amount of transfected DNA was equalized in all conditions by the addition of the empty plasmid *pcDNA3*. Table 19 states the amounts of individual plasmids used in lipofections conducted in this thesis.

**Table 19: Transfection of DNA plasmids using Lipofectamine 2000**

Plasmid	DNA per well in a 24-well plate
<b>Firefly luciferase reporter constructs</b>	200 ng
<b>Renilla luciferase</b>	1 ng
<b>CRISPR/Cas9 fusions</b>	10 fmol
<b>SAM activator complex</b>	10 fmol
<b>SpyCatcher</b>	40 fmol
<b>scFv-VP64</b>	20 fmol
<b>Tet-O-Ascl1, Tet-O-Lmx1a, Tet-O-Nurr1, Tet-O-Smarca1, rTTA</b>	10 fmol
<b>gRNAs, combined amount of all gRNAs per well</b>	10 ng
<b>pcDNA3</b>	Adjustment to highest DNA amount of experiment

Primary cortical astrocytes were transfected using Lipofectamine LTX with Plus Reagent according to the manufacturer's instructions. However, the amounts of DNA, Lipofectamine LTX and Plus Reagent were doubled to approximately 1.1 µg DNA, 5 µl Lipofectamine LTX and 1 µl Plus reagent per well of a 24-well plate with  $5 \times 10^4$  primary astrocytes. The molar ratios of plasmids transfected are shown in Table 20. 100 µl Lipofectamine LTX/DNA mix were added to each well of a 24-well plate.

**Table 20: Transfection of DNA plasmids using Lipofectamine LTX**

Plasmid	DNA per well in a 24-well plate
<b>CRISPR/Cas9 fusions</b>	40 fmol
<b>SAM activator complex</b>	40 fmol
<b>Tet-O-Ascl1, Tet-O-T2A-dsRed, rTTA</b>	40 fmol
<b>gRNAs, combined amount of all gRNAs per well</b>	20 ng
<b>pcDNA3</b>	Adjustment to highest DNA amount of experiment

### 8.2.2 Preparation of lentiviruses and titer determination

Replication incompetent, self-inactivating lentiviruses were generated with a third-generation packaging system [176]. For each virus  $1.6 \times 10^7$  low passage Lenti-X 293T cells were seeded in two T225 flasks, respectively. On the next day, medium was replaced by 18 ml fresh DMEM medium in each flask 2 h before transfection. For the transfection of two T225 flasks DNA was diluted in 9 ml OPTI-MEM medium as indicated in Table 21

**Table 21: Transfection of DNA for lentivirus production**

Plasmid	DNA for an individual virus [ $\mu\text{g}$ ]
Transfer vector with gene of interest	59.5
pMDLg/pRRE	39.8
pRSV-Rev	15.4
pMD2.G	19.5

248  $\mu\text{l}$  Lipofectamine2000 were diluted in 9 ml OPTI-MEM and incubated for 5 min. Lipofectamine and DNA mix were combined and incubated for further 20 min before 9 ml of the mix were added to the two T225 flasks. After 5 h medium was replaced by 21 ml fresh DMEM medium. Virus was harvested 72 h after transfection by combining the supernatant of the two flasks. In order to remove cell debris, the supernatant was centrifuged at 2,200  $\times g$  for 10 min. Afterwards, the supernatant was filtered using a 0.45  $\mu\text{m}$  PES filter and centrifuged in an Avanti J-30I centrifuge at 50,000  $\times g$ , 4°C for 2 h. The pellet was washed with 30 ml cold TBS-5 buffer (Table 6) and centrifuged again at 50,000  $\times g$ , 4°C for 2 h. The supernatant was removed and the pellet dissolved in 100  $\mu\text{l}$  TBS-5 buffer overnight at 4°C. Virus was then aliquoted and stored at -80°C. In order to determine the virus titer  $5 \times 10^4$  HEK293 cells/well were seeded on a 24-well plate. After 4 h of cultivation 2  $\mu\text{l}$  of lentivirus were diluted in 400  $\mu\text{l}$  DMEM medium. 1  $\mu\text{l}$  (containing 0.005  $\mu\text{l}$  virus), 10  $\mu\text{l}$  (containing 0.05  $\mu\text{l}$  virus) or 100  $\mu\text{l}$  (containing 0.5  $\mu\text{l}$  virus) of the virus dilution were added to individual wells, respectively. For viruses containing a *Tet-O* promoter, 1  $\mu\text{l}$  of rTTA2 virus and 2  $\mu\text{g/ml}$  doxycycline were added to each well to enable expression from the *Tet-O*-promoter. 48 h after transduction cells were fixed and stained to detect the expression of the transduced gene (see 8.2.4). The percentage of transduced cells per DAPI<sup>+</sup> cells was determined by scanning 50 fields of each well using the CellInsight NXT High Content Screening Platform. After calculating the corresponding number of transduced cells per  $5 \times 10^4$  cells the titer was calculated as follows:

$$\frac{\# \text{ transduced cells per } 5 \times 10^4 \text{ seeded cells} \cdot 10^3 \frac{\mu\text{l}}{\text{ml}}}{\mu\text{l of virus used (0.005, 0.05 or 0.5 } \mu\text{l})} = \text{infectious particles per ml}$$

### 8.2.3 Direct reprogramming of somatic cells

#### 8.2.3.1 Reprogramming of MEFs

MEFs in passage one were thawed and cultured in a T75 flask in MEF medium (see Table 6) until reaching a confluency of approximately 80%. Cells were trypsinized and  $5 \times 10^4$  cells were seeded on poly-D-lysine coated cover slips (see 8.2.1.4) in 24-well plates. After 24 h cells were transduced with viruses at a multiplicity of infection of three for each individual virus. When using the *Tet-O* system, 1  $\mu$ l rTTA2 lentivirus was co-transfected. 24 h after transduction the medium was replaced with 500  $\mu$ l fresh MEF medium. From this point onwards 2  $\mu$ g/ml doxycycline were added to the medium if *Tet-O* promoters were used. 72 h after transduction the medium was replaced by 500  $\mu$ l differentiation medium (N2-B27 medium, see Table 6). Six days after transduction the medium was replaced by 500  $\mu$ l fresh differentiation medium. Nine days after transduction 250  $\mu$ l of the conditioned differentiation medium were replaced by fresh differentiation medium. At day 12 – 14 cells were fixed and stained for analysis (see 8.2.4). The percentage of neurons per DAPI was determined in 20 random fields (200 x 200  $\mu$ m) on each coverslip using the Stereo Investigator system. Only TUBB3<sup>+</sup> or MAP2<sup>+</sup> cells with a mature neuronal morphology (compact soma, at least one neurite more than three times longer than the cell body) were considered successfully reprogrammed neurons. As an alternative to normalizing to DAPI, cells were stained for the expression of the delivered gene such as Cas9 and the percentage of mature neurons per Cas9<sup>+</sup> cells was determined.

#### 8.2.3.2 Reprogramming of astrocytes

Ten days after isolation of cortical astrocytes (see 8.2.1.3) cells were washed with PBS and trypsinized.  $5 \times 10^4$  cells were seeded in 100  $\mu$ l astrocyte medium carefully in the middle of coated glass cover slips (see 8.2.1.4) in 24-well plates (Table 6). This prevented a loss of cells due to attachment to the plate outside the glass cover slip. 1 h after seeding, 400  $\mu$ l additional astrocyte medium were added. At 3 h past seeding cells were transduced using lentiviruses at different multiplicities of infection (see individual experiments). On the next day, astrocyte plating medium was replaced by 1.5 ml astrocyte reprogramming medium (Table 6) containing 2  $\mu$ g/ml doxycycline if *Tet-O* promoters were used. As an alternative to viral transduction cells were transfected 24h after seeding. In order to remove dead cells before the transfection, the medium was removed, sterile filtered with a 0.22  $\mu$ m PES syringe filter and 400  $\mu$ l of the medium were added to the wells again. The transfection was performed using Lipofectamine LTX as described in chapter 8.2.1.5. On the next day, medium was replaced by 1.5 ml astrocyte reprogramming medium (see Table 6) containing 2  $\mu$ g/ml doxycycline if *Tet-O* promoters were used. Transduced and transfected cells were incubated for 14 days before fixation and staining (see 8.2.4). During these 14 days, BDNF was added at a concentration of 20 ng/ml every fourth day. The percentage of neurons per

DAPI was determined in 25 random fields (500 x 500  $\mu\text{m}$ ) on each coverslip using the Stereo Investigator system. As an alternative to normalizing to DAPI, cells were stained for the expression of the delivered gene such as Cas9 and the percentage of mature neurons per Cas9<sup>+</sup> cells was determined. Due to the significantly lower DNA transfer efficiency of lipofection complete coverslips were analyzed in this case. In lipofection reprogramming experiments marker genes such as dsRed were co-transfected and all dsRed<sup>+</sup> cells on the whole coverslip were checked for co-expression of neuronal markers. Only TUBB3<sup>+</sup> or MAP2<sup>+</sup> cells with a mature neuronal morphology (compact soma, at least one neurite more than three times longer than the cell body) were considered successfully reprogrammed neurons.

### 8.2.4 Immunocytochemistry and microscopy

Immunocytochemistry (ICC) was used to visualize gene expression of cells in *in vitro* experiments. For pre-fixation, an equal volume of 10% formalin was added to the cells in culture medium of a 24-well plate and incubated for 5 min at 37°C. The medium was then removed and replaced by 10% formalin for 10 min at 37°C. Afterwards cells were washed three times using DPBS. Primary antibodies were diluted according to Table 9 in blocking buffer (1% BSA, 0.5 % Triton-X-100 in PBS) and 200  $\mu\text{l}$  antibody solution were added to each well in a 24-well plate. After incubation at 4°C overnight, cells were washed three times with PBS. Suitable secondary antibodies (see Table 10) were diluted in blocking buffer and 200  $\mu\text{l}$  were added to each well and incubated in the dark for 1 h at RT. Afterwards the antibody solution was replaced by 200  $\mu\text{l}$  DAPI (100 ng/ml DPBS) in order to visualize nuclei. DAPI was discarded after 1 min followed by three washing steps using PBS. Finally, cover slips were removed from the 24-well plate and mounted on glass slides using AquaPolyMount. Slides were dried and stored at 4°C in the dark.

Pictures of fluorescence stained cells were taken using an Olympus IX81 confocal microscope and Fluoview 2.0 software. For quantitative analysis, an Axioplan 2 microscope together with Stereoinvestigator software were used. Unless indicated otherwise, 20 – 25 random 200x 200  $\mu\text{m}$  fields evenly distributed over the whole coverslip were analyzed. Only fields with more than 10 cells were counted.

### 8.2.5 Luciferase assay analysis

Luciferase assays were performed to analyze transcription factor binding and intracellular signaling mechanisms. The assay was based on a dual-luciferase system. A *firefly luciferase* was expressed under the control of an assay dependent promoter (i.e. *Pitx3* promoter, binding sites for transcription factors or signaling molecules of interest). From a second plasmid *renilla luciferase* was expressed under the control of a constitutively active *SV40* promoter and served as a control for normalization.  $5 \times 10^4$  HEK293 or N2A cells were

seeded in 24-well plates 24 h prior to transfection. *Firefly luciferase* plasmid and *renilla luciferase* plasmids were transfected together with further plasmids of interest using Lipofectamine 2000 (see 8.2.1.5). Cells were lysed using 100  $\mu$ l passive lysis buffer provided in the promega dual luciferase assay kit 48 h after transfection by shaking at RT for 15 min. 10  $\mu$ l of the lysate were used for the measurement of firefly and renilla luciferase activity in a white 96-well plate using a Centro LB 960 luminometer. The program settings for the MicroWin32 luminometer software are shown in Table 22.

**Table 22: Settings MicroWin32 luminometer software**

Step	Operation	Definition
<b>Dispense</b>	Volume	50 $\mu$ l
	Speed	Middle
	Measured operation	By well
	Repeated operation	Yes
	Duration	2 s
<b>Delay</b>	Measurement option	By well
	Name	Firefly or renilla
<b>Firefly/renilla</b>	Counting time	5 s
	Measurement option	By well

For data analysis firefly values were normalized to renilla activity and these were subsequently normalized to control values in order to receive fold change values. All experiments were performed with three technical replicates.

### 8.2.6 RT-qPCR

RT-qPCR was used to quantitatively assess mRNA levels of different genes of interest in cell culture experiments.  $5 \times 10^4$  cells were seeded in 24-well plates 24 h before transfection. Experiments were performed in triplicates and Lipofectamine 2000 was used for DNA transfer (see 8.2.1.5). Six hours after lipofection medium was replaced and 2  $\mu$ g/ml doxycycline was added to experiments where *Tet-O*-promoters were included. 48 h after transfection RNA was isolated using a RNeasy plus Kit according to the manufacturers protocol. 400 ng RNA were reversely transcribed from each well using the SuperScript VILO cDNA synthesis kit in a 20  $\mu$ l reaction. Subsequently, 80  $\mu$ l RNase free water was added and this 1:10 dilution was used for RT-qPCR analysis. All measurements were carried out in technical triplicates. 9  $\mu$ l cDNA were pipetted into a 384 well-plate. 1  $\mu$ l TaqMan probe and 10  $\mu$ l TaqMan universal PCR mastermix were added and the plate was sealed with adhesive seal sheets. RT-qPCR was carried out using an ABI Prism 7900 HT Real-Time PCR System and SDS 2.4.1 software with settings shown in Table 23.

**Table 23: Running conditions RT-qPCR**

Repetitions	Temperature [°C]	Time [min:s]
1	95	10:00
40	95	0:15
	60	1:00

In order to analyze the data the mean threshold cycle (ct) values of the gene of interest from three technical replicates were normalized to the mean ct of a control gene (*b-actin*, *Gapdh*). This value was termed  $\Delta ct$ . Subsequently, fold changes were calculated as follows:

$$\Delta ct = \frac{ct \text{ gene of interest}}{ct \text{ housekeeping gene}}$$

$$\Delta\Delta ct = \frac{\Delta ct \text{ treated cells}}{\Delta ct \text{ control}}$$

$$\text{Fold change values} = 2^{-\Delta\Delta ct}$$

### 8.2.7 Western blot

24 h after transfection cells were lysed by adding 100  $\mu$ l RIPA buffer (Table 6) to each well of a 24-well plate. Protein concentration was determined using a Pierce BCA protein assay kit according to the manufacturer's instructions. Absorption was measured at 562 nm by a ChemiDoc imaging system. A linear equation was determined from the absorption values of the BSA standard which allowed calculation of protein sample concentration.

Afterwards, 5  $\mu$ l NuPAGE LDS sample buffer containing 4%  $\beta$ -mercaptoethanol were added to 15  $\mu$ l concentration-matched samples which were then incubated at 95°C for 5 min for denaturation. After cooling down on ice samples were pipetted into gel pockets of a 4 - 12% NuPAGE Novex Bis-Tris gel. For size determination 5  $\mu$ l Page Ruler Plus Prestained were used. Gel electrophoresis was performed at 200 V in 1x NuPAGE MOPS SDS running buffer. PVDF membranes were activated prior to blotting by incubation in 100% methanol for 30 s followed by 2 min in water and 5 min in 1x NuPAGE transfer buffer/ 10% methanol. The SDS gel was equilibrated in 1x NuPAGE transfer buffer/ 10% methanol for 15 min. Blotting pads and whatman paper were also soaked in this buffer. Two blotting pads followed by a whatman paper, SDS gel and the PVDF membrane were placed into a blotting chamber. On top, another whatman paper was placed and the chamber was filled with several layers of blotting pads and 1x NuPAGE transfer buffer/ 10% methanol. Transfer of the proteins from gel to PVDF membrane was subsequently performed at 30 V for one hour or at 20 V, 4°C overnight for proteins > 100 kDa. Afterwards, the membrane was washed in TBS-T buffer (see Table 6) for 5 min and blocked in western blot blocking buffer (see Table 6) for 1 h.

Overnight, the membrane was incubated with a primary antibody (see Table 9) diluted in western blot blocking buffer at 4°C. On the next day, the membrane was washed with TBS-T buffer 3 x 5 min. A suitable secondary antibody coupled to horseradish-peroxidase (Table 10) was diluted 1:5000 in blocking buffer and incubated with the membrane for 1 h at room temperature. Subsequently, the membrane was washed 3 x 5 min in TBS-T buffer. For the detection of protein bands 0.5 ml Ace glow luminol enhancer per lane were pipetted onto the membrane. Pictures were taken using a Fusion SL imaging system. Quantitative analysis was performed with ImageJ software. Band intensities of the protein of interest and a housekeeping protein such as  $\beta$ -Actin were determined with ImageJ and the values of the protein of interest were divided by the values of the loading control. Afterwards, all values were normalized to the control condition in order to obtain fold change values.

## **8.2.8 Isolation of nucleic acids**

### **8.2.8.1 Isolation of RNA**

For the isolation of mRNA from cells a RNeasy plus mini kit was used according to manufacturer's instructions.

### **8.2.8.2 Purification of DNA**

In order to remove buffer components, primers or enzymes for subsequent enzymatic steps DNA was purified using a QIAquick PCR Purification Kit according to manufacturer's instructions. For the isolation of DNA fragments from agarose gels the bands of interest were cut from gels with a scalpel and DNA was isolated using a QIAquick Gel Extraction Kit according to the manufacturer's instructions.

### **8.2.8.3 Agarose gel electrophoresis**

Agarose gel electrophoresis was performed for size estimation and separation of DNA fragments. Agarose powder was boiled in 1X TEA buffer (Table 6) and 1  $\mu$ g/ml EtBr was added for the detection of DNA fragments before gels were cast. The agarose concentration was adjusted to the size of the analyzed DNA fragments (1 - 2% agarose for DNA <1 kb, 0.8 - 1% agarose for DNA >1 kb). DNA samples were mixed with loading buffer and applied to the gel. Gel electrophoresis was performed in 1x TAE buffer at 120 V and pictures were taken using a E.A.S.Y Win32 Gel-Documentation system.

## **8.2.9 DNA plasmid preparations**

For mini plasmid preparations 5 ml LB-medium with a suitable selection marker were inoculated with a single bacterial colony from an agar plate. For a maxi plasmid preparation 200 ml of medium were used. Bacteria were cultured in a shaker at 37°C overnight. Plasmid preparations were performed using a QIAprep Spin Miniprep or QIAprep Spin Maxiprep Kit according to the manufacturer's instructions. Plasmids for lentivirus production were isolated

using the PureLink® HiPure Plasmid Filter Maxiprep Kit according to the manufacturer's instructions in order to achieve superior plasmid purity.

## **8.2.10 Cloning of new constructs**

### **8.2.10.1 Polymerase chain reaction**

For PCRs requiring a proof-reading polymerase the Q5 High-Fidelity 2X Master Mix was used according to manufacturer's instructions. For colony PCRs and other reactions not requiring proof reading REDTaq ReadyMix PCR Reaction Mix was used according to manufacturer's instructions. Site-directed mutagenesis was carried out with a QuikChange Lightning Site-Directed Mutagenesis Kit. PCRs were performed in a Mastercycler pro. All primers used for amplification steps are shown in Table 11.

### **8.2.10.2 Digestion of DNA fragments**

For subsequent cloning steps or as a control after cloning 1 – 5 µg of DNA fragments or plasmids were digested with restriction enzymes provided by New England Biolabs according to manufacturer's instructions.

### **8.2.10.3 Ligation of DNA fragments**

DNA fragments were ligated either by using a Rapid DNA Dephos & Ligation Kit or by gibbon assembly (NEBuilder® HiFi DNA Assembly Master Mix) according to manufacturer's instructions. Blunt end cloning was performed using a StrataClone PCR Cloning Kit according to manufacturer's instructions.

### **8.2.10.4 Design and generation of gRNA constructs**

The 20 nucleotide targeting sequence (crRNA) of a gRNA defines the sequence specific binding to DNA. Targeting sequences were designed within positions -250 to -1 upstream of the transcription start site of the respective gene. *gRNAs N1 – N8* targeting the murine *Nurr1* promoter and *gRNAs A1 – A8* binding to the murine *Ascl1* promoter were designed using the online tool <http://crispr.mit.edu/>. For each gene the eight targeting sequences with the highest off-target score (i.e. low probability of off-target binding) and an even distribution over the 250 nucleotides were chosen. Targeting sequences *mA1* to *mA5* binding the murine *Ascl1* promoter were designed using the online platform <https://benchling.com/>. This tool offered an additional on-target score indicating gRNAs with higher binding properties. The five targeting sequences with the highest on-target scores were chosen (*mA1* > *mA5*). Sense and antisense oligos (without PAM sequence) were ordered with the following additions: sense 5'-CACCGG-20nt-3', anti-sense 5'-AAAC-20nt-CC-3'. These overhangs served for later sticky end cloning into the target vector and GG 5' of the 20 nucleotides was required as a start signal for RNA polymerase III.

The lyophilized sense and antisense targeting sequence oligos were dissolved at 1 µg/µl in TE buffer (see Table 6). 1 µl of each oligo was pipetted to 100 µl TE buffer followed by incubation at 100°C for 5 min. The oligos were cooled down slowly to allow hybridization. These double stranded DNA fragments were then cloned into plasmids containing a RNA polymerase III promoter and the gRNA scaffold. As a non-viral gRNA expressing plasmid *pBS-U6-chimaeric-F+E* was used. *pKLV-U6gRNA(BbsI)-PGKpuro2ABFP* served as gRNA vector suitable for lentiviral packaging and *lenti-sgRNA(MS2)-zeo-backbone* was used for gRNA expression in combination with the SAM system and for lentiviral packaging. 5 µg of these target vectors were digested using BbsI or BsmBI leaving suitable sticky end overhangs for ligation with the annealed oligos. After gel purification 50 ng digested gRNA backbone were ligated with 4 µl annealed oligos (see 8.2.10.3) and transformed into DH5α bacteria (see 8.2.11). Successful cloning was checked by sequencing at GATC Biotech.

#### 8.2.10.5 Addition of a FlagTag to the SAM construct

To allow detection and titer determination of SAM the hygromycin resistance cassette of *lenti-MS2-P65-HSF1\_Hygro* (*SAM*) was replaced by a *FlagTag*. The vector was digested by BsrGI and EcoRI. *Flag-oligo-F* and *Flag-oligo-R* (see Table 11) containing a FlagTag and stop codon were annealed similar to gRNA targeting sequences (see chapter 8.2.10.4) and ligated with the digested plasmid.

#### 8.2.10.6 Design and generation of the split-Cas system with *Ef1a* promoters

The split-Cas system was based on an intein split system developed at the IDG previously [141] for adeno-associated virus (AAV) delivery. The system consisted of two vectors containing *N-Cas* (*SpCas9<sup>2-573</sup>*) and *C-Cas* (*SpCas9<sup>574-1368</sup>*) fused to *DnaE-N-Intein* and *DnaE-C-Intein* respectively. Since the packaging limit of AAVs prevented the addition of *SAM* and *VPR* a lentiviral system was chosen. The aim was to generate a two-vector system containing all components necessary: *N-Cas* was combined with one gRNA and *SAM*, *C-Cas* was combined with a second gRNA and *VPR*.

First, a SAM-compatible gRNA scaffold together with a *hU6* promoter from *lenti sgRNA(MS2)zeo* backbone was added to the *SAM* construct (*lenti-MS2-P65-HSF1\_Hygro*) by AelI and AgeI digest and ligation. Next, *N-Cas-N-intein* was amplified by PCR from AAV vector *N-SpCas9(2-573)\_Npu-DnaE-N-Intein* (*N-Cas-Int F* and *N-Cas-Int R* primers) and a gblock containing *Flag-Tag* and *P2A* sequences (*gBlock-Flag-P2A*) to connect *SAM* and *N-Cas* in a single expression cassette was ordered. The newly generated *gRNA-SAM* vector was digested by BsrGI/BstXI followed by gblock assembly of the *gRNA-SAM* backbone, the *N-Cas-N-intein* PCR product and the *FlagTag-Stop* gblock resulting in *hU6-gRNA-Ef1a-SAM-P2A-N-Cas-N-intein* (termed *hU6-mA1-Ef1a-SAM-N-Cas*).

In order to generate a *C-Cas-VPR* construct *pCAG-Cas9v2\_Intein\_C-Part\_v1\_new* was digested using EcoRV and MluI resulting in *pCAG-Cas9v2\_Intein*. The wildtype *C-Cas* was then replaced by *C-Cas-VPR* from the *SP-dCas9-VPR* construct by Gibson assembly thus generating *C-intein-C-cas-VPR*. Finally, the whole coding sequence was amplified (*Int-C-Cas-Fw*, *Int-C-Cas-Rev* primers) and transferred to the lentiviral *lenti sgRNA(MS2)zeo* backbone containing gRNA *mA2*. For this purpose the gRNA vector was digested by BsrGI/EcoRI thus replacing the zeomycine resistance cassette by *C-intein-C-cas-VPR* generating the *hU6-mA2-Ef1a-C-intein-C-Cas-VPR* construct.

#### 8.2.10.7 Design and generation of CRISPR/Cas9 constructs using the *Tet-O* system

These constructs were designed to generate a split-Cas system with an inducible promoter system enabling regulation of the expression level and timing of gene induction. Furthermore, these constructs were generated with the same unique restriction sites allowing simple exchange of individual cassettes. gRNAs including SAM-compatible loops were flanked by NheI/RsrII recognition sites, the *Tet-O-promoter* by RsrII and BsiWI cutting sites, and the open reading frame by BsiWI and SbfI.

The *lenti-sgRNA(MS2)zeo* backbone containing a gRNA scaffold suitable for the SAM system and the *mA1* or *mA2* gRNA was digested using BamHI and EcoRI. The backbone without promoter and zeomycine resistance was isolated by gel electrophoresis. The *Tet-response element (TRE, Tet-O-promoter)* was amplified from *Tet-O-FUW* using the primers *TRE-ampl-F* (containing BamHI, RsrII restriction sites) and *TRE-ampl-R* (containing EcoRI and SbfI restriction sites). The PCR product was blunt-cloned using the StrataClone kit (see 8.2.10.3) into *pSC-B-amp/kan*. The insert was then digested by BamHI/EcoRI and cloned into the digested *lenti-sgRNA(MS2)zeo* backbones. The new vectors were termed *mA1-Tet-O* and *mA2-Tet-O*.

The coding sequences of *SAM-N-Cas* and *SAM* were cloned into *mA1-Tet-O*, the coding sequences of *C-Cas-VPR* and *dCas-VPR* were cloned into *mA2-Tet-O*. The *SAM-N-Intein-N-Cas* coding sequence was amplified from *mA1-Ef1a-SAM-N-Cas-N-intein* using *N-Cas-BsiWI-F* and *N-Cas-SbfI-R* primers and cloned into the *pSC-B-amp/kan* vector using a Strataclone blunt cloning kit. By BsiWI and SbfI digest the coding sequence was then transferred into the *mA1-Tet-O* backbone generating *mA1-Tet-O-SAM-N-Cas-N-intein*. *SAM-Flag* (amplified with *N-Cas-BsiWI-F* and *SAM-SbfI-R* primers from *Ef1a-SAM-Flag*) was also cloned into the *mA1-Tet-O* construct. Similar, *C-Cas-VPR* (amplified using *C-Cas-BsiWI-F*, *C-Cas-SbfI-R*), *dCas-VPR* (amplified with *VPR-BsiWI-F*, *VPR-SbfI-R*), *VP64-dCas-VP64* (amplified by *VP64-Cas-VP64-Fw*, *VP64-Cas-VP64-Rv*) were cloned into *mA2-Tet-O*.

*dCas-VP64* was amplified from *lenti dCAS-VP64\_Blast* (*dCasVP64-BsiWI-F*, *dCasVP64-SbfI-R* primers) and ligated into *pSC-B-amp/kan* using the Strataclone blunt ligation kit. An

internal BsiWI restriction site was removed by site directed mutagenesis (see 8.2.10.1) using *BsiWI-del-F* primer. Afterwards, *dCas-VP64* was digested with BsiWI/SbfI and transferred into the *mA2-Tet-O* vector.

### **8.2.11 Transformation of competent bacteria**

For the multiplication of plasmids chemically competent bacteria were transformed. Bacteria were carefully thawed on ice and 2 µl plasmid DNA were added to 50 µl of bacteria. After incubation on ice for 20 min cells were heat shocked for 30 s at 42°C in a water bath. After 2 min on ice, 250 µl of pre warmed (37°C) LB-medium was added and the tube was shaken at 37°C for 1 h. Afterwards bacteria were spread on agar plates containing suitable selection markers. Bacteria were incubated overnight at 37°C and single colonies were picked for further analysis.

### **8.2.12 Glycerol stock preparations**

For long-term storage of bacteria containing plasmids of interest 700 µl overnight culture were mixed with 300 µl 80% glycerol and stored at -80°C immediately.

### **8.2.13 Statistical analysis**

Statistical analysis of data was performed using GraphPad prism 5 software. Only experiments with at least three biological replicates were analyzed. In order to test for Gaussian distribution of the values a D'Agostino and Pearson omnibus normality test was performed. If data passed the normality test, either a t-test or one-way ANOVA test was conducted. Values with non-Gaussian distributions were analyzed by Mann-Whitney or Kruskal-Wallis tests respectively. Asterisks were assigned as follows: \*P < 0.05. All data are shown with mean ± standard error of the mean (SEM).

## REFERENCES

## 9 References

1. Meiser, J., D. Weindl, and K. Hiller, *Complexity of dopamine metabolism*. Cell Commun Signal, 2013. **11**(1): p. 34.
2. Prakash, N., et al., *A Wnt1-regulated genetic network controls the identity and fate of midbrain-dopaminergic progenitors in vivo*. Development, 2006. **133**(1): p. 89-98.
3. Dahlstrom, A. and K. Fuxe, *Localization of monoamines in the lower brain stem*. Experientia, 1964. **20**(7): p. 398-9.
4. Abeliovich, A. and R. Hammond, *Midbrain dopamine neuron differentiation: factors and fates*. Dev Biol, 2007. **304**(2): p. 447-54.
5. Lang, A.E. and A.M. Lozano, *Parkinson's disease. Second of two parts*. N Engl J Med, 1998. **339**(16): p. 1130-43.
6. Riederer, P. and S. Wuketich, *Time course of nigrostriatal degeneration in parkinson's disease. A detailed study of influential factors in human brain amine analysis*. J Neural Transm, 1976. **38**(3-4): p. 277-301.
7. Fritsch, T., et al., *Parkinson disease: research update and clinical management*. South Med J, 2012. **105**(12): p. 650-6.
8. Gaillard, A. and M. Jaber, *Rewiring the brain with cell transplantation in Parkinson's disease*. Trends Neurosci, 2011. **34**(3): p. 124-33.
9. Chaudhuri, K.R., et al., *Non-motor symptoms of Parkinson's disease: diagnosis and management*. Lancet Neurol, 2006. **5**(3): p. 235-45.
10. Lees, A.J., J. Hardy, and T. Revesz, *Parkinson's disease*. Lancet, 2009. **373**(9680): p. 2055-66.
11. Dick, F.D., et al., *Environmental risk factors for Parkinson's disease and parkinsonism: the Geoparkinson study*. Occup Environ Med, 2007. **64**(10): p. 666-72.
12. Wood-Kaczmar, A., S. Gandhi, and N.W. Wood, *Understanding the molecular causes of Parkinson's disease*. Trends Mol Med, 2006. **12**(11): p. 521-8.
13. Salama, M. and O. Arias-Carrion, *Natural toxins implicated in the development of Parkinson's disease*. Ther Adv Neurol Disord, 2011. **4**(6): p. 361-73.
14. Luk, K.C., et al., *The transcription factor Pitx3 is expressed selectively in midbrain dopaminergic neurons susceptible to neurodegenerative stress*. J Neurochem, 2013. **125**(6): p. 932-43.
15. Peng, C., et al., *Pitx3 is a critical mediator of GDNF-induced BDNF expression in nigrostriatal dopaminergic neurons*. J Neurosci, 2011. **31**(36): p. 12802-15.
16. Hwang, D.Y., et al., *Selective loss of dopaminergic neurons in the substantia nigra of Pitx3-deficient aphakia mice*. Brain Res Mol Brain Res, 2003. **114**(2): p. 123-31.
17. Lindvall, O. and A. Bjorklund, *Cell therapeutics in Parkinson's disease*. Neurotherapeutics, 2011. **8**(4): p. 539-48.
18. Fearnley, J.M. and A.J. Lees, *Ageing and Parkinson's disease: substantia nigra regional selectivity*. Brain, 1991. **114** ( Pt 5): p. 2283-301.
19. Lindvall, O., et al., *Grafts of fetal dopamine neurons survive and improve motor function in Parkinson's disease*. Science, 1990. **247**(4942): p. 574-7.
20. Backlund, E.O., et al., *Transplantation of adrenal medullary tissue to striatum in parkinsonism. First clinical trials*. J Neurosurg, 1985. **62**(2): p. 169-73.
21. Itakura, T., et al., *Transplantation of autologous sympathetic ganglion into the brain with Parkinson's disease. Long-term follow-up of 35 cases*. Stereotact Funct Neurosurg, 1997. **69**(1-4 Pt 2): p. 112-5.
22. Freed, C.R., et al., *Transplantation of embryonic dopamine neurons for severe Parkinson's disease*. N Engl J Med, 2001. **344**(10): p. 710-9.
23. Olanow, C.W., et al., *A double-blind controlled trial of bilateral fetal nigral transplantation in Parkinson's disease*. Ann Neurol, 2003. **54**(3): p. 403-14.
24. Takahashi, K. and S. Yamanaka, *Induction of pluripotent stem cells from mouse embryonic and adult fibroblast cultures by defined factors*. Cell, 2006. **126**(4): p. 663-76.

25. Takahashi, K., et al., *Induction of pluripotent stem cells from adult human fibroblasts by defined factors*. Cell, 2007. **131**(5): p. 861-72.
26. Javoy, F., et al., *Specificity of dopaminergic neuronal degeneration induced by intracerebral injection of 6-hydroxydopamine in the nigrostriatal dopamine system*. Brain Res, 1976. **102**(2): p. 201-15.
27. Wernig, M., et al., *Neurons derived from reprogrammed fibroblasts functionally integrate into the fetal brain and improve symptoms of rats with Parkinson's disease*. Proc Natl Acad Sci U S A, 2008. **105**(15): p. 5856-61.
28. Erdo, F., et al., *Host-dependent tumorigenesis of embryonic stem cell transplantation in experimental stroke*. J Cereb Blood Flow Metab, 2003. **23**(7): p. 780-5.
29. Miura, K., et al., *Variation in the safety of induced pluripotent stem cell lines*. Nat Biotechnol, 2009. **27**(8): p. 743-5.
30. Kim, H.S., et al., *Direct lineage reprogramming of mouse fibroblasts to functional midbrain dopaminergic neuronal progenitors*. Stem Cell Res, 2014. **12**(1): p. 60-8.
31. Lim, M.S., et al., *Generation of Dopamine Neurons from Rodent Fibroblasts through the Expandable Neural Precursor Cell Stage*. J Biol Chem, 2015. **290**(28): p. 17401-14.
32. Kim, J., et al., *Functional integration of dopaminergic neurons directly converted from mouse fibroblasts*. Cell Stem Cell, 2011. **9**(5): p. 413-9.
33. Liu, X., et al., *Direct reprogramming of human fibroblasts into dopaminergic neuron-like cells*. Cell Res, 2012. **22**(2): p. 321-32.
34. Pfisterer, U., et al., *Direct conversion of human fibroblasts to dopaminergic neurons*. Proc Natl Acad Sci U S A, 2011. **108**(25): p. 10343-8.
35. Torper, O., et al., *Generation of induced neurons via direct conversion in vivo*. Proc Natl Acad Sci U S A, 2013. **110**(17): p. 7038-43.
36. Sheng, C., et al., *Generation of dopaminergic neurons directly from mouse fibroblasts and fibroblast-derived neural progenitors*. Cell Res, 2012. **22**(4): p. 769-72.
37. Caiazzo, M., et al., *Direct generation of functional dopaminergic neurons from mouse and human fibroblasts*. Nature, 2011. **476**(7359): p. 224-7.
38. Liu, G.H., et al., *Induced neural stem cells: a new tool for studying neural development and neurological disorders*. Cell Res, 2012. **22**(7): p. 1087-91.
39. Matsui, T., et al., *Neural stem cells directly differentiated from partially reprogrammed fibroblasts rapidly acquire gliogenic competency*. Stem Cells, 2012. **30**(6): p. 1109-19.
40. Yung, S.Y., et al., *Differential modulation of BMP signaling promotes the elaboration of cerebral cortical GABAergic neurons or oligodendrocytes from a common sonic hedgehog-responsive ventral forebrain progenitor species*. Proc Natl Acad Sci U S A, 2002. **99**(25): p. 16273-8.
41. Bertrand, N., D.S. Castro, and F. Guillemot, *Proneural genes and the specification of neural cell types*. Nat Rev Neurosci, 2002. **3**(7): p. 517-30.
42. Kele, J., et al., *Neurogenin 2 is required for the development of ventral midbrain dopaminergic neurons*. Development, 2006. **133**(3): p. 495-505.
43. Park, C.H., et al., *Differential actions of the proneural genes encoding Mash1 and neurogenins in Nurr1-induced dopamine neuron differentiation*. J Cell Sci, 2006. **119**(Pt 11): p. 2310-20.
44. Guillemot, F., et al., *Mammalian achaete-scute homolog 1 is required for the early development of olfactory and autonomic neurons*. Cell, 1993. **75**(3): p. 463-76.
45. Wapinski, O.L., et al., *Hierarchical mechanisms for direct reprogramming of fibroblasts to neurons*. Cell, 2013. **155**(3): p. 621-35.
46. Zaret, K.S. and J.S. Carroll, *Pioneer transcription factors: establishing competence for gene expression*. Genes Dev, 2011. **25**(21): p. 2227-41.
47. Chanda, S., et al., *Generation of induced neuronal cells by the single reprogramming factor ASCL1*. Stem Cell Reports, 2014. **3**(2): p. 282-96.
48. Heinrich, C., et al., *Directing astroglia from the cerebral cortex into subtype specific functional neurons*. PLoS Biol, 2010. **8**(5): p. e1000373.

49. Heinrich, C., et al., *Generation of subtype-specific neurons from postnatal astroglia of the mouse cerebral cortex*. Nat Protoc, 2011. **6**(2): p. 214-28.
50. Andersson, E., et al., *Identification of intrinsic determinants of midbrain dopamine neurons*. Cell, 2006. **124**(2): p. 393-405.
51. Yan, C.H., et al., *Lmx1a and Lmx1b function cooperatively to regulate proliferation, specification, and differentiation of midbrain dopaminergic progenitors*. J Neurosci, 2011. **31**(35): p. 12413-25.
52. Chung, S., et al., *Wnt1-Lmx1a forms a novel autoregulatory loop and controls midbrain dopaminergic differentiation synergistically with the SHH-FoxA2 pathway*. Cell Stem Cell, 2009. **5**(6): p. 646-58.
53. Deng, Q., et al., *Specific and integrated roles of Lmx1a, Lmx1b and Phox2a in ventral midbrain development*. Development, 2011. **138**(16): p. 3399-408.
54. Wallen, A. and T. Perlmann, *Transcriptional control of dopamine neuron development*. Ann N Y Acad Sci, 2003. **991**: p. 48-60.
55. Colon-Cesario, W.I., et al., *Knockdown of Nurr1 in the rat hippocampus: implications to spatial discrimination learning and memory*. Learn Mem, 2006. **13**(6): p. 734-44.
56. Xiao, Q., S.O. Castillo, and V.M. Nikodem, *Distribution of messenger RNAs for the orphan nuclear receptors Nurr1 and Nur77 (NGFI-B) in adult rat brain using in situ hybridization*. Neuroscience, 1996. **75**(1): p. 221-30.
57. Wallen, A., et al., *Fate of mesencephalic AHD2-expressing dopamine progenitor cells in NURR1 mutant mice*. Exp Cell Res, 1999. **253**(2): p. 737-46.
58. Sakurada, K., et al., *Nurr1, an orphan nuclear receptor, is a transcriptional activator of endogenous tyrosine hydroxylase in neural progenitor cells derived from the adult brain*. Development, 1999. **126**(18): p. 4017-26.
59. Sacchetti, P., et al., *Nurr1 enhances transcription of the human dopamine transporter gene through a novel mechanism*. J Neurochem, 2001. **76**(5): p. 1565-72.
60. Volpicelli, F., et al., *Bdnf gene is a downstream target of Nurr1 transcription factor in rat midbrain neurons in vitro*. J Neurochem, 2007. **102**(2): p. 441-53.
61. Saucedo-Cardenas, O., et al., *Nurr1 is essential for the induction of the dopaminergic phenotype and the survival of ventral mesencephalic late dopaminergic precursor neurons*. Proc Natl Acad Sci U S A, 1998. **95**(7): p. 4013-8.
62. Volpicelli, F., et al., *Direct regulation of Pitx3 expression by Nurr1 in culture and in developing mouse midbrain*. PLoS One, 2012. **7**(2): p. e30661.
63. Zetterstrom, R.H., et al., *Dopamine neuron agenesis in Nurr1-deficient mice*. Science, 1997. **276**(5310): p. 248-50.
64. Makarova, K.S., et al., *Evolution and classification of the CRISPR-Cas systems*. Nat Rev Microbiol, 2011. **9**(6): p. 467-77.
65. Barrangou, R., et al., *CRISPR provides acquired resistance against viruses in prokaryotes*. Science, 2007. **315**(5819): p. 1709-12.
66. Jinek, M., et al., *A programmable dual-RNA-guided DNA endonuclease in adaptive bacterial immunity*. Science, 2012. **337**(6096): p. 816-21.
67. Jinek, M., et al., *Structures of Cas9 endonucleases reveal RNA-mediated conformational activation*. Science, 2014. **343**(6176): p. 1247997.
68. Deltcheva, E., et al., *CRISPR RNA maturation by trans-encoded small RNA and host factor RNase III*. Nature, 2011. **471**(7340): p. 602-7.
69. Fonfara, I., et al., *Phylogeny of Cas9 determines functional exchangeability of dual-RNA and Cas9 among orthologous type II CRISPR-Cas systems*. Nucleic Acids Res, 2014. **42**(4): p. 2577-90.
70. Gasiunas, G., et al., *Cas9-crRNA ribonucleoprotein complex mediates specific DNA cleavage for adaptive immunity in bacteria*. Proc Natl Acad Sci U S A, 2012. **109**(39): p. E2579-86.
71. Deveau, H., et al., *Phage response to CRISPR-encoded resistance in Streptococcus thermophilus*. J Bacteriol, 2008. **190**(4): p. 1390-400.

72. Shah, S.A., et al., *Protospacer recognition motifs: mixed identities and functional diversity*. RNA Biol, 2013. **10**(5): p. 891-9.
73. Zhang, Y., et al., *Comparison of non-canonical PAMs for CRISPR/Cas9-mediated DNA cleavage in human cells*. Sci Rep, 2014. **4**: p. 5405.
74. Sampson, T.R., et al., *A CRISPR/Cas system mediates bacterial innate immune evasion and virulence*. Nature, 2013. **497**(7448): p. 254-7.
75. Garneau, J.E., et al., *The CRISPR/Cas bacterial immune system cleaves bacteriophage and plasmid DNA*. Nature, 2010. **468**(7320): p. 67-71.
76. Sorek, R., C.M. Lawrence, and B. Wiedenheft, *CRISPR-mediated adaptive immune systems in bacteria and archaea*. Annu Rev Biochem, 2013. **82**: p. 237-66.
77. Gratz, S.J., et al., *Genome engineering of Drosophila with the CRISPR RNA-guided Cas9 nuclease*. Genetics, 2013. **194**(4): p. 1029-35.
78. Hwang, W.Y., et al., *Efficient genome editing in zebrafish using a CRISPR-Cas system*. Nat Biotechnol, 2013. **31**(3): p. 227-9.
79. Wang, H., et al., *One-step generation of mice carrying mutations in multiple genes by CRISPR/Cas-mediated genome engineering*. Cell, 2013. **153**(4): p. 910-8.
80. Yang, H., et al., *One-step generation of mice carrying reporter and conditional alleles by CRISPR/Cas-mediated genome engineering*. Cell, 2013. **154**(6): p. 1370-9.
81. Shalem, O., et al., *Genome-scale CRISPR-Cas9 knockout screening in human cells*. Science, 2014. **343**(6166): p. 84-7.
82. Wang, T., et al., *Genetic screens in human cells using the CRISPR-Cas9 system*. Science, 2014. **343**(6166): p. 80-4.
83. Cong, L., et al., *Multiplex genome engineering using CRISPR/Cas systems*. Science, 2013. **339**(6121): p. 819-23.
84. Mali, P., et al., *RNA-guided human genome engineering via Cas9*. Science, 2013. **339**(6121): p. 823-6.
85. Wood, A.J., et al., *Targeted genome editing across species using ZFNs and TALENs*. Science, 2011. **333**(6040): p. 307.
86. Miller, J.C., et al., *An improved zinc-finger nuclease architecture for highly specific genome editing*. Nat Biotechnol, 2007. **25**(7): p. 778-85.
87. Christian, M., et al., *Targeting DNA double-strand breaks with TAL effector nucleases*. Genetics, 2010. **186**(2): p. 757-61.
88. Gaj, T., C.A. Gersbach, and C.F. Barbas, 3rd, *ZFN, TALEN, and CRISPR/Cas-based methods for genome engineering*. Trends Biotechnol, 2013. **31**(7): p. 397-405.
89. Cheng, A.W., et al., *Multiplexed activation of endogenous genes by CRISPR-on, an RNA-guided transcriptional activator system*. Cell Res, 2013. **23**(10): p. 1163-71.
90. Chavez, A., et al., *Highly efficient Cas9-mediated transcriptional programming*. Nat Methods, 2015. **12**(4): p. 326-8.
91. Konermann, S., et al., *Genome-scale transcriptional activation by an engineered CRISPR-Cas9 complex*. Nature, 2015. **517**(7536): p. 583-8.
92. Zlotorynski, E., *Genome engineering: NHEJ and CRISPR-Cas9 improve gene therapy*. Nat Rev Mol Cell Biol, 2016. **18**(1): p. 4.
93. Chu, V.T., et al., *Increasing the efficiency of homology-directed repair for CRISPR-Cas9-induced precise gene editing in mammalian cells*. Nat Biotechnol, 2015. **33**(5): p. 543-8.
94. Gilbert, L.A., et al., *CRISPR-mediated modular RNA-guided regulation of transcription in eukaryotes*. Cell, 2013. **154**(2): p. 442-51.
95. Gilbert, L.A., et al., *Genome-Scale CRISPR-Mediated Control of Gene Repression and Activation*. Cell, 2014. **159**(3): p. 647-61.
96. Lin, Y.S., et al., *Binding of general transcription factor TFIIB to an acidic activating region*. Nature, 1991. **353**(6344): p. 569-71.
97. Buratowski, S. and H. Zhou, *Functional domains of transcription factor TFIIB*. Proc Natl Acad Sci U S A, 1993. **90**(12): p. 5633-7.

98. Zakeri, B., et al., *Peptide tag forming a rapid covalent bond to a protein, through engineering a bacterial adhesin*. Proc Natl Acad Sci U S A, 2012. **109**(12): p. E690-7.
99. Zakeri, B. and M. Howarth, *Spontaneous intermolecular amide bond formation between side chains for irreversible peptide targeting*. J Am Chem Soc, 2010. **132**(13): p. 4526-7.
100. Tanenbaum, M.E., et al., *A protein-tagging system for signal amplification in gene expression and fluorescence imaging*. Cell, 2014. **159**(3): p. 635-46.
101. Schmitz, M.L., et al., *Interaction of the COOH-terminal transactivation domain of p65 NF-kappa B with TATA-binding protein, transcription factor IIB, and coactivators*. J Biol Chem, 1995. **270**(13): p. 7219-26.
102. Perkins, N.D., et al., *Regulation of NF-kappaB by cyclin-dependent kinases associated with the p300 coactivator*. Science, 1997. **275**(5299): p. 523-7.
103. Gwack, Y., et al., *CREB-binding protein and histone deacetylase regulate the transcriptional activity of Kaposi's sarcoma-associated herpesvirus open reading frame 50*. J Virol, 2001. **75**(4): p. 1909-17.
104. Peabody, D.S., *The RNA binding site of bacteriophage MS2 coat protein*. EMBO J, 1993. **12**(2): p. 595-600.
105. Anckar, J. and L. Sistonen, *Regulation of HSF1 function in the heat stress response: implications in aging and disease*. Annu Rev Biochem, 2011. **80**: p. 1089-115.
106. Wei, S., et al., *Conversion of embryonic stem cells into extraembryonic lineages by CRISPR-mediated activators*. Sci Rep, 2016. **6**: p. 19648.
107. Black, J.B., et al., *Targeted Epigenetic Remodeling of Endogenous Loci by CRISPR/Cas9-Based Transcriptional Activators Directly Converts Fibroblasts to Neuronal Cells*. Cell Stem Cell, 2016. **19**(3): p. 406-14.
108. Chakraborty, S., et al., *A CRISPR/Cas9-based system for reprogramming cell lineage specification*. Stem Cell Reports, 2014. **3**(6): p. 940-7.
109. Hilton, I.B., et al., *Epigenome editing by a CRISPR-Cas9-based acetyltransferase activates genes from promoters and enhancers*. Nat Biotechnol, 2015. **33**(5): p. 510-7.
110. Chavez, A., et al., *Comparison of Cas9 activators in multiple species*. Nat Methods, 2016. **13**(7): p. 563-7.
111. Bannister, A.J. and T. Kouzarides, *Regulation of chromatin by histone modifications*. Cell Res, 2011. **21**(3): p. 381-95.
112. Creyghton, M.P., et al., *Histone H3K27ac separates active from poised enhancers and predicts developmental state*. Proc Natl Acad Sci U S A, 2010. **107**(50): p. 21931-6.
113. Perez-Pinera, P., et al., *RNA-guided gene activation by CRISPR-Cas9-based transcription factors*. Nat Methods, 2013. **10**(10): p. 973-6.
114. Gossen, M., et al., *Transcriptional activation by tetracyclines in mammalian cells*. Science, 1995. **268**(5218): p. 1766-9.
115. de Felipe, P., et al., *Inhibition of 2A-mediated 'cleavage' of certain artificial polyproteins bearing N-terminal signal sequences*. Biotechnol J, 2010. **5**(2): p. 213-23.
116. Donnelly, M.L., et al., *Analysis of the aphthovirus 2A/2B polyprotein 'cleavage' mechanism indicates not a proteolytic reaction, but a novel translational effect: a putative ribosomal 'skip'*. J Gen Virol, 2001. **82**(Pt 5): p. 1013-25.
117. de Felipe, P., et al., *E unum pluribus: multiple proteins from a self-processing polyprotein*. Trends Biotechnol, 2006. **24**(2): p. 68-75.
118. Theodorou, M., et al., *Limitations of In Vivo Reprogramming to Dopaminergic Neurons via a Tricistronic Strategy*. Hum Gene Ther Methods, 2015. **26**(4): p. 107-22.
119. Kim, J.H., et al., *High cleavage efficiency of a 2A peptide derived from porcine teschovirus-1 in human cell lines, zebrafish and mice*. PLoS One, 2011. **6**(4): p. e18556.
120. Qin, J.Y., et al., *Systematic comparison of constitutive promoters and the doxycycline-inducible promoter*. PLoS One, 2010. **5**(5): p. e10611.
121. Liu, M.L., et al., *Small molecules enable neurogenin 2 to efficiently convert human fibroblasts into cholinergic neurons*. Nat Commun, 2013. **4**: p. 2183.

122. Seamon, K.B., W. Padgett, and J.W. Daly, *Forskolin: unique diterpene activator of adenylate cyclase in membranes and in intact cells*. Proc Natl Acad Sci U S A, 1981. **78**(6): p. 3363-7.
123. Mayr, B. and M. Montminy, *Transcriptional regulation by the phosphorylation-dependent factor CREB*. Nat Rev Mol Cell Biol, 2001. **2**(8): p. 599-609.
124. Montminy, M., *Transcriptional regulation by cyclic AMP*. Annu Rev Biochem, 1997. **66**: p. 807-22.
125. Tasken, K. and E.M. Aandahl, *Localized effects of cAMP mediated by distinct routes of protein kinase A*. Physiol Rev, 2004. **84**(1): p. 137-67.
126. Chen, X., et al., *Activation of tyrosine hydroxylase mRNA translation by cAMP in midbrain dopaminergic neurons*. Mol Pharmacol, 2008. **73**(6): p. 1816-28.
127. Xu, L., C.R. Sterling, and A.W. Tank, *cAMP-mediated stimulation of tyrosine hydroxylase mRNA translation is mediated by polypyrimidine-rich sequences within its 3'-untranslated region and poly(C)-binding protein 2*. Mol Pharmacol, 2009. **76**(4): p. 872-83.
128. Misra, U.K. and S.V. Pizzo, *Coordinate regulation of forskolin-induced cellular proliferation in macrophages by protein kinase A/cAMP-response element-binding protein (CREB) and Epac1-Rap1 signaling: effects of silencing CREB gene expression on Akt activation*. J Biol Chem, 2005. **280**(46): p. 38276-89.
129. Kilmer, S.L. and R.C. Carlsen, *Forskolin activation of adenylate cyclase in vivo stimulates nerve regeneration*. Nature, 1984. **307**(5950): p. 455-7.
130. Sulaiman, O.A. and T. Gordon, *Transforming growth factor-beta and forskolin attenuate the adverse effects of long-term Schwann cell denervation on peripheral nerve regeneration in vivo*. Glia, 2002. **37**(3): p. 206-18.
131. Treutlein, B., et al., *Dissecting direct reprogramming from fibroblast to neuron using single-cell RNA-seq*. Nature, 2016. **534**(7607): p. 391-5.
132. Heinrich, C., M. Gotz, and B. Berninger, *Reprogramming of postnatal astroglia of the mouse neocortex into functional, synapse-forming neurons*. Methods Mol Biol, 2012. **814**: p. 485-98.
133. Hsu, P.D., et al., *DNA targeting specificity of RNA-guided Cas9 nucleases*. Nat Biotechnol, 2013. **31**(9): p. 827-32.
134. Castro, D.S., et al., *Proneural bHLH and Brn proteins coregulate a neurogenic program through cooperative binding to a conserved DNA motif*. Dev Cell, 2006. **11**(6): p. 831-44.
135. Doench, J.G., et al., *Rational design of highly active sgRNAs for CRISPR-Cas9-mediated gene inactivation*. Nat Biotechnol, 2014. **32**(12): p. 1262-7.
136. Qi, L.S., et al., *Repurposing CRISPR as an RNA-guided platform for sequence-specific control of gene expression*. Cell, 2013. **152**(5): p. 1173-83.
137. Voronova, A., et al., *Ascl1/Mash1 is a novel target of Gli2 during Gli2-induced neurogenesis in P19 EC cells*. PLoS One, 2011. **6**(4): p. e19174.
138. Gompf, H.S., et al., *Targeted genetic manipulations of neuronal subtypes using promoter-specific combinatorial AAVs in wild-type animals*. Front Behav Neurosci, 2015. **9**: p. 152.
139. Varma, N., et al., *Lentiviral Based Gene Transduction and Promoter Studies in Human Hematopoietic Stem Cells (hHSCs)*. J Stem Cells Regen Med, 2011. **7**(1): p. 41-53.
140. Kumar, M., et al., *Systematic determination of the packaging limit of lentiviral vectors*. Hum Gene Ther, 2001. **12**(15): p. 1893-905.
141. Truong, D.J., et al., *Development of an intein-mediated split-Cas9 system for gene therapy*. Nucleic Acids Res, 2015. **43**(13): p. 6450-8.
142. Choi, J.H., et al., *Optimization of AAV expression cassettes to improve packaging capacity and transgene expression in neurons*. Mol Brain, 2014. **7**: p. 17.
143. Cheriyan, M., et al., *Faster protein splicing with the Nostoc punctiforme DnaE intein using non-native extein residues*. J Biol Chem, 2013. **288**(9): p. 6202-11.
144. Mizuguchi, H., et al., *IRES-dependent second gene expression is significantly lower than cap-dependent first gene expression in a bicistronic vector*. Mol Ther, 2000. **1**(4): p. 376-82.
145. Hennecke, M., et al., *Composition and arrangement of genes define the strength of IRES-driven translation in bicistronic mRNAs*. Nucleic Acids Res, 2001. **29**(16): p. 3327-34.

146. Gascon, S., et al., *Identification and Successful Negotiation of a Metabolic Checkpoint in Direct Neuronal Reprogramming*. Cell Stem Cell, 2016. **18**(3): p. 396-409.
147. Wernig, M., et al., *Tau EGFP embryonic stem cells: an efficient tool for neuronal lineage selection and transplantation*. J Neurosci Res, 2002. **69**(6): p. 918-24.
148. Bottenstein, J.E. and G.H. Sato, *Growth of a rat neuroblastoma cell line in serum-free supplemented medium*. Proc Natl Acad Sci U S A, 1979. **76**(1): p. 514-7.
149. Zhao, S., et al., *Generation of embryonic stem cells and transgenic mice expressing green fluorescence protein in midbrain dopaminergic neurons*. Eur J Neurosci, 2004. **19**(5): p. 1133-40.
150. Sawamoto, K., et al., *Visualization, direct isolation, and transplantation of midbrain dopaminergic neurons*. Proc Natl Acad Sci U S A, 2001. **98**(11): p. 6423-8.
151. Dixon, S.J., et al., *Ferroptosis: an iron-dependent form of nonapoptotic cell death*. Cell, 2012. **149**(5): p. 1060-72.
152. Michel, P.P. and Y. Agid, *Chronic activation of the cyclic AMP signaling pathway promotes development and long-term survival of mesencephalic dopaminergic neurons*. J Neurochem, 1996. **67**(4): p. 1633-42.
153. Kriks, S., et al., *Dopamine neurons derived from human ES cells efficiently engraft in animal models of Parkinson's disease*. Nature, 2011. **480**(7378): p. 547-51.
154. Ribeiro, D., et al., *Efficient expansion and dopaminergic differentiation of human fetal ventral midbrain neural stem cells by midbrain morphogens*. Neurobiol Dis, 2013. **49**: p. 118-27.
155. Chambers, S.M., et al., *Highly efficient neural conversion of human ES and iPS cells by dual inhibition of SMAD signaling*. Nat Biotechnol, 2009. **27**(3): p. 275-80.
156. Lin, L.F., et al., *GDNF: a glial cell line-derived neurotrophic factor for midbrain dopaminergic neurons*. Science, 1993. **260**(5111): p. 1130-2.
157. Engele, J. and B. Franke, *Effects of glial cell line-derived neurotrophic factor (GDNF) on dopaminergic neurons require concurrent activation of cAMP-dependent signaling pathways*. Cell Tissue Res, 1996. **286**(2): p. 235-40.
158. Fang, J., et al., *Stable antibody expression at therapeutic levels using the 2A peptide*. Nat Biotechnol, 2005. **23**(5): p. 584-90.
159. Szymczak, A.L., et al., *Correction of multi-gene deficiency in vivo using a single 'self-cleaving' 2A peptide-based retroviral vector*. Nat Biotechnol, 2004. **22**(5): p. 589-94.
160. McIntyre, G.J., et al., *Cassette deletion in multiple shRNA lentiviral vectors for HIV-1 and its impact on treatment success*. Virol J, 2009. **6**: p. 184.
161. Hampton, R.Y., *ER stress response: getting the UPR hand on misfolded proteins*. Curr Biol, 2000. **10**(14): p. R518-21.
162. Nakajima, K., et al., *An improved retroviral vector for assaying promoter activity. Analysis of promoter interference in pIP211 vector*. FEBS Lett, 1993. **315**(2): p. 129-33.
163. Emerman, M. and H.M. Temin, *Comparison of promoter suppression in avian and murine retrovirus vectors*. Nucleic Acids Res, 1986. **14**(23): p. 9381-96.
164. de Felipe, P., *Polycistronic viral vectors*. Curr Gene Ther, 2002. **2**(3): p. 355-78.
165. Maeder, M.L., et al., *CRISPR RNA-guided activation of endogenous human genes*. Nat Methods, 2013. **10**(10): p. 977-9.
166. Vierbuchen, T. and M. Wernig, *Direct lineage conversions: unnatural but useful?* Nat Biotechnol, 2011. **29**(10): p. 892-907.
167. Lin, Y., et al., *CRISPR/Cas9 systems have off-target activity with insertions or deletions between target DNA and guide RNA sequences*. Nucleic Acids Res, 2014. **42**(11): p. 7473-85.
168. Zhang, X.H., et al., *Off-target Effects in CRISPR/Cas9-mediated Genome Engineering*. Mol Ther Nucleic Acids, 2015. **4**: p. e264.
169. Chen, X., J.L. Zaro, and W.C. Shen, *Fusion protein linkers: property, design and functionality*. Adv Drug Deliv Rev, 2013. **65**(10): p. 1357-69.
170. Cohen, R.N., et al., *Quantification of plasmid DNA copies in the nucleus after lipoplex and polyplex transfection*. J Control Release, 2009. **135**(2): p. 166-74.

171. Schildge, S., et al., *Isolation and culture of mouse cortical astrocytes*. J Vis Exp, 2013(71).
172. Zhang, F., et al., *Multimodal fast optical interrogation of neural circuitry*. Nature, 2007. **446**(7136): p. 633-9.
173. Cooper, A.R., et al., *Rescue of splicing-mediated intron loss maximizes expression in lentiviral vectors containing the human ubiquitin C promoter*. Nucleic Acids Res, 2015. **43**(1): p. 682-90.
174. Koike-Yusa, H., et al., *Genome-wide recessive genetic screening in mammalian cells with a lentiviral CRISPR-guide RNA library*. Nat Biotechnol, 2014. **32**(3): p. 267-73.
175. Kadi, A.M., et al., *Multiplex CRISPR/Cas9-based genome engineering from a single lentiviral vector*. Nucleic Acids Res, 2014. **42**(19): p. e147.
176. Dull, T., et al., *A third-generation lentivirus vector with a conditional packaging system*. J Virol, 1998. **72**(11): p. 8463-71.

# APPENDIX

## 10 Appendix

### 10.1 Supplementary data

This section includes supplementary information as indicated in the results or discussion sections.

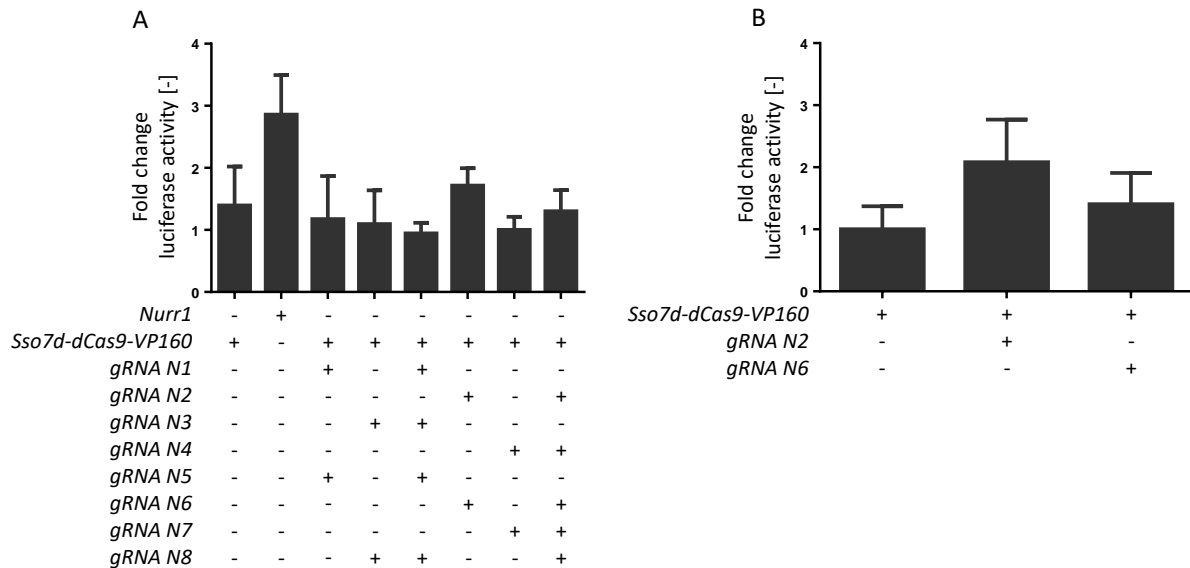


**Figure 25: gRNA N2 successfully induces *Nurr1* in Neuro 2a cells**

Luciferase assay screen for suitable gRNAs to induce murine *Nurr1* 48 h after transfection of Neuro 2a cells. **(A)** The combination of gRNAs N2/N6 showed the strongest luciferase activity. **(B)** gRNA N2 alone reached comparable levels as the combination of gRNAs N2/N6 together for *Nurr1* induction in (A). gRNA N2 was therefore chosen for further screenings regarding the induction of murine *Nurr1*. **Abbreviations:** gRNAs N1-8: gRNAs targeting the murine *Nurr1* promoter, *Sso7d*: *S. solfataricus* DNA binding protein 7d, VP160: ten repeats of the *Herpes simplex virus* protein vmw65 (VP16) transactivation domain. Data was derived from one experiment. Error bars represent mean  $\pm$  SEM.

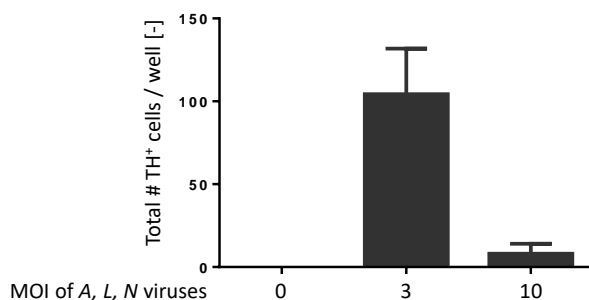


**Figure 26: Increasing the MOI of *Ascl1*, *Lmx1a*, *Nurr1* encoding lentiviruses to ten results in a decrease of TH<sup>+</sup> cells**

Quantification of reprogrammed TH<sup>+</sup> neurons 14 days after transduction of MEFs with individual lentiviruses encoding *Ascl1*, *Lmx1a* and *Nurr1*. Here, the total number of TH<sup>+</sup> cells / well was determined. An increase in the viral load from MOI3 to MOI10 (three and ten times more viral particles than cells, respectively) resulted in a reduction of reprogrammed TH<sup>+</sup> cells indicating adverse effects of high lentiviral particle concentrations. **Abbreviations:** A: *Ascl1*, L: *Lmx1a*, MOI: multiplicity of infection, N: *Nurr1*. Data was derived from one experiment. Error bars represent mean  $\pm$  SEM.

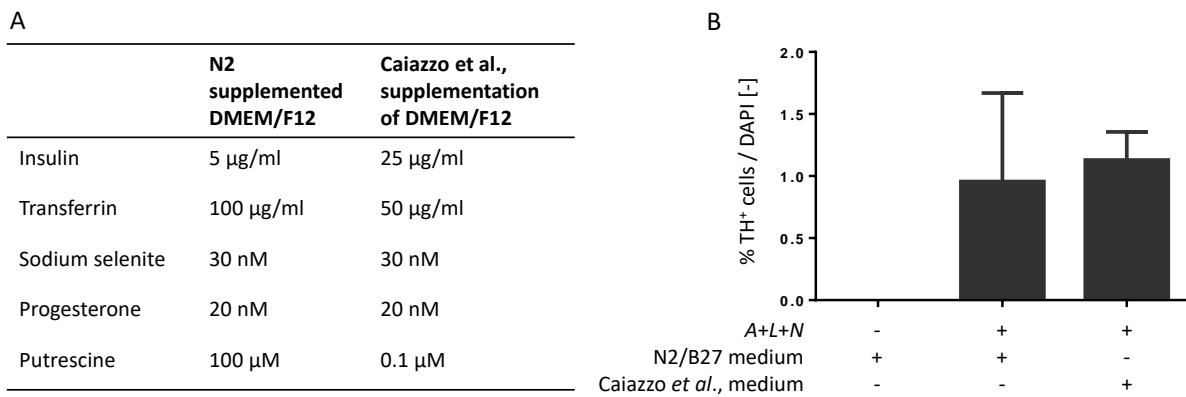


**Figure 27: Switching from N2/B27 to the medium used by Caiazzo et al., does not influence the reprogramming efficiency**

**(A)** Concentrations of N2 supplement components compared to concentrations used by Caiazzo *et al.*, [37]. How final concentrations of these substances in a 50:50 mixture of N2/B27 medium used in this thesis (see Table 6 for details) compare to the medium by Caiazzo *et al.*, is unclear as all substances shown in the table above are also included in B27 supplement at unknown concentrations. **(B)** Quantification of reprogrammed TH<sup>+</sup> neurons 14 days after transduction of MEFs with individual lentiviruses encoding *Ascl1*, *Lmx1a* and *Nurr1*. Switching from the previously used N2/B27 medium to the differentiation medium used by Caiazzo *et al.*, did not significantly affect the percentage of reprogrammed TH<sup>+</sup> cells. Abbreviations: A: *Ascl1*, L: *Lmx1a*, N: *Nurr1*, N2/B27 medium: 50:50 mixture of DMEM/F12 medium (addition of N2 supplement) and Neurobasal medium (addition of B27 supplement). Data was derived from one experiment. Error bars represent mean ± SEM.

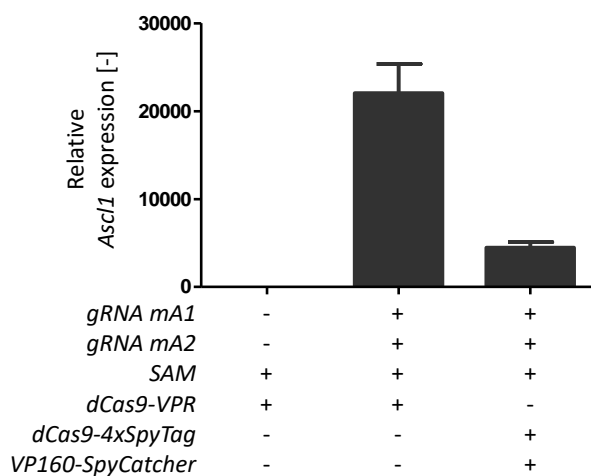


**Figure 28: The combination of SAM and 4x-SpyTag does not reach the levels of *Ascl1* activation observed for SAM and VPR**

RT-qPCR analysis of *Ascl1* mRNA levels 48h after transfection. Using a dCas9 version with four SpyTag repeats in combination with SAM did not induce *Ascl1* expression at levels observed for the combination of SAM and VPR together. Abbreviations: *gRNAs mA1*, *mA2*: *gRNAs* targeting the murine *Ascl1* promoter, SAM: MS2-P65-HSF1 fusion protein, VP160: ten repeats of *Herpes simplex virus* protein VP16, VPR: VP64-P65-RTA fusion protein. Data derived from one experiment, error bars represent mean ± SEM.

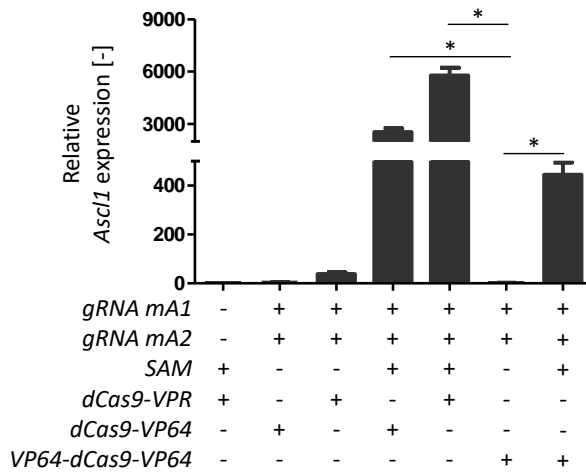


**Figure 29: VP64-dCas9-VP64 fails to induce *Ascl1* expression in Neuro 2a cells when used alone with gRNAs *mA1* and *mA2***

RT-qPCR analysis of *Ascl1* mRNA levels 48h after transfection of Neuro 2a cells. Using VP64-dCas9-VP64 in combination with gRNAs *mA1* and *mA2* did not induce *Ascl1* at detectable levels. By combining VP64-dCas9-VP64 with SAM, *Ascl1* expression was induced although not reaching the levels of SAM and dCas9-VP64. **Abbreviations:** gRNAs *mA1*, *mA2*: gRNAs targeting the murine *Ascl1* promoter, SAM: MS2-P65-HSF1 fusion protein, VP64: four repeats of *Herpes simplex virus* protein VP16, VPR: VP64-P65-RTA fusion protein. Data was derived from three independent experiments, error bars represent mean  $\pm$  SEM, Kruskal-Wallis test, Dunn's multiple comparison test, \*P < 0.05.

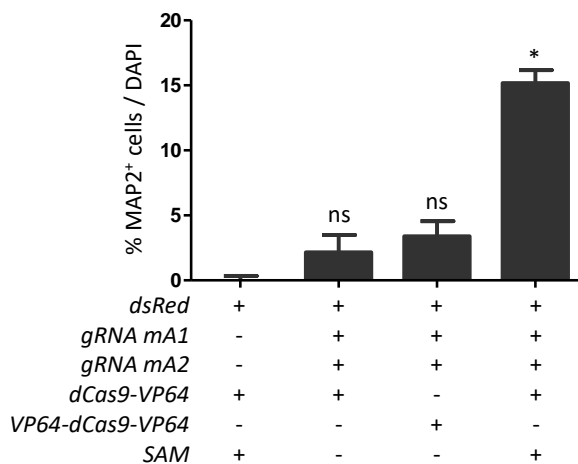


**Figure 30: VP64-dCas9-VP64 is not sufficient to induce direct conversion of astrocytes to neurons**

Quantification of reprogrammed cells 16 days after lipofection. In each condition *dsRed* was co-transfected allowing identification of cells which had received the DNA mix. All *dsRed*<sup>+</sup> cells were checked for neuronal morphology and MAP2 expression and counted for the analysis. Due to different background levels of neurons in control wells, the percentage of *dsRed*<sup>+</sup> neurons in control wells was subtracted from all wells of an individual experiment. The percentage of neurons obtained by VP64-dCas9-VP64 was not significantly different to dCas9-VP64 or the control. **Abbreviations:** gRNAs *mA1*, *mA2*: gRNAs targeting the murine *Ascl1* promoter, VP64: four repeats of *Herpes simplex virus* protein VP16. Data derived from three independent experiments, error bars represent mean  $\pm$  SEM, Kruskal-Wallis test, Dunn's multiple comparison test, ns: not significant, \*P < 0.05.

## 10.2 Abbreviations

6-OHDA	6-hydroxy dopamine
A	Ascl1 expressed from single vector
A+L+N	Ascl1, Lmx1a and Nurr1 expressed from single vectors
A1 – A8	gRNAs 1 – 29 targeting murine Ascl1 promoter
ALN	Ascl1, Lmx1a, Nurr1 expressed from tri-cistronic vector
Ascl1	Achaete-scute family bHLH transcription factor 1
Bdnf	Brain derived neurotrophic factor
Brn2	POU domain, class 3, transcription factor 2
cAMP	Cyclic adenosine monophosphate
cMyc	Myelocytomatosis oncogene
CREB	cAMP response element binding protein
CRISPR	Clustered regularly interspaced short palindromic repeats
crRNA	CRISPR-RNA
DA	Dopaminergic
DAT	Dopamine transporter
dCas9	Nuclease deficient CRISPR associated protein
Ef1a	Eukaryotic translation initiation factor 1A promoter
En1	Engrailed 1
FbaB	Fibronectin-binding protein
Foxa2	Forkhead box A2
GCN4	General control protein 4
Gdnf	Glial cell-line derived neurotrophic factor
GFAP	Glial fibrillary acidic protein
Gli2	Glioma-associated oncogene family zinc finger 2
gRNA	guide RNA
hA1 - hA4	gRNAs A – D targeting the human Ascl1 promoter
HDR	Homology directed repair
HSF1	Heat shock factor 1
hUBC	Human Ubiquitin C promoter
IMR90	Human fetal lung fibroblast cell line
iPSC	Induced pluripotent stem cell
IRES	Internal ribosomal entry site
Klf4	Kruppel-like factor 4
L	Lmx1a expressed from single vector
L-DOPA	L-Dihydroxyphenylalanine
Lmx1a	LIM homeobox transcription factor 1 alpha

Lmx1b	LIM homeobox transcription factor 1 beta
mA1 - mA5	gRNAs A – E targeting murine Ascl1 promoter
mdDA	Meso-diencephalic dopaminergic
MEF	Mouse embryonic fibroblast
MOI	Multiplicity of infection
MS2	MS2 coat protein
Msx1	Msh homeobox 1
Myt1l	Myelin transcription factor 1-like
N	Nurr1 expressed from single vector
N1 - N8	gRNAs 1 - 38 targeting murine Nurr1 promoter
Ngn2	Neurogenin 2
NHEJ	Non-homologous end joining
NPC	Neuronal precursor cells
NSC	Neuronal stem cell
nt	Nucleotide
Nurr1	Nuclear receptor subfamily 4, group A, member 2 (Nr4a2)
Oct4	POU domain, class 5, transcription factor 1 (Pou5f1)
Otx2	Orthodenticle homeobox 2
P2A	2A peptide of Porcine teschovirus-1
P65	P65 subunit of human NF- $\kappa$ B (residues 287-546)
PAM	Protospacer adjacent motifs
PD	Parkinson's disease
Pitx3	Paired-like homeodomain transcription factor 3
PM	Pluripotency mediated
RTA	Regulator of transcription activation (residues 416 – 605)
SAM	Synergistic activation mediator, consists of VP64-P65-HSF1
SNc	Substantia nigra pars compacta
Sox2	Sex determining region Y-box 2
Sso7d	<i>S. solfataricus</i> DNA binding protein 7d
SWI/SNF	Switching defective/ Sucrose non-fermenting
T2A	2A peptide of Thoseaasigna virus
TALEN	Transcription activator-effector nuclease
TF	Transcription factor
TFIIB	General transcription factor IIB
TH	Tyrosine hydroxylase
TNAP	TRAFs and NIK-associated protein
<i>tracrRNA</i>	Transactivating CRISPR RNA

VP16, -64, -160	Herpes simplex virus protein 16 (residues 437-448) repeats
VPR	Fusion protein of VP64-P65-RTA
VTA	Ventral tegmental area

### 10.3 Danksagung

Meinem Doktorvater Herrn Prof. Dr. Wolfgang Wurst bin ich sehr dankbar dafür, dass ich meine Doktorarbeit am Institut für Entwicklungsgenetik habe anfertigen dürfen. Insbesondere möchte ich mich für die regelmäßigen und offenen Diskussionen zu meinem Projekt und die hervorragende wissenschaftliche und persönliche Unterstützung bedanken. Ebenso gilt mein Dank meinen Betreuern Frau Prof. Dr. Nilima Prakash, Herrn Dr. Oskar Ortiz und Herrn Dr. Florian Giesert für die vielfältige Unterstützung und die zahlreichen Ratschläge. Ich möchte auch den Mitgliedern meines Thesis Komitees Frau Prof. Dr. Magdalena Götz und Frau Dr. Stefanie Hauck für ihre Unterstützung danken, die mich in vielerlei Hinsicht vorangebracht hat. Im Weiteren bin ich den Mitgliedern meines Prüfungskomitees Frau Prof. Angelika Schnieke, Ph.D. und Frau Prof. Dr. Aphrodite Kapurniotu dankbar für ihre Unterstützung bei meiner Verteidigung.

Besonderer Dank gilt auch meinem Kollegen Jeffery Truong für die Entwicklung und Bereitstellung der SpyTag und Sso7d Cas9 Varianten und für die zahlreichen konstruktiven Diskussionen. Zusätzlich danke ich meinen Kollegen Dr. Florian Meier, Dr. Sebastian Götz, Dr. Marina Theodorou, Dr. Jingzhong Zhang und Jessica Schwab für die wissenschaftliche und persönliche Unterstützung. Ich danke Susanne Badeke und Davina Fischer für die Hilfe im Labor und Anja Folchert für ihren Einsatz bei den Mäusen. Danke auch an Dietrich Trümbach für die Promoteranalysen und an Christoph Bach für die vergleichenden Experimente an humanen und murinen Promotoren. Zusätzlich gilt Annerose Kurz-Drexler ein besonderer Dank für ihre moralische Unterstützung, ihr stets offenes Ohr und das außergewöhnliche Fachwissen in sämtlichen Laborfragen. Außerdem danke ich meinen Kollegen Constantin, Artem, Petra, Clara, Anke, Michi und Luise für die gute Zeit im Labor und außerhalb der Arbeit. Vielen Dank auch an alle anderen Mitglieder des IDG für die gute Zusammenarbeit.

Schließlich möchte ich meiner Familie und meinen Schwiegereltern für die großartige Unterstützung während meines Studiums und meiner Doktorarbeit danken. Ein ganz besonderer Dank geht aber an meine Frau Julia. Du warst als Rückhalt immer für mich da, insbesondere wenn es stressig und kompliziert wurde. Ohne deine Unterstützung im privaten wie beruflichen hätte ich all das nicht erreichen können. Ich freue mich auf die weitere gemeinsame Zukunft.

Vielen Dank!

## 10.4 Lebenslauf

Benedict Samuel Rauser  
Eisnergutbogen 56  
80639 München

Geboren am 26.02.1986 in Filderstadt  
deutsch

### Ausbildung

---

- 05/2013 – 06/2017: **Promotion im Bereich Parkinson-Forschung / Zellersatztherapie**  
Helmholtz Zentrum München  
“Direct conversion of somatic cells utilizing CRISPR/Cas9”
- 04/2011 - 04/2013: **Master of Science, Studiengang Molekulare Biotechnologie**  
Technische Universität München
- Masterthesis am Helmholtz Zentrum München  
“Charakterisierung der Expression und Funktion neuer Gene in der Entwicklung Wnt-responsiver mdDA Neurone im Mittelhirn der Maus“ (Abschlussnote: 1,2)
- 10/2007 - 02/2011: **Bachelor of Science, Studiengang Biotechnologie**  
Hochschule Mannheim
- Bachelorthesis bei Rentschler Biotechnologie GmbH in Laupheim  
"Multivariate Analyse von CHO-Prozessen im Bioreaktor"  
(Abschlussnote: 1,5)
- 09/1992 - 06/2005: **Fachhochschulreife**  
Freie Waldorfschule Engelberg (Abschlussnote: 1,3)

### Praktische Erfahrung

---

- 12/2011 - 10/2012: Ascenion GmbH in München  
Teilzeittätigkeit
- Markt- und Patentrecherche
- 03/2011 - 04/2011: Rentschler Biotechnologie GmbH in Laupheim  
Nebentätigkeit in der Technologieentwicklung
- Überwachung von CHO-Prozessen mittels Infrarotspektroskopie
  - Multivariate Datenanalyse
- 07/2010 - 09/2010: Rentschler Biotechnologie GmbH in Laupheim  
Praktikum in der Technologieentwicklung
- Studien zu Single-Use Bioreaktoren und Filtrationstechnologien

- 07/2008 - 09/2008: BioGeneriX AG in Mannheim  
Nebentätigkeit in der Abteilung für Operative Entwicklung /  
Proteinchemie und Analytik
- Herstellung von Puffern und Analytik unter GLP Bedingungen
- 11/2006 - 08/2007: Atelier Busche, Werbefotografie  
Anerkennungsjahr der Fachhochschulreife

### Auslandserfahrungen

---

- 08/2009 - 02/2010: Ludwig Institute for Cancer Research Ltd., in Melbourne, Australien  
Praxissemester
- Darmkrebs-Forschung
- 10/2005 - 09/2006: Camphill Village USA, Inc. in Copake, NY, USA  
Alternativer Zivildienst im Ausland

## 10.5 Eidesstattliche Erklärung



Ich erkläre an Eides statt, dass ich die bei der promotionsführenden Einrichtung  
Fakultät Wissenschaftszentrum Weihenstephan für Ernährung, Landnutzung und Umwelt

der TUM zur Promotionsprüfung vorgelegte Arbeit mit dem Titel:

Direct conversion of somatic cells utilizing CRISPR/Cas9

in Institut für Entwicklungsgenetik, HelmholtzZentrum München

(Fakultät, Institut, Lehrstuhl, Klinik, Krankenhaus, Abteilung)

unter der Anleitung und Betreuung durch: Prof. Dr. Wolfgang Wurst

ohne sonstige Hilfe erstellt und bei der Abfassung nur die gemäß § 6 Abs. 6 und 7 Satz 2  
 angegebenen Hilfsmittel benutzt habe.

Ich habe keine Organisation eingeschaltet, die gegen Entgelt Betreuerinnen und Be-  
 treuer für die Anfertigung von Dissertationen sucht, oder die mir obliegenden Pflich-  
 ten hinsichtlich der Prüfungsleistungen für mich ganz oder teilweise erledigt.

Ich habe die Dissertation in dieser oder ähnlicher Form in keinem anderen Prüfungs-  
 verfahren als Prüfungsleistung vorgelegt.

Die vollständige Dissertation wurde in \_\_\_\_\_  
 veröffentlicht. Die promotionsführende Einrichtung

\_\_\_\_\_ hat der Vorveröffentlichung zugestimmt.

Ich habe den angestrebten Doktorgrad noch nicht erworben und bin nicht in einem  
 früheren Promotionsverfahren für den angestrebten Doktorgrad endgültig geschei-  
 tert.

Ich habe bereits am \_\_\_\_\_  
 bei der Fakultät für \_\_\_\_\_  
 der Hochschule \_\_\_\_\_  
 unter Vorlage einer Dissertation mit dem Thema \_\_\_\_\_

\_\_\_\_\_ die Zulassung zur Promotion beantragt mit dem Ergebnis:

\_\_\_\_\_ Die öffentlich zugängliche Promotionsordnung der TUM ist mir bekannt, insbesonde-  
 re habe ich die Bedeutung von § 28 (Nichtigkeit der Promotion) und § 29 (Entzug des  
 Doktorgrades) zur Kenntnis genommen. Ich bin mir der Konsequenzen einer falschen  
 Eidesstattlichen Erklärung bewusst.

Mit der Aufnahme meiner personenbezogenen Daten in die Alumni-Datei bei der TUM  
 bin ich

einverstanden,  nicht einverstanden.

\_\_\_\_\_  
(Ort, Datum, Unterschrift)